Article

Identification of a New Heterocyclic Scaffold for Inhibitors of the Polo-Box Domain of Polo-like Kinase 1

Celeste N. Alverez, Jung-Eun Park, Kiran S. Toti, Yangliu Xia, Kristopher W. Krausz, Ganesha Rai, Jeong K. Bang, Frank J. Gonzalez, Kenneth A. Jacobson,* and Kyung S. Lee*
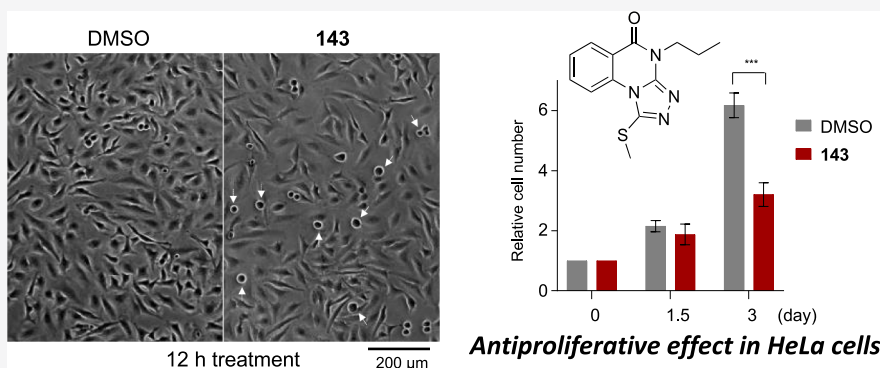
Cite This: https://dx.doi.org/10.1021/acs.jmedchem.0c01669

Read Online

ACCESS | Metrics & More | Article Recommendations | Supporting Information

Antiproliferative effect in HeLa cells

ABSTRACT: As a mitotic-specific target widely deregulated in various human cancers, polo-like kinase 1 (Plk1) has been extensively explored for anticancer activity and drug discovery. Although multiple catalytic domain inhibitors were tested in preclinical and clinical studies, their efficacies are limited by dose-limiting cytotoxicity, mainly from off-target cross reactivity. The C-terminal noncatalytic polo-box domain (PBD) of Plk1 has emerged as an attractive target for generating new protein−protein interaction inhibitors. Here, we identified a 1-thioxo-2,4-dihydro-[1,2,4]triazolo[4,3-*a*]quinazolin-5(1*H*)-one scaffold that efficiently inhibits Plk1 PBD but not its related Plk2 and Plk3 PBDs. Structure−activity relationship studies led to multiple inhibitors having ≥10-fold higher inhibitory activity than the previously characterized Plk1 PBD-specific phosphopeptide, PLHSpT ($K_d \sim 450$ nM). In addition, *S*-methyl prodrugs effectively inhibited mitotic progression and cell proliferation and their metabolic stability was determined. These data describe a novel class of small-molecule inhibitors that offer a promising avenue for future drug discovery against Plk1-addicted cancers.
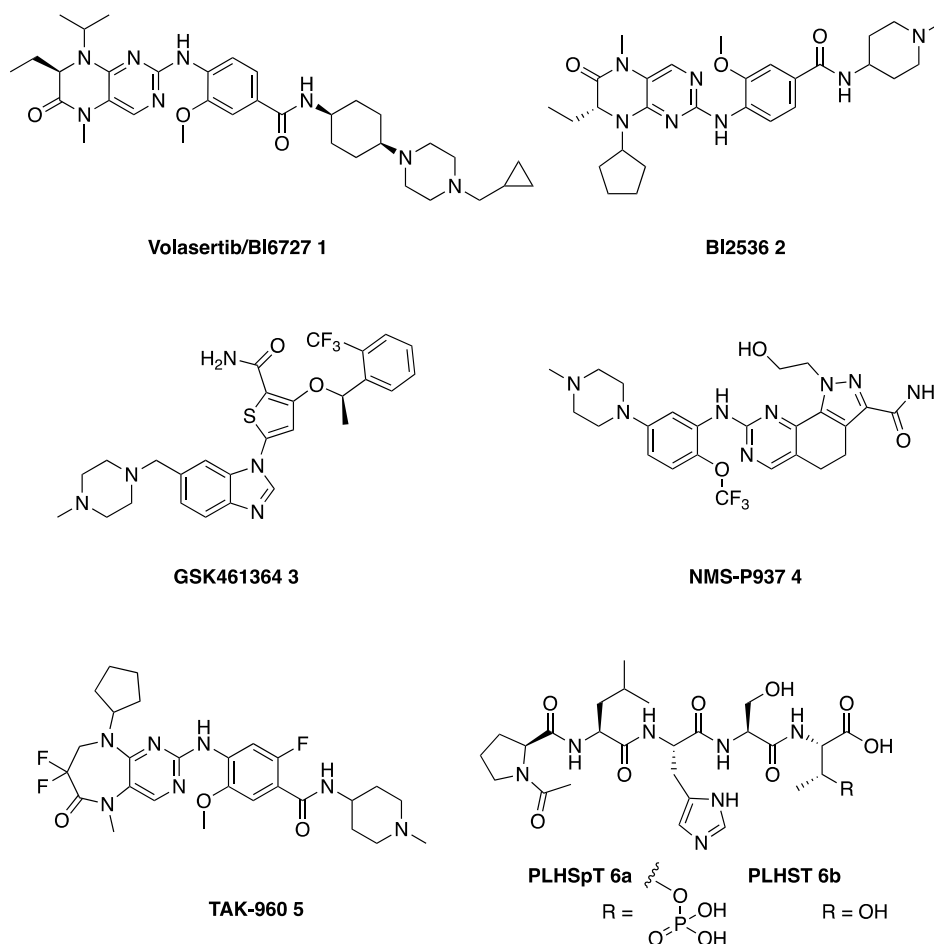
INTRODUCTION

Members of the polo subfamily of Ser/Thr protein kinases [collectively, polo-like kinases (Plks)] play a key role in regulating various aspects of the cell cycle and cell proliferation.[1] Among them, Plk1 is critically required for proper mitotic progression, whereas other members play distinct roles during interphase progression and exhibit little functional overlap with other Plk family members.[1,2] In accordance with its importance in promoting mitosis, Plk1 is largely upregulated in a broad range of human cancers and its level of overexpression appears to correlate with aggressiveness and poor prognosis for a wide spectrum of human cancers.[3,4] Notably, various cancer cells, but not their isogenic normal cells, are addicted to high Plk1 levels and consequently require Plk1 overexpression for their viability.[5−7] As the reversal of addicted protein functions in cancer cells has proven to be an attractive strategy to selectively kill cancer cells,[8−10] Plk1 is considered a discriminating target for anticancer therapy.

Plk1 contains an N-terminal kinase domain (KD) for ATP-dependent catalysis and is characterized by the presence of the C-terminal noncatalytic, but functionally essential, polo-box domain (PBD).[11,12] The PBD plays a key role in mediating Plk1 functions by targeting its N-terminal catalytic activity to distinct subcellular structures, such as centrosomes, kinetochores, and midbody, through specific protein−protein interactions (PPIs).[12,13] For more than a decade, extensive efforts were made to develop Plk1 inhibitors targeting the KD, resulting in several advanced Plk1 ATP-competitive inhibitors (Chart 1), such as volasertib/BI6727 **1**,[14] BI2536 **2**,[15] GSK461364 **3**,[16] NMS-P937 **4**,[17] and TAK-960 **5**,[18] that

Chart 1. Structures of Inhibitors of the KD (1−5) and the PBD (6) of Plk1

Volasertib/BI6727 1

BI2536 2

GSK461364 3

NMS-P937 4

TAK-960 5

PLHSpT 6a   PLHST 6b

R = [phosphate]   R = OH

have been examined against various cancers.[2] However, they all showed limited efficacy with more-than-acceptable dose-limiting toxicity in various preclinical or clinical trials. As dose-limiting toxicity arises mainly from nonspecific activity of these inhibitors,[19] improving the Plk1 specificity is likely the major concern that needs to be addressed to achieve better clinical outcomes. In fact, one of the common problems associated with the currently available Plk1 ATP-competitive inhibitors appears to be their low degree of selectivity against other kinases,[20,21] including two closely related Plk2 and Plk3 with potential tumor suppressor roles.[22,23]

Unlike the KD inhibitors aimed at annihilating all Plk1 catalytic activity-dependent processes, inhibiting the Plk1 PBD is expected to be less drastic because it could selectively mitigate a subset of essential Plk1 functions requiring PBD-dependent interactions.[7,24] In addition, given a high affinity (low nM K_d values) interaction between Plk1 PBD and its binding target sequence,[25] the effect of PBD inhibition is expected to be less severe than that of KD inhibition. As Plk1 is also required for the viability of normal cells, a moderate level of inhibition could serve as a fail-safe mechanism that helps prevent undesirable normal cell killing.

At the structural level, Plk1 PBD represents a well-characterized PPI domain that interacts with its short phosphopeptide targets with a high affinity.[11] The unique nature of PBD, which requires strict structural elements for binding, holds the promise of generating specific inhibitors capable of overcoming nonspecific toxicities associated with

the KD inhibitors.[20,21] Intriguingly, the blockade of Plk1 PBD-dependent PPIs by short peptides or peptide mimetics is sufficient for effectively abrogating the proper mitotic progression, thus imposing potent mitotic arrest and apoptotic cell death in cancer cells but less in normal cells.[7,25,26] These findings suggest that PBD is an attractive target amenable for in vitro PPI- and in vivo cell-based assays required to carry out optimization and preclinical studies for potential leads.

Over the years, various Plk1 PBD inhibitors were generated by either derivatizing the well-characterized minimal phospho-peptide, PLHSpT 6a,[27] or isolating small molecules interfering with Plk1 PBD-dependent PPI.[20,21] However, although peptide-derived inhibitors provide valuable insights into the binding interface of Plk1 PBD-dependent interactions, whether they can serve as a lead for developing anti-PBD agents is disputable, largely because of their poor permeability and limited bioavailability.[21] In addition, although multiple small molecule inhibitors targeting the Plk1 PBD were reported, most exhibit a low level (IC$_{50}$ of 50−1000 μM) of anti-Plk1 activity in cell-based assays,[28−35] while others are not sufficiently characterized at the cellular level.[36−41]

Here, we report the identification and exploration of triazoloquinazolinone-based small-molecule compounds that exhibit specific anti-Plk1 PBD activity in both in vitro biochemical and cell-based assays. These compounds are anticipated not to be chemically reactive as are many of the current probes of Plk1 PBD that contain electrophilic groups.[42,43] Their low molecular weight (MW) (generally

~300−400 Da) along with moderate hydrophobicity and activity of uncharged analogues predict facile availability in intracellular compartments. Notably, the two heterocyclic moieties of the inhibitors (i.e., quinazoline and triazole) are frequently found in various FDA-approved drugs, suggesting the potential druggability of this inhibitor class. We propose the triazoloquinazolinone-based compounds described here as attractive compounds that may lead to the development of a new class of anti-PBD therapeutics against various Plk1-addicted cancers.

RESULTS

Screening Small Molecules to Target Plk1 PBD. A small chemical library of ~400 drug-like molecules in the Molecular Recognition Section, National Institute of Diabetes and Digestive and Kidney Diseases (NIDDK), National Institutes of Health (NIH), was screened for the ability to bind to the PBD of Plk1. The principle screening assay consisted of an ELISA-based Plk1 PBD inhibition assay that utilizes the specific interaction between the full-length human Plk1 and a specific phospho-Thr (pT)-containing peptide (Biotin-Ahx-C-ETFDPPLHSpTAI-NH$_2$) derived from a kinetochore-localizing Plk1-binding protein, PBIP1.[27,44] When necessary, secondary fluorescence polarization (FP) assays were carried out using a 5-carboxyfluorescein-labeled peptide (FITC-Ahx-DPPLHSpTAI-NH$_2$)[26] to confirm the anti-Plk1 PBD activity from the primary ELISA-based assay and eliminate false positives.

Among four hits identified was triazoloquinazolinone **7** (Chart 1), which inhibited PBD binding in the ELISA assay with an IC$_{50}$ of 4.38 μM. When compared to the previously characterized phosphopeptide, PLHSpT **6a** (IC$_{50}$ of 14.74 μM), showing a K_d of ~450 nM,[27] the affinity of the lead compound **7** is anticipated to be at least threefold higher than that of peptide **6a** (Table 1). Compound **7** was previously reported as a weak hit in a structure-based in silico screen to identify ligands of the adenosine receptors.[45] From this hit, a family of congeners was synthesized by substitutions introduced on all of the moieties of the lead compound **7** (Figure 1). Various substituents were introduced as R^1 groups, and aza analogues of the phenyl ring were also introduced. Many alkyl, heteroalkyl, and arylalkyl modifications of the R^2 group (phenylethyl in compound **7**) were included. Some of the analogues were obtained from commercial sources and their identity confirmed by ^{1}H NMR and mass spectrometry.

Chemical Synthesis. The synthesis of analogues of **7** generally began with either the corresponding isatoic anhydride (Scheme 1) or anthranilic acid (Supporting Information). An isatoic anhydride (e.g., **10**) was heated in the presence of the desired amine to give the corresponding intermediate 2-aminobenzamide (structure not shown). This intermediate was heated in the presence of carbon disulfide and potassium hydroxide to give the cyclized 2-thioxo-2,3-dihydroquinazolin-4(1H)-one derivative (e.g., **11**), which was isolated by precipitation with treatment of water, followed by filtration. The corresponding 3-thione-1,2,4-triazole (e.g., **12**) was then typically formed in a one-pot procedure by first stirring with hydrazine in refluxing ethanol to form the hydrazine intermediate. This intermediate, after cooling, was treated with pyridine and carbon disulfide. The desired triazoloquinazolinone **12** was formed after heating the reaction again to 80 °C. The 2-thioxo-2,3-dihydroquinazolin-4(1H)-one intermediate could also be formed by reacting the desired

Table 1. Inhibitory Activity of Triazoloquinazolinones Modified in Zones 5 and 6 at the Plk1 PBD[a,b]
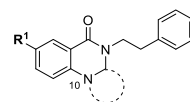
Cmpd	Triazole	R^1 =	IC$_{50}$ (μM, ELISA)	t$_{1/2}$ (min, RLM)	PAMPA (1e-6 cm/s)	Solub. (μg/ml)
PLHSpT 6a	--	--	14.74 ± 0.48 (12)	ND	ND	ND
7		H	4.38 ± 0.41 (6)	ND	ND	ND
15		H	>50	ND	ND	<1
16		F	>50	29.4	885	2.2
17		F	>50	10.7	1084	11.0
18		F	>50	11.8	924	14.8
19		H	>50	ND	ND	ND

[a](IC$_{50}$ values are n = 3 unless noted in parentheses) and microsomal half-life, PAMPA assays, and aqueous solubility. [b]ND, not determined.

2-aminobenzoic acid with an isothiocyanate. However, because of the limited availability of isothiocyanates, the preferred route for preparation of the triazoloquinazolinones is shown in Scheme 1. With the core triazoloquinazolinone formed, additional analogues could be generated with a terminal amine (e.g., **13**, Scheme 2). Amides of this amino congener (e.g., **14**) were selected as a primary focus, and (1-cyano-2-ethoxy-2-oxoethylidenaminooxy)dimethylamino-morpholino-carbenium hexafluorophosphate (COMU) was found to be the best coupling agent and therefore used to synthesize all additional analogues.

Structure−Activity Relationship. The structure−activity relationship (SAR) of the 1-thioxo-2,4-dihydro-[1,2,4]triazolo-[4,3-a]quinazolin-5(1H)-one scaffold as PBD inhibitors was explored (compounds **15−138**, Tables 1−9). All compounds were evaluated for their efficacy against the full-length human Plk1 in an ELISA assay (representative data shown in Figure 2) and for their in vitro physicochemical properties (half-life, permeability, and solubility). Because of the lack of structural information for the binding of **7** to the PBD domain of Plk1, early SAR studies began by exploring the 2,4-dihydro-3H-1,2,4-triazole-3-thione moiety to determine empirically the requirements for binding. Despite the prevalence of sulfur atoms in small-molecule drug discovery, we began by replacing and modifying the thiourea portion of the molecule. First, we replaced the sulfur with a range of additional atoms including oxygen in **15**. We found that any replacement of the sulfur resulted in complete loss of activity, indicating that a free 1-thioxo group is essential for activity (Table 1). To determine whether the thiocarbonyl was required, sulfur was methylated and product **19** tested, but this methyl thioether was also inactive. In addition, many alkyl groups were tried, and all were found to be inactive (see Table S1, Supporting Information). This showed that unmodified thiourea was required for activity.
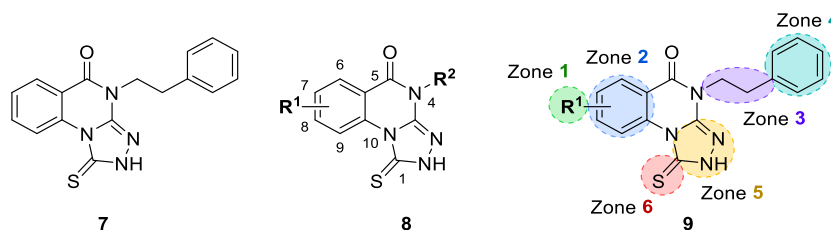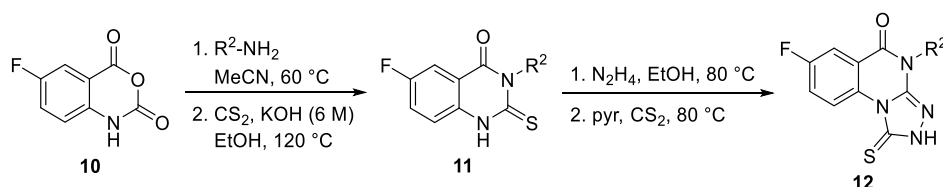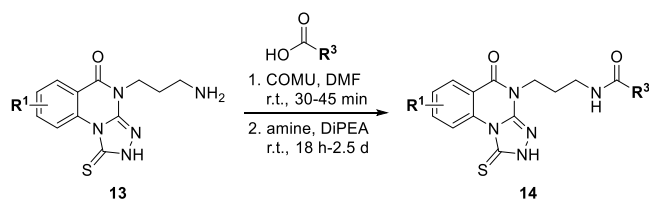
Figure 1. Delineation of zones of SAR focus in the triazoloquinazolinone series.

Scheme 1. General Synthesis of 7-Fluoro Analogues
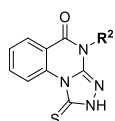

Scheme 2. Synthesis of Zone 4 Amides

We also explored S-methyl and S-acetyl derivatives (compounds 139−144, Table 9) as potential prodrugs of the corresponding active 1-thioxo derivatives. By decreasing the polarity of the molecules, we expected to achieve better intracellular levels of the active species, with the expectation that the masking moiety on the S could be labile prior to reaching the site of action.

We then explored the SAR of the side chain, R^2, by systematically modifying the length and composition of the linker as well as the end group of the side chain. First, we simplified the side chain by removing the terminal phenyl ring and maintaining the simpler alkyl chain of various lengths (Table 2, 20−34). All alkyl chain lengths tested, from the shorter ethyl group through the pentyl group, which maintain a linear length similar to that of 7, showed improved potency relative to the aryl-containing 7. This suggests a potential size restriction in the area of the pocket where the side chain binds. To further explore this, branching was introduced into the alkyl side chain with the 3-methylbutane of 25 and the isopropyl group of 26. However, these bulkier alkyl groups, relative to their linear counterparts 23 and 20, respectively, maintained potency in the range of 1−2 μM, suggesting that the improvement in potency was not strictly due to removal of the bulkier phenyl group.

Next, we tried to evaluate if incorporation of heteroatoms on the alkyl group (R^2) was tolerated (Table 2, 27−29). The CF$_3$ group of 27 also had the added benefit of blocking potential cytochrome P450 (CYP)-mediated metabolism of the side chain. Though there was no observable change in the metabolic stability of 27 relative to 21, 27 did maintain a potency relative to that of 21. Incorporation of oxygen to give ether side chains also improved the activity of 28 and 29 relative to 7 and maintained the activity relative to the hydrocarbon chains. We also incorporated amide groups into

Table 2. Inhibitory Activity of Early Triazoloquinazolinones Modified in Zones 3 and 4 at the Plk1 PBD (IC$_{50}$ Values Are $n = 3$ Unless Noted in Parentheses) and Microsomal Half-Life, PAMPA Assays, and Aqueous Solubility

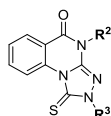| Cmpd	R^2 =	IC$_{50}$ (μM, ELISA)	$t_{1/2}$ (min, RLM)	PAMPA (1e-6 cm/s)	Solub. (μg/ml)
7	(phenethyl)	4.38 ± 0.41 (6)	ND	ND	ND
20	Et	1.49 ± 0.22 (6)	>30	427	>36
21	Pr	1.03 ± 0.08 (9)	>30	37.0	21.3
22	(allyl)	1.31 ± 0.03	ND	ND	19.4
23	Bu	1.03 ± 0.14 (5)	>30	77.5	8.5
24	Pent	1.97 ± 0.11 (6)	ND	ND	4.2
25	(3-methylbutyl)	1.73 ± 0.08 (6)	ND	ND	8.0
26	i-Pr	1.30 ± 0.06	ND	ND	19.5
27	CF$_3$	1.25 ± 0.11 (5)	>30,	82	23.3
28	(OMe ether)	1.75 ± 0.19	ND	ND	31.2
29	(OEt ether)	1.68 ± 0.11	ND	ND	15.5
30[a]	(sec-butyl amide)	3.23 ± 0.44	ND	ND	ND
31	(isopropyl amide)	3.90 ± 0.43	ND	ND	ND
32	(isobutyl amide)	2.92 ± 0.56	ND	ND	30.8
33	(2,6-dimethylphenyl)	1.85 ± 0.12	ND	ND	ND
34	(4-fluorobenzyl)	3.54 ± 0.57	ND	ND	ND

[a]Racemic. ND, not determined.

the side chain to see if there were additional H-bonding interactions that could be established with the PBD (Table 2, 30−32). All three amide-containing analogues showed a slight improvement over 7 (IC$_{50}$ = 2.92−3.90 μM vs IC$_{50}$ = 4.38 μM, respectively) but reduced activity relative to the alkyl chain-

Table 3. Inhibitory Activity of Zone 5-Modified Triazoloquinazolinone Derivatives at the Plk1 PBD (IC$_{50}$ Values Are n = 3 Unless Noted in Parentheses) and Microsomal Half-Life, PAMPA Assays, and Aqueous Solubility[a]

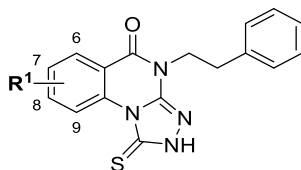| Cmpd	R^2 =	R^3 =	IC$_{50}$ (μM, ELISA)	$t_{1/2}$ (min, RLM)	PAMPA (1e-6 cm/s)	Solub. (μg/ml)
21	Pr	H	1.03 ± 0.08 (9)	>30	37	21.3
35	Pr	(N-ethyl cyclopropyl)	1.63 ± 0.05	ND	ND	Insol.
36	CH$_3$	(N-ethyl propyl)	1.20 ± 0.03	ND	ND	ND
37	Pr	(N-ethyl propyl)	1.83 ± 0.04	ND	ND	ND
38	Pr	(N-ethyl isobutyl)	1.67 ± 0.06	ND	ND	8.7
39	Pr	(phenyl ketone)	>50	ND	ND	ND

[a]ND, not determined

containing analogues (IC$_{50}$ = 2.92−3.90 μM vs IC$_{50}$ = 1.03−1.97 μM, respectively). This reduction in potency relative to the alkyl chain-containing analogues could be due to the branching of the fragment attached at the nitrogen, although branching appeared to be tolerated for analogues **25** and **26**. In addition, the combination of the branching along with the carbonyl of the amide resulted in an apparently less favorable orientation of the side chain and reduced potency. The final side chains tested for these early SARs studied included shorter-chain aryl groups (Table 2, **33** and **34**). For analogue **33**, the 2,3-dimethylphenyl group was attached directly to the core and resulted in an improved activity relative to **7** (IC$_{50}$ =

1.85 μM vs 4.38 μM, respectively). However, when the 4-fluorobenzyl group was present, it failed to show significant improvement over **7** (IC$_{50}$ = 3.54 μM vs 4.38 μM, respectively). This indicates that, unless directly connected to the core, phenyl groups are not well tolerated when a linker is present.

Once an initial SAR was analyzed for the 2,4-dihydro-3H-1,2,4-triazole-3-thione and the side chain, we chose to revisit the triazole and determined whether alkylation of N-2 could be tolerated. Four analogues (**35−38**) included a tertiary amine with various small alkyl groups (Table 3). All four N-substituted triazole analogues showed good activity, particularly the three analogues where R^2 was the longer propyl group (IC$_{50}$ = 1.63−1.83 μM). The ketone-containing analogue **39** lacking a basic nitrogen was inactive (IC$_{50}$ > 50 μM).

We then explored the fused phenyl ring of the core to determine whether substitution would be tolerated in this region. First, we began with halogenation at the 7-position (Table 4, **40−42**). As the size of the halogen increased, the affinity decreased (F, IC$_{50}$ = 12.9 μM; Br, IC$_{50}$ = 14.7 μM; I, IC$_{50}$ = 30.7 μM). The larger, hydrophobic 7-methyl group (**43**) showed a potency similar to that of the 7-F analogue. However, these analogues were still less potent overall than the unsubstituted **7**. We then wanted to determine if larger substituents would be tolerated if a heteroatom was introduced to make additional interactions. The 7-acetamide **44**, 7-dimethylamine **45**, and 7-(1-morpholino) **46** were prepared (Table 4). All three of these analogues with H-bonding capabilities were approximately twofold more potent than **7** (IC$_{50}$ = 1.54−2.77 μM vs IC$_{50}$ = 4.38 μM, respectively). Next, we explored the substitution pattern around the ring. To do so, the mono-fluoro analogues were prepared including 7-F (**40**), 8-F (**41**), and 9-F (**42**). They were shown to increase in potency as the fluorine moved around the ring from the 7- to 8- to 9-position (IC$_{50}$ = 12.9, 8.29, and 2.58 μM, respectively). Finally, we explored the replacement of the phenyl ring with

Table 4. Inhibitory Activity of Triazoloquinazolinones Modified in Zones 1 and 2 at the Plk1 PBD (IC$_{50}$ Values Are n = 3 Unless Noted in Parentheses) and Microsomal Half-Life, PAMPA Assays, and Aqueous Solubility[a]

cmpd	R^1=	IC$_{50}$ (μM, ELISA)	$t_{1/2}$ (min, RLM)	PAMPA (1 × 10^{-6} cm/s)	solub. (μg/mL)
7	H	4.38 ± 0.41 (6)	ND	ND	ND
40	7-F	12.92 ± 1.85	>30	77.0	ND
41	7-Br	14.74 ± 0.81	>30	162	<1
42	7-I	30.71 ± 1.31	>30	1025	<1
43	7-Me	11.29 ± 0.92	>30	ND	<1
44	7-NHAc	2.19 ± 0.10	>30	253	2.2
45	7-N(CH$_3$)$_2$	2.77 ± 0.33	13.3	356	<1
46	7-(1-morpholino)	1.54 ± 0.21	>30	1.2	3.4
47	8-F	8.29 ± 0.59	22.7	91.0	<1
48	9-F	2.58 ± 0.12	>30	141	3.4
49	H (6-aza)	6.16 ± 0.44	>30	16.8	26.9
50	H (8-aza)	27.78 ± 4.07	15.8	202	17.3
51	H (9-aza)	7.55 ± 0.44	>30	51.8	4.9

[a]ND, not determined.

Table 5. Inhibitory Activity of Triazoloquinazolinones Modified in Combined Zones 1, 2, 3, and 4 at the Plk1 PBD (IC$_{50}$ Values Are n = 3 Unless Noted in Parentheses) and Microsomal Half-Life, PAMPA Assays, and Aqueous Solubility[a]
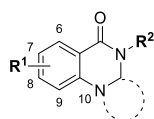
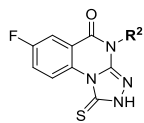| Cmpd	R^1 =	R^2 =	Triazole	IC$_{50}$ (μM, ELISA)	t$_{1/2}$ (min, RLM)	PAMPA (1e-6 cm/s)	Solub. (μg/ml)
52	7-F	(benzyl)	(triazole-thiol)	6.42 ± 0.44	>30	841	8.3
53	7-F	(phenylpropyl)	(triazole-thiol)	6.63 ± 0.39	8.8	1269	<1
54	7-Cl	(propyl)	(triazole-thiol)	1.77 ± 0.15 (6)	ND	ND	ND
55	7-Cl	(CF$_3$ propyl)	(triazole-thiol)	2.14 ± 0.12	>30	257	5.1
56	7-Cl	(isopropoxy propyl)	(triazole-thiol)	1.62 ± 0.17	ND	ND	8.6
57	7-Cl	(N-isopropyl amide)	(triazole-thiol)	1.49 ± 0.09	ND	ND	8.1
58	7-CH$_3$	(N-isopropyl amide)	(triazole-thiol)	2.01 ± 0.21	ND	ND	ND
59	8- (N-isopropyl amide)	(propyl)	(triazole-thiol)	3.01 ± 0.10	ND	ND	ND
60	8- (N-cyclopentyl amide)	(3-methylbutyl)	(triazole-thiol)	11.11 ± 0.90	ND	ND	ND
61	8- (N-cyclopentyl amide)	CH$_3$	(triazole-thiol)	2.75 ± 0.17	ND	ND	ND
62	7-F	(phenylpropyl)	(N-methyl thiourea)	>50	2.2	161	4.5

[a]ND, not determined.

pyridine. The 6-aza (49), 8-aza (50), and 9-aza (51) analogues were prepared; however, these heteroaryl derivatives were found to be less potent than 7 (>2−6-fold).

The next stage of our SAR exploration involved combining features from each of the regions explored so far (Table 5). First, we incorporated substitutions on the phenyl ring and modified the side chain. On the 7-fluoro core, we shortened (52) and extended (53), the alkyl phenyl side chain. Both the longer propyl and shorter methyl homologues showed similar activity that was slightly less potent than that of the parent 7 with the ethyl linker (propyl, IC$_{50}$ = 6.63 μM; methyl, IC$_{50}$ = 6.42 μM; ethyl, IC$_{50}$ = 4.38 μM). We then revisited the alkyl chains with the 7-chloro core (Table 5, 54−57). Compound 54 with the propyl side chain showed a small decrease in potency from the unsubstituted 21 (IC$_{50}$ = 1.77 μM and IC$_{50}$ = 1.03 μM, respectively). For compound 55 with the 3,3,3-trifluoropropane side chain, the 7-chloro core resulted in a nearly twofold loss of potency compared to its unsubstituted counterpart, 27 (IC$_{50}$ = 2.14 μM and IC$_{50}$ = 1.25 μM,

respectively). The ether-containing analogue 56 was equipotent to its most similar 29. The two amide-containing side chain analogues 57 and 58 with the 7-chloro and 7-methyl cores, respectively, were about twofold more potent than the unsubstituted 31 (IC$_{50}$ = 1.49 μM, IC$_{50}$ = 2.01 μM, and IC$_{50}$ = 3.90 μM, respectively).

After the promising results shown in Table 4 for the 7-acetamide 44, three additional amides were prepared this time in the 8-position to determine the tolerability of a larger group in the 8-position. The 8-isopropyl amide with the propyl chain (59, IC$_{50}$ = 3.01 μM) was shown to be less potent than the unsubstituted 21 (IC$_{50}$ = 1.03 μM) but more potent than either the 8-fluoro (47, IC$_{50}$ = 8.29 μM) or the 8-aza (50, IC$_{50}$ = 27.8 μM). Compounds 60 and 61 have an 8-cyclopentyl amide substitution with alkyl side chains. However, when comparing 60 and 25, both of which have a 3-methylbutane side chain, the substitution in the 8-position was not beneficial as 60 was found to be sixfold less potent than 25. We had already discovered that modifying the thiourea portion of the

Table 6. Inhibitory Activity at the Plk1 PBD of Triazoloquinazolinones Modified in Zones 3 and 4 with a Preferred 7-Fluoro Substitution, Except for 69 with 9-Fluoro (IC$_{50}$ Values Are n = 3 Unless Noted in Parentheses) and Microsomal Half-Life, PAMPA Assays, and Aqueous Solubility

63 – 68, 70 – 93

Cmpd	R^2 =	IC$_{50}$ (µM, ELISA)	t$_{1/2}$ (min, RLM)	PAMPA (1e-6 cm/s)	Solub. (µg/ml)
63	Et	1.98 ± 0.07	>30	39.5	>39
64	Pr	1.16 ± 0.06 (12)	>30	195	>28
65	CF$_3$	0.75 ± 0.06 (5)	>30	117	17.3
66	OH	1.44 ± 0.10 (9)	>30	222	>43
67	NH$_2$	4.33 ± 0.18	>30	8.2	>41
68	NH$_2$	2.26 ± 0.07 (4)	>30 [c] / >30 [d]	<1 [c] / 16.8 [d]	>43 [c] / 27 [d]
69	NH$_2$ (9-F)	5.07 ± 0.16	>30	4.2	15.9
70	N(CH$_3$)$_2$	2.45 ± 0.25	>30	177	>45
71[a]	N(CH$_3$)$_2$	6.12 ± 0.17	>30	186	>47
72	NHC(O)CH$_3$	2.48 ± 0.20	>30	12.9	>47
73	NHC(O)CH$_3$	2.48 ± 0.08 (6)	>30	18.0	>50
74	NHC(O)Ph	1.60 ± 0.19 (4)	>30	267	21.9
75	NHSO$_2$CH$_3$	2.77 ± 0.31	>30	8.9	>53
76	NHSO$_2$CH$_3$	1.87 ± 0.06	>30	10.8	34
77	P(O)(OH)$_2$	21.70 ± 1.73	ND	9.3	>51
78	P(O)(OEt)$_2$	13.89 ± 0.59	>30	16.7	>59
79	cyclopropyl	0.77 ± 0.08 (8)	>30	46.0	16.2

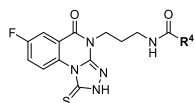| Cmpd	R^2 =	IC$_{50}$ (µM, ELISA)	t$_{1/2}$ (min, RLM)	PAMPA (1e-6 cm/s)	Solub. (µg/ml)
80[b]	cyclopropyl	1.19 ± 0.05 (4)	>30	188	13.2
81	2-Cl-phenyl	14.37 ± 0.33	22.8	56.3	3.0
82	4-Cl-phenyl	5.71 ± 0.44	>30	<1	1.2
83	2-pyridyl	0.87 ± 0.07 (4)	>30	355	13.0
84	3-pyridyl	1.07 ± 0.13 (9)	>30	<1	25.1
85	4-pyridyl	0.89 ± 0.05 (4)	>30	32.7	10.9
86	NBoc-azetidine	5.67 ± 0.30	ND	229	15
87[a]	pyrrolidine	5.67 ± 0.42	>30	53.8	17.8
88	piperidine	1.51 ± 0.19 (4)	>30	358	2.4
89	4,4-difluoropiperidine	1.37 ± 0.08 (5)	>30	234	20.2
90	morpholine	1.63 ± 0.22 (5)	>30	67.0	>52
91	N-methylpiperazine	6.72 ± 0.17	>30	12.7	>54
92	NBoc-piperazine	1.84 ± 0.01	26.3	33.1	20.5
93	4,4-difluorocyclohexyl	2.83 ± 0.36	>30	201	<1

[a]Racemic. [b]Relative stereochemistry, trans. [c]TFA salt. [d]Free base. ND, not determined.

2,4-dihydro-3H-1,2,4-triazole-3-thione was not tolerated; however, we wanted to determine whether the triazole ring itself was required. To test this, we prepared the thiourea, 62, which maintained the thiocarbonyl as well as the NH of the 2,4-dihydro-3H-1,2,4-triazole-3-thione. Similar to most other modifications of the 2,4-dihydro-3H-1,2,4-triazole-3-thione, the thiourea of 62 was not tolerated and also resulted in a highly metabolically labile analogue (IC$_{50}$ > 50 µM, $t_{1/2}$ RLM = 2.2 min).

Based on the observed results thus far, it became clear that we could make the most significant positive modifications to the chemotype in the side chain. Therefore, we made a large number of analogues on the 7-fluoro core and varied the side chain to expand our SAR. We began with linear alkyl groups, which we had previously found to lead to low micromolar affinity. The shorter ethyl group (63) led to a small reduction in affinity compared to the unsubstituted 20 (IC$_{50}$ = 1.98 µM and IC$_{50}$ = 1.49 µM, respectively), while the propyl analogue (64) was found to be equipotent to the unsubstituted

equivalent (21). Previously the 3,3,3-trifluoropropyl group led to one of the most potent analogues. Therefore, we combined this group with the 7-F and found that the 7-F analogue 65 was at least as potent as the corresponding unsubstituted 27. We then chose to introduce additional H-bonding groups that might increase interactions within the binding site. To this end, hydroxy (66), amino (67−76), and phosphorus (77, 78) derivatives were synthesized and tested. The 1-propanol group, which is similar in length to the butyl analogue (23), maintained good potency at 1.44 µM. For the primary amines, both ethyl and propyl chains were tested, and the three-carbon linker was found to be twice as potent as the two-carbon linker. Also, as the 9-fluoro substitution was previously shown to be the most potent of the mono-fluoro substituents, the 9-F analogue with a propylamine chain (69) was prepared but found to be less potent than the 7-F derivative 68. This is unexpected as it is opposite to the trend seen for the phenethyl series. When relatively simple dimethyl amine analogues 70 and 71 were prepared, 70 was shown to be

Table 7. Inhibitory Activity of Amide-Containing Triazoloquinazolinones Modified in Zones 3 and 4 with Preferred 7-Fluorine at the Plk1 PBD (IC$_{50}$ Values Are $n = 3$ Unless Noted in Parentheses) and Microsomal Half-Life, PAMPA Assays, and Aqueous Solubility
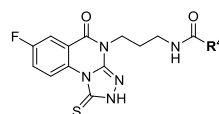

Cmpd	R^2 =	IC$_{50}$ (μM, ELISA)	t$_{1/2}$ (min, RLM)	PAMPA (1e-6 cm/s)	Solub. (μg/ml)
94	(structure)	5.36 ± 0.40	ND	ND	ND
95	(structure)	3.22 ± 0.12	ND	ND	ND
96	(structure)	13.13 ± 0.36	>30	13.4	>99
97	(structure)	9.40 ± 0.35	>30	18.1	>107
98	(structure)	5.02 ± 0.29	>30	8.8	36.1
99	(structure)	2.88 ± 0.21	27.9	44.3	>88
100	(structure)	3.04 ± 0.16	>30	3.5	31.8
101	(structure)	3.23 ± 0.15	>30	405	>75
102	(structure)	8.19 ± 0.26	25.1	1214	20.4
103	(structure)	3.31 ± 0.14	3.8	744	41.6
104	(structure)	2.33 ± 0.13	>30	8.7	37.5
105	(structure)	12.65 ± 0.44	>30	20.1	32.0
106	(structure)	5.05 ± 0.22	>30	<1	>58
107	(structure)	2.18 ± 0.19	>30	3.0	42.4
108	(structure)	1.47 ± 0.18	>30	155	>58
109[a]	(structure)	>50	>30	66.9	1.1
110[b]	(structure)	2.38 ± 0.74	24.8	330	>77
111[b]	(structure)	3.97 ± 0.26	>30	1.6	38.8
112[b]	(structure)	27.66 ± 1.25	>30	ND	>60
113[b]	(structure)	30.20 ± 1.09	>30	ND	29.6
114	(structure)	44.01 ± 2.32	>30	ND	>60
115	(structure)	1.79 ± 0.11 (4)	ND	8.0	<1
116	(structure)	3.96 ± 0.37	>30	4.4	37.5
117	(structure)	4.66 ± 0.23	>30	<1	>64
118	(structure)	3.77 ± 0.19	>30	<1	>62
119	(structure)	1.48 ± 0.12 (4)	>30	46.8	13.7
120	(structure)	1.23 ± 0.09 (6)	18.7	248	31.7
121	(structure)	1.78 ± 0.13 (4)	6.3	27.6	37.6

Table 7. continued

[a]Relative stereochemistry, trans. [b]Racemic. ND, not determined.

Table 8. Inhibitory Activity of 4 Phenylacetic Acid Amide Triazoloquinazolinone Derivatives Modified in Zones 3 and 4 with Preferred 7-Fluorine at the Plk1 PBD (IC$_{50}$ Values Are $n = 3$ Unless Noted in Parentheses) and Microsomal Half-Life, PAMPA Assays, and Aqueous Solubility[a]

Cmpd	R^4 =	IC$_{50}$ (μM, ELISA)	t$_{1/2}$ (min, RLM)	PAMPA (1e-6 cm/s)	Solub. (μg/ml)
122	(structure, 3-F)	1.42 ± 0.18 (4)	26.5	364	>63
123	(structure, 4-F)	1.35 ± 0.17 (4)	26.3	8.5	8.5
124	(structure, 3-Cl)	1.15 ± 0.03 (4)	8.4	861	>66
125	(structure, 4-Br)	1.59 ± 0.12	20.6	767	<1
126	(structure, 4-Me)	1.18 ± 0.01	23.9	621	12.9
127	(structure, 4-OH)	1.16 ± 0.06	>30	3.7	31.0
128	(structure, 2-OMe)	1.15 ± 0.11 (5)	16.1	379	>65
129	(structure, 3-OMe)	0.96 ± 0.08 (4)	20.1	300	>65
130	(structure, 4-OMe)	1.06 ± 0.08 (5)	>30	233	3.2
131	(structure, 2-CF$_3$)	1.40 ± 0.07 (4)	3.7	825	40.3
132	(structure, 3-CF$_3$)	2.23 ± 0.33	17.3	1088	26.8
133	(structure, 2-CN)	1.24 ± 0.14 (4)	>30	156	20.9
134	(structure, 4-CN)	0.99 ± 0.14	>30	172	2.0
135	(structure, 4-NHBoc)	2.72 ± 0.63	>30	910	17.4
136	(structure, pyridin-2-yl)	5.34 ± 0.64	>30	68.0	41.4
137	(structure, pyridin-3-yl)	2.50 ± 0.28	>30	21.0	31.8
138	(structure, pyridin-4-yl)	3.01 ± 0.26	>30	<1	9.6

[a]ND, not determined.

slightly more potent than the equivalent primary amine **67**, while the branched 1-dimethylaminoprop-2-yl analogue (**71**) was slightly less potent. In the case of amide (**72−74**) and sulfonamide (**75** and **76**) derivatives, regardless of the linker length or the type of derivative, all analogues essentially performed similarly (IC$_{50}$ = ∼2.0 μM) with the benzamide **74** showing the most potent affinity of the five. The phosphorus-containing analogues, phosphonic acid **77** and phosphonate diester **78**, both showed significantly weaker affinity, with the phosphonic acid being essentially inactive. In addition to these

Table 9. Inhibitory Activity of Prodrug Triazoloquinazolinones and Their Corresponding Parent Drugs at the Plk1 PBD (IC$_{50}$ Values Are n = 3 Unless Noted in Parentheses)
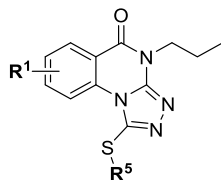
cmpd	R^1=	R^5=	IC$_{50}$ (μM)
21	H	H[a]	1.03 ± 0.08 (9)
64	7-F	H[a]	1.16 ± 0.06 (12)
139	9-F	H[a]	2.06 ± 0.07 (4)
140	9-Cl	H[a]	2.49 ± 0.02
141	9-OMe	H[a]	2.43 ± 0.01
142	H	Ac	1.33 ± 0.08
143	H	Me	>50
144	7-F	Me	>50
145	9-F	Me	>50
146	9-Cl	Me	>50
147	9-OMe	Me	>50

[a]Shown as the enol tautomers, while this series is shown in the thiocarbonyl form elsewhere. ND, not determined.

heteroatom-containing analogues, several cyclopropane derivatives were prepared (**79** and **80**). Both **79** and **80**, which differ in the location of the cyclopropane in the chain, showed good potency of approximately 1.0 μM, indicating that although heteroatoms are well tolerated in the side chain, they are not required.

Next, we explored the phenethyl side chain (Table 6), first, by substituting the phenyl moiety with chloro groups (**81** and **82**). While the 4-chloro analogue maintained an affinity similar to that of **7** (**82**, IC$_{50}$ = 5.71 μM) and was over twofold more potent than **40**, the 2-chloro analogue was less potent than either **7** or **40** (**81**, IC$_{50}$ = 14.4 μM). This indicates that ortho substitution is not well tolerated, which supports the earlier conclusion that for the phenethyl derivatives the binding pocket around the phenyl group is restrictive, and substituents that make it bulkier led to negative interactions. Concluding that the space around the phenyl ring was sterically limited, we next chose to replace it with a pyridine to determine if H-bonding opportunities are available without increasing the steric bulk. All three pyridine analogues were synthesized, and all were found to be ≥12-fold more potent than the phenyl-containing **40**. The trend for the potency (4-pyridine ≈ 2-pyridine > 3-pyridine, best to worst) differs from that observed for the chloro substitution, which clearly indicated that the 4-

position is the most favorable for affinity. However, in the case of the pyridines, all three N positions were well tolerated. This could be due to the chloro group extending into the pocket, creating steric clashes, which were absent for the pyridines. Nonaromatic heterocycles were also tested to determine whether they would be more beneficial than the aromatic heterocycles. Azetidine **86**, pyrrolidine **87**, and piperidine **88** were all prepared to determine if there was a size preference for the ring, and a clear preference was observed for the six-membered piperidine (IC$_{50}$ = 5.67 μM, IC$_{50}$ = 5.67 μM, and IC$_{50}$ = 1.51 μM, respectively). With this information, we then explored whether additional heteroatoms in the 4-position would be tolerated. The 4,4-difluoropiperidine **89** and the N-morpholino **90** were equipotent to **88**, that is, all near IC$_{50}$ = 1.5 μM. However, when a second nitrogen was incorporated into the ring in analogues **91** and **92**, a discrepancy was observed in the SAR. Based on the chloro-substituted phenyl rings, both **91** and **92** were expected to be potent; however, only **92** showed an affinity similar to the other six-membered ring heterocycles. Because the methyl group is much smaller than the Boc group, the difference in affinity is not due to the size of the group. The more likely source of the difference is the basicity of the nitrogen in the 4-position, given that the Boc group significantly decreases the pK_a of the nitrogen relative to **91**. Finally, we also prepared the carbocyclic version of **89** to determine if the heteroatom in the ring was required at all. Compound **93** maintained the difluoro substitution, which could potentially generate H-bonding interactions. However, there were no other heteroatoms with which to form H-bonds or salt bridges, and as a result, the potency showed a small (approximately twofold) decrease, indicating that though the nitrogen is not required, it is beneficial.

Expanding upon the SAR established above, we continued to explore the side chain region by focusing on the propyl amide motif, given that this serves as a good handle for further modification to probe the binding pocket (Table 7) and that compound **74** with the benzamide was one of the more potent analogues thus far. First, we prepared analogues **94** and **95** with polyethylene glycol (PEG) linkers to extend the primary amine further into the pocket. While both compounds maintained single-digit micromolar affinity, the Boc-protected **95** was more potent than the free amine **94** (IC$_{50}$ = 3.22 μM and IC$_{50}$ = 5.36 μM, respectively), which suggests a preference for a less basic group and that the size of the terminal group is unimportant. To determine whether this was related to a preference for uncharged species or unprotonated species, the L-Glu derivatives were prepared (**96** and **97**). While the fully deprotected **96** was shown to be >twofold less potent than **94**, the t-butyl ester-protected **97** was <twofold less potent. This does support the conclusion that, in the region where these highly extended compounds reside, an uncharged species is
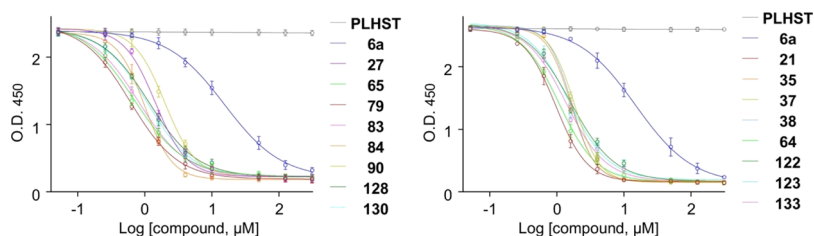
Figure 2. Representative inhibition curves in the ELISA assay. A previously characterized phosphopeptide, PLHSpT **6a** (K_d of ~450 nM[27]), is included for comparison. The curve numbers correspond to compound numbers.
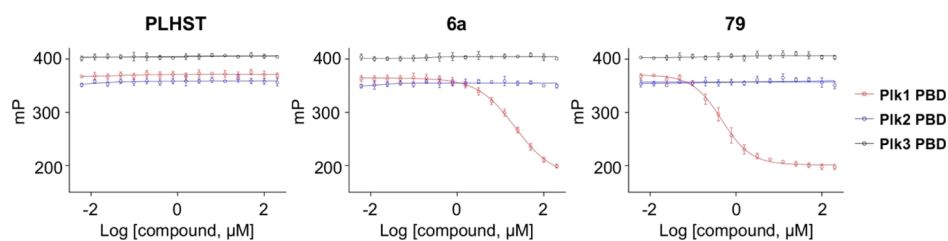
Figure 3. Comparative FP-based assays showing that compound **79** potently inhibits the PBD of Plk1 but not Plk2 and Plk3 with an IC_{50} of 0.47 μM. Under the same experimental conditions, PLHSpT **6a** shows an IC_{50} of 22 μM, whereas its control nonphosphorylated form, PLHST **6b**, exhibits no detectable activity. Bars, mean $\pm$ standard deviation (s.d.).

preferred. We then chose to look at increasingly shorter chains to determine their tolerability in the binding pocket. The PEG_3 chain analogues (**98** and **99**) showed the same preference for the less basic, Boc-protected amine that was observed for the PEG_4 chain. However, when the chain was shorted further to the hexylamine, the primary amine and the corresponding Boc-protected amine were equipotent, indicating that the preference for uncharged species begins at greater distances from the main binding site for the chemotype. The Boc-D-Glu-OtBu (**102**) and Boc-L-Glu-OtBu (**103**) derivatives showed a preference for the natural amino acid derivative (>twofold more potent than **102**). Compound **103** was then deprotected, giving either the Boc deprotected L-Glu-O^{t}Bu **104** or the fully deprotected **105**. These analogues show that a negatively charged species is not well tolerated (**105** IC_{50} = 12.7 μM). The succinic acid derivative, **106**, still exhibited an intolerance for negatively charged species as well, indicating that the two charges likely present in **105** are not beneficial either. Moreover, the sulfonamide **107**, which is thought to maintain many of the same potential interactions without being negatively charged, was shown to be the most potent of these extended linear analogues with an IC_{50} = 2.18 μM.

After determining that the shorter chain molecules were preferred, we focused on smaller, cyclic analogues. Beginning with carbocyclic groups, the cyclopentyl amide **108** showed a relatively good potency (IC_{50} = 1.47 μM), but the sterically much bulkier *trans*-4-(*t*-butyl)cyclohexane amide **109** was inactive. Consistent with the finding that a highly bulky group was not tolerated, the 4-Boc-aminocyclohexane amide **110** was found to be moderately potent (IC_{50} = 2.38 μM). However, once again, when the Boc group was removed (**111**), the potency decreased slightly, suggesting the preference for uncharged species. A series of piperidine analogues (**112**–**114**) were prepared to further assess this. In agreement with the data above, all three piperidines, despite the location of the nitrogen in the ring, were significantly less active and nearly inactive (IC_{50} = 27.7–44.0 μM). Notably, 4-tetrahydropyran **115** was found to show good potency (IC_{50} = 1.79 μM), indicating that the protonation of the amine, which likely occurs at physiological pH, is the feature not tolerated rather than the presence of a heteroatom in the ring. Three additional analogues with a methylene linker between the amide carbonyl and the heterocycle were also prepared (**116**–**118**). All three analogues contained a basic nitrogen in the ring and all three showed moderate affinity, reinforcing the preference for neutral compounds in this side chain region. Finally, a series of aromatic analogues of differing lengths were prepared (**119**–**121**). All three analogues, despite the presence of heteroatoms or the overall length of the side chain, showed good affinity (IC_{50} = 1.23–1.78 μM).

Given that compound **120** showed the best affinity of these amide analogues, we decided to explore substitution around the phenylacetamide portion (Table 8). Beginning with simple halogen-containing analogues, compounds **122**–**125** were prepared. Though not all positions were tested for each halogen, a general trend did emerge. When comparing **122** and **123**, the position of the halogen was found not to have a significant impact on the potency (meta IC_{50} = 1.42 μM and para IC_{50} = 1.35 μM). Also, the halogen size had no effect on the affinity of the analogue as seen by all four analogues showing essentially the same potency, indicating that the size of the group does not have a large impact on binding. Next, we looked at substituents that would modulate the electronic character of the ring (**126**–**134**). For electron-donating groups, methyl (**126**), hydroxy (**127**), and methoxy (**128**–**130**) analogues were prepared. Overall, electron-donating groups were well tolerated, maintaining a similar affinity relative to **120**. Similar to the trend observed for the halogens, the location of these groups did not have a large impact on the potency of the compound either. The electron-withdrawing groups, trifluoromethyl (**131**–**132**) and cyano (**133**–**134**), showed similar results. They were also well tolerated in all positions, but the 3-CF_3 derivative (**132**) was the least potent but only slightly (<twofold) less potent than all other substituted phenylacetamide analogues. The Boc-protected 4-amino analogue was also twofold less potent than the parent **120**. Finally, in the case of a series of pyridine analogues prepared (**136**–**138**), all three analogues were less potent than the phenyl analogue **120** and 2-pyridine was the weakest at IC_{50} = 5.34 μM.

Plk1 PBD Specificity. To determine whether the above modified compounds show Plk1 PBD-binding specificity, we carried out FP-based inhibition assays using fluorescein isothiocyanate (FITC)-labeled peptides that specifically bind to each of the PBDs from Plk1, Plk2, and Plk3.[26] Under these experimental settings, PLHSpT **6**, but not its respective nonphosphorylated peptide, specifically inhibited Plk1 PBD with an IC_{50} of 22 μM (Figure 3). Under the same conditions, representative, potent compound **79** inhibited Plk1 PBD with an IC_{50} of 0.47 μM and failed to exhibit any detectable level of inhibition against the PBDs from Plk2 and Plk3. An approximately 40-fold increased potency for compound **79** over PLHSpT **6** is largely in good agreement with the data obtained with ELISA-based assays described above. Similar to this observation, expanded FP assays showed that several additional compounds tested showed approximately the same degree of Plk1 PBD specificity (Figure S3, Supporting Information). The all-or-none selectivity for Plk1 PBD is significant, given that the well-characterized Plk1 KD inhibitor BI2536 exhibits Plk1 selectivity of only around fourfold.[49] These data collectively suggest that, while the exact binding
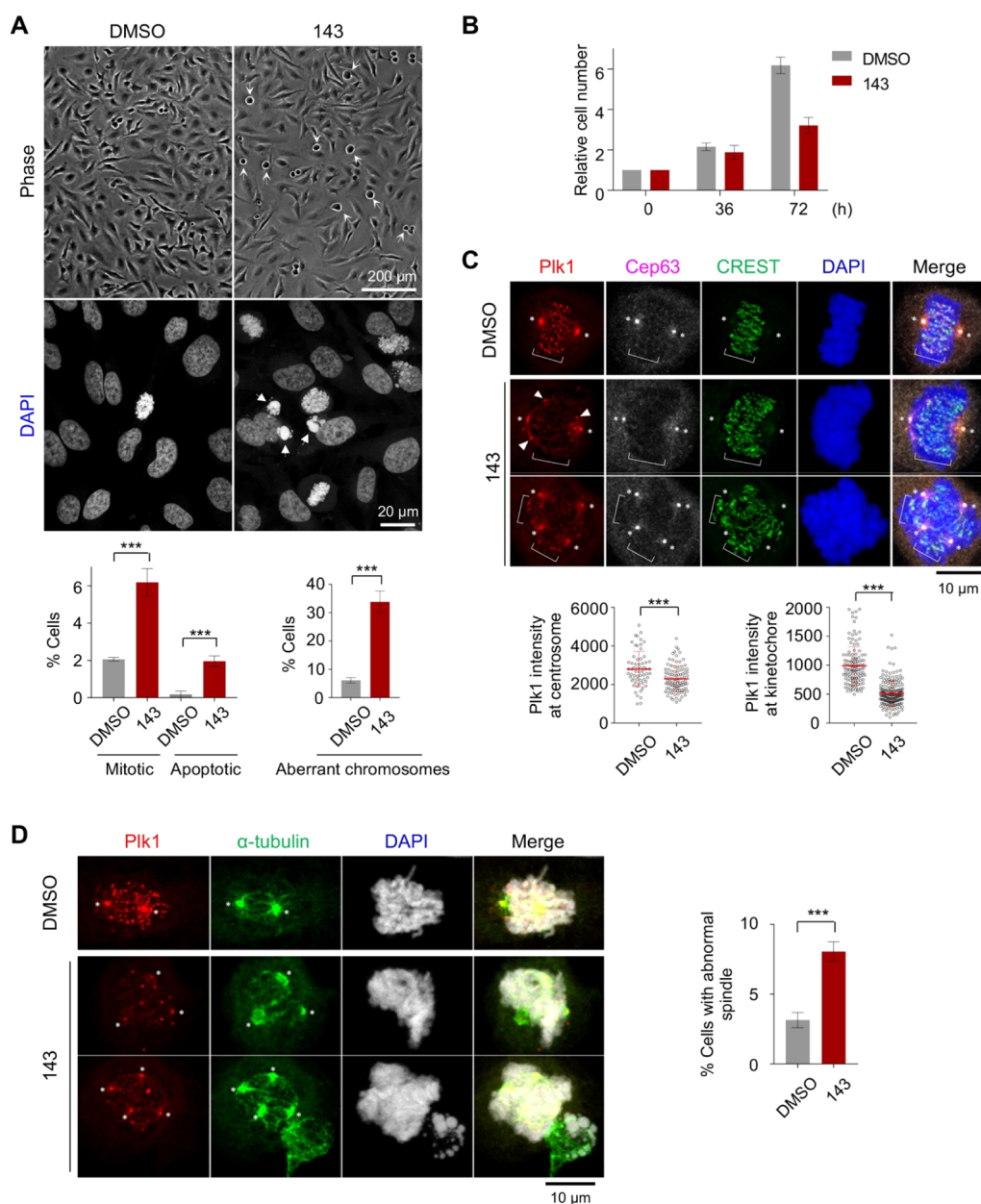
Figure 4. Antiproliferative effect of **143** in HeLa cells. (A) Asynchronously growing HeLa cells were treated with 100 μM of compound **143** for 12 h, subjected to phase-contrast micrography (cells with a rounded morphology are marked with barbed arrows) and stained with DAPI. Cells exhibiting mitotic and apoptotic DNA morphologies (arrows in DAPI) (bottom left) and abnormally misaligned or lagging chromosomes (bottom right) were quantified from three independent experiments ($n > 515$ cells/sample/experiment). Bars, mean $\pm$ s.d., ***, $P < 0.001$ (unpaired two-tailed t-test). (B) Cell numbers at the indicated time points were quantified from three independent experiments (n = an average of 2547 cells/experiment for DMSO and 1673 cells/experiment for **143**). Bars, mean $\pm$ s.d. (C,D) Cells in (A) were immunostained with the indicated antibodies to reveal delocalized Plk1 signals from centrosomes (marker: Cep63) and kinetochores (marker: CREST) (C) and abnormal spindle morphologies (marker: α-tubulin) (D). Asterisks, centrosome-localized Plk1; brackets, kinetochore-associated Plk1. Arrowheads in (C), delocalized Plk1 aggregates in the cytosol. Quantification was carried out from three independent experiments [$\geq$20 (DMSO) or 32 (**143**) centrosomes/sample/experiment and $\geq$42 (DMSO) or 64 (**143**) kinetochores ($\sim$4 kinetochores per cell)/sample/experiment for (C); $\geq$106 (DMSO) or 102 (**143**) cells/sample/experiment for (D)]. Bars, means $\pm$ s.d., ***, $P < 0.001$ (unpaired two-tailed t-test).

mode of these compounds is yet to be determined, they may at least partially block the canonical S-pT/pS-P/X-binding region of Plk1 PBD described previously.[11,27]

Prodrug and Cellular Efficacy. Having confirmed that many of the compounds generated through SAR exhibited submicromolar IC_{50} values with a superb specificity for Plk1 PBD, we then examined their activities in whole-cell studies. However, likely due to limited intracellular bioavailability arising from low membrane permeability, we failed to observe

mitotic arrest, the phenotype that can be expected by interfering with the function of Plk1 PBD.[25,26] We reasoned that alkylating the thiocarbonyl could improve the cellular uptake of the compounds. In addition, it would directly block oxidative metabolism of the thiourea as well as prevent potential oxidation of the phenyl ring via steric factors, consequently reducing clearance and allowing for greater exposure of the drug at a site of action. Therefore, we selected a small alkyl group or small alkyl ester as a starting point as
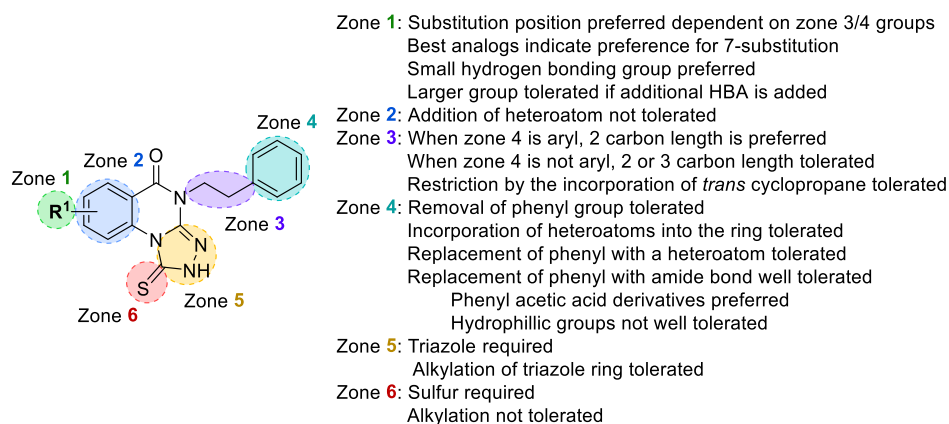
they should be relatively readily cleaved within the body and could allow us to gauge the level of stability necessary for the prodrug to be beneficial. Accordingly, compounds **142−147** were prepared as thioester or S-methyl prodrugs and examined in the ELISA assay (Table 9) and in metabolic studies (see below). The corresponding parent drugs were unsubstituted **21** for **142** and **143**, 7-F analogue **64** for **144**, 9-F analogue **139** for **145**, 9-Cl analogue **140** for **146**, and 9-OMe analogue **141** for **147**. Not surprisingly, these prodrugs, except the S-acyl group-containing **142**, were inactive with IC_{50} > 50 μM (Table 9). Compound **142** appeared to rapidly become active by releasing the active parental compound **21** because of the reactivity of the S-acyl group toward electron-rich moieties (see below and Figure S4, Supporting Information).

In HeLa cells, compounds **143**, **144**, and **145** were compared for their ability to induce mitotic arrest and an antiproliferation effect, which are characteristics of Plk1 PBD inhibition.[25,27] Results showed that treatment of cells with 100 μM of either compound **143** or **145** effectively induced rounded cells with apoptotic or aberrant chromosome morphologies (Figure 4A,B), indicative of a sustained mitotic arrest. Consequently, both compounds inhibited cell proliferation, decreasing the total cell population nearly by 50% 3 days after treatment. Considering that blocking the function of Plk1 PBD-dependent PPI is destined to be less drastic than that of Plk1 KD[20,21] and that several purported inhibitors reported to date show a low level (IC_{50} of 50−1000 μM) of cellular activities,[28−35] the activity of **143** or **145** is a modest but clear improvement. Treatment with compound **144** also induced mitotic arrest but at a somewhat reduced level, whereas control DMSO failed to induce any detectable phenotype under the same conditions. As expected, if the arrest was caused by interfering with the PBD-dependent Plk1 function, compound **143** significantly inhibited Plk1 localization to centrosomes (approximately 20% inhibition) and kinetochores (approximately 50% inhibition), frequently yielding cytosolic aggregates of delocalized Plk1 as observed previously[44] (Figure 4C). A weaker blocking of Plk1 localization to the centrosome is likely due to the presence of PBD-independent Plk1-binding targets at this structure. Consistent with impaired Plk1 localization, spindle bipolarity was significantly compromised in **143**-treated cells (Figure 4D). Under the same conditions, the parent drugs, that is, **21**, **64**, and **139**, lacked a detectable level of cellular response. These findings suggest that, although the prodrugs themselves failed to inhibit Plk1 PBD (Table 9) because of the absence of a free 1-thioxy group, the S-methyl thioethers had a more pronounced response, presumably by promoting cell membrane permeability while regenerating the parent drug intracellularly.

Analysis of Pharmacokinetics. To obtain metabolic stability information, the half-life of the selected compounds was determined in rat liver microsomes (RLMs) containing the NADPH-generating system, which permits CYP-mediated metabolic reactions.[46] Parallel artificial membrane permeability assay (PAMPA) permeability was measured using a high-throughput protocol, as reported.[47] Aqueous solubility was determined by a published procedure.[48] Most compounds tested showed a half-life of >30 min, indicating that they could be relatively stable in the CYP system. To further elucidate their metabolic pathway and to prioritize compounds for in vivo testing, several were selected as representative compounds from each group with different substitution patterns to characterize the metabolites that may be generated during

incubation with CYP using mouse liver microsomes (MLMs). By inspection of the triazoloquinazolinone structures, they display a potential for CYP-mediated hydroxylation on the main quinazolinone aromatic ring as a preferred target. To our surprise, not only were the expected hydroxylated metabolites undetectable, but no other metabolites were produced in the CYP incubation system for most of the tested compounds. To further understand the metabolic pathways, similar MLM incubations of the selected compound set were conducted with uridine 5′-diphospho-glucuronic acid (UDPGA) as a cofactor to allow glucuronidation reactions. As shown in Figure S1, a new peak with 176 Da increase of the corresponding parent, which is a characteristic gain for a glucuronide, appeared for each of the tested compounds. It should be noted that for some of these compounds, two peaks with the MWs corresponding to one and two glucuronide additions were apparent, but for the remainder, only one peak appeared with the fragmentation pattern and MW representing a glucuronide. To characterize the glucuronidated site, the MS/MS analysis was performed to generate a fragment pattern for each of the glucuronides. Upon entering the source, however, the parent ions of the glucuronides fragmented into the daughter ions, which are generated from the parent ion, rather than giving a characteristic fragment to indicate the glucuronidation site (Figure S2). Examining the structure of these compounds, the thiocarbonyl S and the triazole ring secondary amine are two sites that could potentially be attacked by uridine 5′-diphospho-glucuronosyltransferase (UGT). Thus, it is highly likely that one of the two glucuronides was generated from the S-glucuronidation and the other from N-glucuronidation. Remarkably, a considerable amount of parent ion remained for the earlier-eluted glucuronides, while the parent ions of the later-eluted glucuronides almost completely fragmented. This is indicative of an N-glucuronide for the former and an S-glucuronide for the latter, given that the C−N bond linking the parent and the glucuronic acid in the former is much more stable than the corresponding C−S bond in the latter. In addition, only the S-glucuronide could be generated for the amide- or pyridine-containing compounds as the parent ions of their glucuronides were also completely fragmented. Thus, it is reasonable to hypothesize that the hydrogen-bonding capabilities of the amide- or pyridine-containing compounds may account for their altered glucuronidation profile where they interacted with UGT in a pattern from which N-glucuronidation was not favored. These results demonstrated that noncirculating metabolites other than the circulating products are expected to appear in vivo when these triazoloquinazolinones are administrated to mice.

Stability of Selected Compounds and Their Prodrugs in Mice. Despite the in vitro data suggesting that most analogues were stable in RLMs up to 30 min (Tables 1−8), further assays were required to fully understand the stability in both in vitro and in vivo systems. Therefore, for selected compounds, additional microsome-based stability assays were performed to determine the major metabolites and class of enzymes responsible for the modifications. Several molecules including early hit-compounds (**23**, **46**) and compounds with submicromolar affinity (i.e., **65**, **79**, **83**, and **134**) were subjected to in vitro MLM assay. LC−MS/MS analysis revealed that glucuronidation is the major metabolite. Note that, in vitro glucuronidation resulted in two products, S- and N-glucuronides in varying amounts, which resulted in two glucuronidation peaks in LC-traces for some compounds

Zone **1**: Substitution position preferred dependent on zone 3/4 groups
Best analogs indicate preference for 7-substitution
Small hydrogen bonding group preferred
Larger group tolerated if additional HBA is added
Zone **2**: Addition of heteroatom not tolerated
Zone **3**: When zone 4 is aryl, 2 carbon length is preferred
When zone 4 is not aryl, 2 or 3 carbon length tolerated
Restriction by the incorporation of *trans* cyclopropane tolerated
Zone **4**: Removal of phenyl group tolerated
Incorporation of heteroatoms into the ring tolerated
Replacement of phenyl with a heteroatom tolerated
Replacement of phenyl with amide bond well tolerated
Phenyl acetic acid derivatives preferred
Hydrophillic groups not well tolerated
Zone **5**: Triazole required
Alkylation of triazole ring tolerated
Zone **6**: Sulfur required
Alkylation not tolerated

Figure 5. Summary of SAR studies on a 1-thioxo-2,4-dihydro-[1,2,4]triazolo[4,3-*a*]quinazolin-5(1*H*)-one scaffold for inhibition of Plk1 PBD.

(Figures S1 and S2, Supporting Information). To mitigate this issue, the *S*-acetyl thioester prodrug **142** was made and found to be active but also toxic and rapidly cleaved by liver microsomes. The instability and toxicity of this compound was expected, given the reactivity of the *S*-acyl group toward electron-rich moieties. To confirm this hypothesis, a model reaction on **142** with ammonium acetate at pH 7.4 was performed, which resulted in efficient acyl transfer releasing the parent drug **21** (Figure S4, Supporting Information). Therefore, to enhance the stability of prodrugs, our attention was turned to *S*-methyl thioether analogues (**143**−**145**), which exhibited anti-Plk1 PBD activity in HeLa cells (Figure 4). Our analyses with two of these analogues (**143** and **144**) revealed that although they were stable in human, mouse, and rat cytosol with $t_{1/2}$ values up to 120 min, unlike their parental **21** and **64**, they exhibited much shorter $t_{1/2}$ values when reacted with the microsomes from the corresponding three species (Table S2). These findings suggest that the membrane-bound enzymes in the microsomes are mainly responsible for the metabolism of these prodrugs rather than the soluble cytosolic enzymes.

The CYP-mediated reactions are the most likely metabolic pathways these prodrugs would undergo given the nature of the NADPH-containing microsome-based incubation system. To further identify the metabolites generated in the microsome reaction, **143** was incubated with MLMs for 1 h, and the resulting mixture processed and subjected to LC−MS/MS analysis (Figure S5A, Supporting Information). As expected, CYP catalysis generated a hydroxylated product, which was further shown by MS/MS fragmentography to be hydroxylated on the main aromatic ring of the quinazolinone (Figure S5B, Supporting Information). In addition, an *S*-demethylated metabolite, also mediated by CYP, was found, for which the structure was determined by comparing the fragmentation pattern with that of the parent drug, **21**. As demonstrated by the in vitro results of MLM-treated nonprodrugs (Figures S1 and S2, Supporting Information), a glucuronidation could also be expected for the demethylated product. To detect a subsequent glucuronidation, **143** was incubated in a mixed system containing both NADPH and UDPGA, the cofactor for UDP-glucuronosyltransferase. After MS analysis, glucuronidation of the demethylated metabolite was evidenced by the appearance of a new peak having a 176 Da increase compared to the demethylated product (Figure S5A, top, Supporting Information).

Next, to achieve a comprehensive understanding of the metabolic stability of the prodrugs, we performed the in vivo experiment by injecting **143** in mice [20 mg/kg, intraperitoneal (IP) injection] under a protocol approved by the National Cancer Institute Animal Care and Use Committee. During the whole period of the experiment, no signs of toxicity was observed under these conditions. Serum was collected at 15, 30, 60, 120, and 240 min after injection. In close agreement with in vitro results in Figure S5, both the hydroxylated and demethylated products were detected in the serum ≥15 min postinjection (Figure S6, Supporting Information). While both metabolites decreased time-dependently, the demethylated product markedly increased in the serum ≥240 min postinjection (Figure S6, Supporting Information). A trace amount of the subsequent glucuronide of the demethylated metabolite was also seen in the serum as it could be promptly excreted from the liver to the bile, once generated, and can then undergo enterohepatic circulation through which the demethylated product is reabsorbed to the circulation. This could also serve as an explanation for the increased demethylated metabolite at the last time point. Compound **145** yielded similar metabolites with a somewhat improved $t_{1/2}$ value of 51.26 min (Table S3 and Figure S6, Supporting Information). These results illustrated that the prodrugs could release the corresponding parent drugs enzymatically, and the released parent drugs levels could be longer lasting because of an enterohepatic circulation. As the glucuronides are considered pharmacologically inactive, whether the hydroxylated metabolite could also interact with Plk1 to exert an inhibitory effect requires further investigation.

■ DISCUSSION

Antimitotic drugs, such as taxanes and vinca alkaloids, that are directed at inhibiting the dynamic function of microtubules (MTs), have proven to be effective in the treatment of cancer.[50] However, given the significant side effects of these conventional anti-MT agents, targeting mitosis-specific and cancer cell-addicted Plk1 has been considered an attractive strategy for generating a cancer cell-selective therapeutic agent.[3,20] Indeed, a large body of studies show that several Plk1 ATP-competitive inhibitors developed over the years exhibit significant activities against hematological malignancies[51−55] and several advanced solid tumors,[56−60] although their less-than-acceptable specificities and dose-limiting toxicities have hampered further clinical applications.

PBD has emerged as an alternative target for developing a new class of Plk1 inhibitors that can potentially overcome the hurdles facing ATP-competitive inhibitors. As PBD inhibitors interfere only with the PBD-dependent Plk1 functions, they are anticipated to incur mitotic stress sufficient to induce cell death in cancer cells but not in normal cells.[7] Completely disrupting Plk1 function would be detrimental even for normal cell proliferation. While a high level of target specificity is one of the inherent advantages that PPI inhibitors can achieve, the primary challenge has been developing small (<500 Da) molecules that still exhibit high affinity to the shallow and often nondescript interface of a target PPI.[61,62] Because of this difficulty, most of the purported PBD inhibitors reported to date exhibit a poor (IC_{50} of 50−1000 μM) anti-Plk1 activity in cell-based assays.[28−35] In addition, many of these compounds appear to exhibit cross-reacting alkylating activities[42,43] that could impose dose-limiting nonspecific cytotoxicity.

SAR Summary. The overall conclusions of our SAR studies are summarized in Figure 5. Our SAR studies identified six analogues which showed submicromolar affinity (**65**, **79**, **83**, **85**, **129**, and **134**), which is at least an order of magnitude more potent than the previously characterized Plk1 PBD-specific phosphopeptide, PLHSpT **6a** (K_d ∼450 nM). All the six compounds appeared to share two distinct features: (1) 7-F substitution in zone 1 and (2) an unsubstituted triazole (zone 5). These are distinct because in our initial analogues exploring zone 1, there was no obvious preference for the 7-substitution. Then, when we combined early zone 1 and zone 3/4 modification unsubstituted triazoles, the fluorine was not obviously the preferred group. The inactivity of thiourea-containing analogue **62** and preference for an intact triazole indicated that a π-stacking interaction rather than H-bonding of the free NH is the important interaction. In addition, five of the six analogues contained zone 4 groups that could form H-bonding interactions, either CF_3 (**65**), pyridine (**83**, **85**), or amides and an additional H-bond acceptor (HBA) (**129**, **134**). All five of these analogues contain HBA in positions that would all be in the same general region of the binding pocket. Compounds **129** and **134** have methoxy and cyano groups that might interact in adjacent regions of the pocket. The only submicromolar analogue that did not have additional H-bonding capabilities, that is, the methyl cyclopropane zone 3/4 analogue (**79**), might still establish stabilizing hydrophobic interactions.

Absorption distribution metabolism excretion (ADME) data were compared for the six most potent analogues (**65**, **79**, **83**, **85**, **129**, and **134**). Five of the six analogues had half-lives of >30 min in RLMs, and the sixth (**129**) had a fairly good (20.1 min) half-life (Tables 6 and 8). Notably, the PAMPA permeability at pH 7.4 was favorable for six compounds (**65**, **83**, **129**, and **134**) with moderate to good permeability (100 to >200 × 10^{-6} cm/s). However, only three analogues (**65**, **79**, and **129**) showed moderate to good solubility (10 to >60 μg/mL). Only compound **129** displayed both good permeability and solubility (P = 311 × 10^{-6} cm/s, S >65 μg/mL) (Table 8). Despite its relatively shorter half-life than other analogues, **129** may represent the best balance of PLK1 PBD affinity and ADME properties.

Some regions of the scaffold tolerated broad structural modification, while a few did not. In zone 1, interdependence on the groups in zones 3 and 4 defined the preferred substitution. This suggests that the core (zones 1, 2, and the quinazolinone) binding region might have been unfilled to

allow for flexibility in the binding pose of molecules with various zone 1 substitutions. However, for the best analogues, the 7-position with a small H-bonding group is preferred; larger groups are tolerated but only with additional HBA groups. Zone 2 did not tolerate modification; the phenyl ring was optimal. Zones 3 and 4 proved to be the most generally amenable to modification. When zone 4 was cyclic, the linker length was best unmodified; however, when zone 4 was acyclic (an alkyl chain, a heteroatom, or another functional group), the entire chain could contain two or three carbons. This linker could also be sterically restricted with a *trans* cyclopropane, but this conclusion may not apply to all analogues differing in zone 4. In zone 4, removal and replacement of the phenyl group with unsubstituted heteroaryl groups was well tolerated, as was replacement with amides, especially for phenylacetyl derivatives. However, beyond the amide, hydrophilic or negatively charged moieties were disfavored. This extreme difference in affinity between phosphorus derivatives **77** and **78** and the other heteroatom-containing analogues could be due to the much larger size of these groups or the highly negatively charged phosphonic acid **77** at physiological pH.

All three nitrogen atoms of the triazole played an important role in binding, and alkylation of the triazole NH but not the S was accommodated. The tertiary amine substituents in **35−38** likely reside in a region that was formerly not accessed by the scaffold and therefore can establish new interactions, allowing for the improvement in affinity. The reason for the inactivity of N-substituted triazole analogue **39** is undetermined tertiary amines can form salt bridges, which ketones cannot form, and this could account for the potency differences. The difference could be due to either electrostatic or steric interactions (the acetophenone group in **39** is both larger and less flexible than the tertiary amines **35−38**). Given that both tertiary amines and carbonyl oxygens can form H-bonding interactions, H-bonding may not account for the significant affinity difference.

The results provided here suggest that a 1-thioxo-2,4-dihydro-[1,2,4]triazolo[4,3-a]quinazolin-5(1H)-one scaffold offers promising structural and chemical features that can be exploited for anti-Plk1 PBD drug discovery. While the triazole moiety is one of the main components of antifungal drugs widely used for the prophylaxis and treatment of invasive fungal disease,[63,64] the quinazoline moiety is frequently found in several FDA-approved EGFR or HER2 inhibitors, such as gefitinib, erlotinib, lapatinib, afatinib, and vandetanib.[65] As these approved drugs have been extensively tested in humans for safety, available information from their prior clinical trials could facilitate further development of the above-described triazoloquinazolinone-based Plk1 PBD inhibitors. Drugs containing the conjoined triazoloquinazolinone backbone have not yet been reported in the drug depository (Drugbank; https://www.drugbank.ca/), indicating the uniqueness of the current triazoloquinazolinone leads. Remarkably, unlike previously reported several Plk1 PBD inhibitors with unacceptable alkylating activities,[42,43] the identified triazoloquinazolinone chemotype does not bear any hallmark structural features that could be a reactive liability. In addition, triazoloquinazolinone-based compounds generally remain inert in multiple inhibitor screenings[66−69] and specific modifications, such as a methyl group at N-3 of the quinazolinone lead, are required to induce biological efficacy.[70,71] These chemical properties suggest a lower likelihood of off-target effects when dosed. In fact, potential off-target interactions for the initial hit, 7, and three other high-affinity compounds (**21**, **68**, and **127**)

were not detected at 10 μM, when they were screened at 45 receptors and channels by the National Institute of Mental Health Psychoactive Drug Screening Program (https://pdsp.unc.edu/pdspweb/) using standard radioligand binding and functional assay methods.[72] The only hits among these compounds at 10 μM causing >50% binding inhibition were for the primary amine **68** at M_3 (100%), M_4 (73%), and M_5 (84%) muscarinic acetylcholine receptors. Thus, there was no pharmacological promiscuity observed for these four representative analogues.

The low MWs (300−450 Da) of several promising triazoloquinazolinone-based inhibitors described here offer considerable room for optimizations. Our extensive SAR analyses revealed distinct patterns (Figure 3) that could serve as a roadmap for further development. Notably, the ELISA-based IC_{50} values for several compounds (**65**, **79**, **83**, **85**, **129**, and **134**) reached <1 μM. As the previously characterized Plk1 PBD-binding PLHSpT **6a** (K_d of ~450 nM)[27] shows an IC_{50} of 14.74 μM under the same conditions, these compounds are expected to have at least an order-of-magnitude-higher affinity than **6a**. Moreover, the superb Plk1 PBD specificity of triazoloquinazolinone-derived inhibitors (Figure 4) along with the cellular efficacy of multiple prodrugs (**143**, **144**, and **145**) (Figure 5) provides clear proof-of-principle evidence that intervene in the Plk1 PBD-mediated PPI is feasible with small drug-like compounds amenable for potential clinical applications.

CONCLUSIONS AND PERSPECTIVE

In this study, we used a 1-thioxo-2,4-dihydro-[1,2,4]triazolo-[4,3-a]quinazolin-5(1H)-one scaffold to synthesize S-methyl prodrugs that effectively inhibit PBD-dependent Plk1 function in cultured cells. Further development of these inhibitors may yield a new class of Plk1 PBD inhibitors that could offer superb specificity with versatile applicability either as a single agent or as a part of combination chemotherapy. Combination therapeutic regimens with various chemotherapeutic agents, including cisplatin, cytarabine, methotrexate, and doxorubicin, have already shown an improved antitumor activity with Plk1's ATP-competitive inhibitors in numerous studies.[52,54,73−77] In addition, as the most advanced ATP-competitive inhibitor **1**[14] was doomed in phase III clinical trials because of its less-than-acceptable tolerability, combination treatment strategy with this inhibitor may allow to achieve the synergistic anti-Plk1 efficacy without causing the dose-limiting toxicity that narrowed their therapeutic windows. As a promising avenue for anti-Plk1 drug discovery, PBD inhibitors may prove to be effective in overcoming the hurdles facing current anti-Plk1 therapy and improving clinical outcomes.

EXPERIMENTAL SECTION

Chemical Synthesis. *General Methods for Chemistry.* All reactions were carried out under the nitrogen atmosphere using anhydrous solvents. All moisture-sensitive reactions were also performed with oven-dried glassware. Chemical reagents and anhydrous solvents were obtained from commercial sources and used as-is. Room temperature or rt refers to 25 ± 2 °C. Preparative purification was performed on a Waters semipreparative HPLC equipment. The column used was a Phenomenex Luna C18 (5 μm, 30 × 75 mm) at a flow rate of 45 mL/min. The mobile phase consisted of acetonitrile and water (each containing 0.1% trifluoroacetic acid). A gradient of 10−50% acetonitrile over 8 min was used during the purification. Fraction collection was triggered by UV detection (220 nm). Initial analytical analysis during compound synthesis was

performed on an Agilent 1200 LC−MS system (Agilent Technologies) using a 3-min gradient of 4−100% acetonitrile (containing 0.025% trifluoroacetic acid) in water (containing 0.05% trifluoroacetic acid) was used with an 8-min run time at a flow rate of 1 mL/min. The purity of compounds newly synthesized was demonstrated on an Agilent 1200 LC−MS system (Agilent Technologies) using a 7-min linear gradient of 4−100% acetonitrile (containing 0.025% trifluoroacetic acid) in water (containing 0.05% trifluoroacetic acid) followed by a 4.5 min run time at a flow rate of 1 mL/min and a Phenomenex Luna C18 column (3 μm, 3 × 75 mm) at 50 °C. The purity of the purchased compounds was determined using an Agilent ZORBAX Eclipse XDB C18 column (5 mm, 4.6 × 250 mm) with a linear gradient of 5−95% acetonitrile in water (containing 10 mM triethylammonium acetate) for 20 min at a flow rate of 1.0 mL/min. ^{1}H and ^{13}C NMR spectra were recorded on either a Varian 400 (100) MHz spectrometer or a Bruker 400 MHz spectrometer. Chemical shifts are given in ppm (δ), calibrated to the residual solvent signals and frequency calibrated internally by solvent for ^{19}F NMR (BrukerTopspin/MestReNova 10.0.2 or 14.1.0). High-resolution mass spectrometry was recorded on either an Agilent 6210 time-of-flight LCMS system or a Waters Micromass spectrometer equipped with a standard electrospray ionization (ESI) and modular Lock-SprayTM interface. The purity of all the tested compounds (including both newly synthesized and purchased, active compounds) were demonstrated to be >95% at 254 nm, except commercially procured compound **58**, which was 93.5% pure. The synthesis of compounds **7**−**64** is described in the Supporting information.

Intermediate A
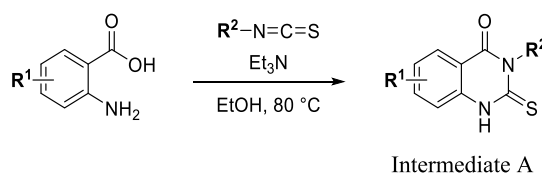
General Procedure A. To a solution of appropriate 2-aminobenzoic acid (1 equiv) and isothiocyanate (1.2 equiv) in EtOH (0.37 M) was added triethylamine (1.2 equiv). The reaction was stirred at 80 °C for 1−2 h. The reaction was cooled to room temperature (RT) and diluted with water. The solid (intermediate A) was filtered and dried under vacuum and used without further purification.
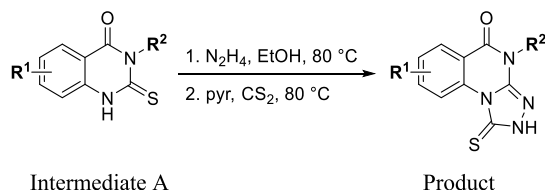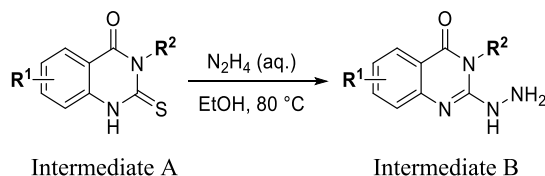

Intermediate A
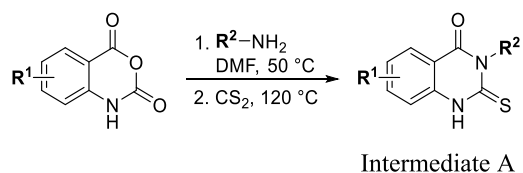
General Procedure B. A solution of isatoic anhydride (1 equiv) in acetonitrile (0.67 M) was added to the amine (1.5 equiv). In the case of amine salts, triethylamine (1.5 equiv) was added to a solution of the amine in acetonitrile (0.67 M), the salt was removed by filtration, and the free based amine solution was added to the reaction. The reaction was heated at 50 °C for 30 min. The reaction was cooled to RT and carbon disulfide (7 equiv) was added cold. The reaction was then heated to 120 °C for 45 min. The reaction was diluted with Et$_2$O, filtered, rinsed with Et$_2$O, and dried. The solid (intermediate A) was dried under vacuum and used without further purification.

isatoic anhydride | Intermediate A
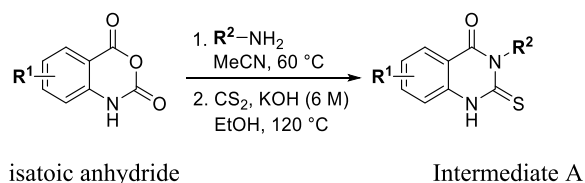
General Procedure C. A solution of isatoic anhydride (1 equiv) in acetonitrile (0.67 M) was added to the amine (1.5 equiv). In the case of amine salts, triethylamine (1.5 equiv) was added to a solution of

the amine in acetonitrile (0.67 M), the salt was removed by filtration, and the free based amine solution was added to the reaction. The reaction was heated at 60 °C for 3 h. The reaction was concentrated and the residue dissolved in EtOH (0.67 M), and aq KOH (1.2 equiv) was added, followed by carbon disulfide (2 equiv). The reaction was then heated to 120 °C for 2 h. The reaction was cooled to RT, diluted with water, and washed with Et$_2$O. The solid (intermediate A) was dried under vacuum and used without further purification.

Intermediate A   Product

General Procedure D. To a solution of intermediate A (1 equiv) in EtOH (0.25−0.35 M) was added hydrazine (7 equiv). The reaction was then heated to 80 °C for 4 h. The reaction was then cooled to RT and pyridine (10 equiv) and carbon disulfide (10 equiv) were added. The reaction was heated to 80 °C for 1−2 h. The reaction was poured into cold water, and the product was filtered and washed with water or purified by HPLC.

Intermediate A   Intermediate B

General Procedure E. To a solution of intermediate A (1 equiv) in EtOH (0.35 M) was added water (2.8 equiv), followed by hydrazine (7 equiv). The reaction was then heated to 80 °C for 4 h. The reaction was then poured into cold water and concentrated. The crude material was purified on a Teledyne ISCO CombiFlash System by (dry-loading) (EtOAc/DCM: 0−3%) to give intermediate B.

General Procedure F. To a solution of carboxylic acid (1.5 equiv) in DMF (0.2 M) was added COMU (1.5 equiv) and the reaction stirred at RT for 30−45 min. Then, the amine (1 equiv) was added, followed by DIPEA (2.2 equiv). The reaction was then stirred for 18 h or 2.5 d at RT. The crude material was purified by HPLC.

4-Phenethyl-1-thioxo-2,4-dihydro-[1,2,4]triazolo[4,3-a]-quinazolin-5(1H)-one (7). Note: Compound **7** previously appeared as an in silico hit in a screen for A$_{2A}$ adenosine receptor antagonists {compound **30** in PMC2865168}.

2-Amino-N-phenethylbenzamide: A mixture of methylanthranilate (0.856 mL, 6.615 mmol) and phenethylamine (1.3 mL, 10 mmol) was stirred in a round-bottom flask at 190 °C for 5 h. The product was purified by silica-gel column chromatography (0.44 g, 28%). ^{1}H NMR (400 MHz, CDCl$_3$): δ 7.40−7.14 (m, 6H), 6.68 (dd, J = 1.1, 8.1 Hz, 1H), 6.62 (ddd, J = 1.2, 7.2, 8.1 Hz, 1H), 6.06 (s, 1H), 5.49 (s, 2H), 3.70 (td, J = 5.8, 6.8 Hz, 2H), 2.94 (t, J = 6.9 Hz, 2H); HRMS: (M + H) for C$_{15}$H$_{16}$N$_2$O calcd 241.1341; found, 241.1339.

3-Phenethyl-2-thioxo-2,3-dihydroquinazolin-4(1H)-one: Route 1: To a solution of 2-amino-N-phenethylbenzamide (100 mg, 0.416 mmol) in anhydrous DMF (2 mL) at RT was added carbon disulfide (72 µL, 1.248 mmol) and DBU (136 µL, 0.916 mmol) sequentially.

After stirring the reaction mixture for 18 h at RT, cold 1 N aq HCl was added with vigorous stirring. The precipitate was collected by filtration, washed with cold water and hexanes, and dried to afford a practically pure product (60 mg, 50%). Route 2: To a solution of 2-amino-N-phenethylbenzamide (100 mg, 0.416 mmol) in anhydrous ethanol (2 mL) at RT were added carbon disulfide (75 µL, 1.25 mmol) and solid KOH (32 mg, 0.916 mmol) sequentially. The reaction mixture was stirred at 80 °C for 18 h at RT, cooled, and was added to a cold 1 N aq HCl with vigorous stirring. The precipitate was collected by filtration, washed with cold water and hexanes, and dried to afford a practically pure product (70 mg, 60%). Note: The product was purified further by silica-gel column chromatography using 0−2% methanol in dichloromethane as an eluent. The purified product gave better yield in the next step. ^{1}H NMR (400 MHz, CDCl$_3$): δ 9.99 (s, 1H), 8.25−8.10 (m, 1H), 7.69 (ddd, J = 1.5, 7.3, 8.4 Hz, 1H), 7.45−7.40 (m, 2H), 7.38−7.32 (m, 2H), 7.27 (d, J = 5.6 Hz, 1H), 7.13 (dt, J = 0.7, 8.2 Hz, 1H), 4.82−4.65 (m, 2H), 3.19−3.07 (m, 2H); HRMS: (M + H) for C$_{16}$H$_{14}$N$_2$OS calcd, 283.0905; found, 283.0909.

2-Hydrazineyl-3-phenethylquinazolin-4(3H)-one: To a suspension of 3-phenethyl-2-thioxo-2,3-dihydroquinazolin-4(1H)-one (200 mg, 0.708 mmol) in anhydrous ethanol (5 mL) was added anhydrous hydrazine (0.33 mL, 10.62 mmol) and heated at 85 °C for 18 h. The volatiles were evaporated under high vacuum, followed by coevaporation with toluene (2×), giving 2-hydrazineyl-3-phenethyl-quinazolin-4(3H)-one as a yellow solid and was used as such without further purification (200 mg, quantitative). ^{1}H NMR (400 MHz, CDCl$_3$): δ 8.16 (dd, J = 1.6, 7.9 Hz, 1H), 7.68−7.56 (m, 1H), 7.45−7.14 (m, 5H), 4.21 (dd, J = 6.7, 8.4 Hz, 2H), 3.09−2.99 (m, 1H); HRMS: (M + H) for C$_{16}$H$_{16}$N$_4$O calcd, 281.1402; found, 281.1405.

4-Phenethyl-1-thioxo-2,4-dihydro-[1,2,4]triazolo[4,3-a]quinazolin-5(1H)-one: 2-Hydrazineyl-3-phenethylquinazolin-4(3H)-one (200 mg, 0.713 mmol) was dissolved in anhydrous ethanol (10 mL). To the solution was added carbon disulfide (0.13 mL, 2.14 mmol), followed by solid KOH (120 mg, 2.14 mmol), and it was heated to 80 °C for 18 h. The reaction mixture was cooled and poured into cold 1 N aq HCl solution. The precipitates were collected and purified by silica-gel column chromatography using 0−2% methanol in dichloromethane as an eluent to afford a pure product as a white solid (200 mg, 87%). ^{1}H NMR (400 MHz, DMSO-d$_6$): δ 14.10 (s, 1H), 10.23 (dd, J = 1.1, 8.6 Hz, 1H), 8.22 (dd, J = 1.6, 7.9 Hz, 1H), 7.91 (ddd, J = 1.7, 7.3, 8.7 Hz, 1H), 7.62 (td, J = 1.1, 7.6 Hz, 1H), 7.38−7.15 (m, 4H), 4.32−4.15 (m, 2H), 3.08−2.92 (m, 2H); HRMS: (M + H) for C$_{17}$H$_{14}$N$_4$OS, calcd 323.0967; found, 323.0966.

4-Phenethyl-2,4-dihydro-[1,2,4]triazolo[4,3-a]quinazoline-1,5-dione (15). 2-Hydrazineyl-3-phenethylquinazolin-4(3H)-one (35 mg, 0.117 mmol) was suspended in anhydrous toluene (2 mL), and to it was added carbonyl diimidazole (22 mg, 0.135 mmol) and heated to reflux (115 °C) for 1.5 h. The volatiles evaporated under vacuum and the residue was treated with 1 N aq HCl and 5% isopropanol-dichloromethane. The organic layer was separated, dried over Na$_2$SO$_4$, evaporated, and the residue was purified by silica-gel column chromatography to afford **7b** as a white solid (13 mg, 34%). ^{1}H NMR (400 MHz, DMSO-d$_6$): δ 12.07 (s, 1H), 8.65 (dd, J = 4.6, 9.1 Hz, 1H), 7.84 (dd, J = 3.0, 8.6 Hz, 1H), 7.75 (td, J = 3.1, 8.7 Hz, 1H), 7.35−7.19 (m, 4H), 4.26−4.05 (m, 2H), 3.08−2.92 (m, 2H); ^{19}F NMR (376 MHz, DMSO-d$_6$): δ −113.33 (td, J = 4.5, 8.1 Hz); HRMS: (M + H) for C$_{17}$H$_{13}$N$_4$O$_2$F calcd, 325.1101; found, 325.1107.

Amine component   Product
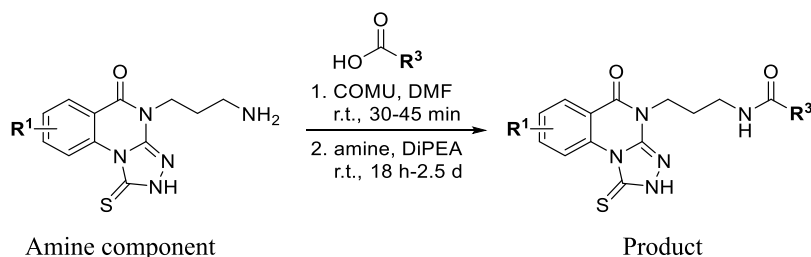
1-Amino-7-fluoro-4-phenethyl-[1,2,4]triazolo[4,3-a]quinazolin-5(4H)-one (16). 6-Fluoro-3-phenethyl-2-thioxo-2,3-dihydroquinazolin-4(1H)-one was synthesized according to General Procedure A. 6-Fluoro-2-hydrazineyl-3-phenethylquinazolin-4(3H)-one was synthesized according to General Procedure E. Then, to a solution of 6-fluoro-2-hydrazinyl-3-phenethylquinazolin-4(3H)-one (0.1 g, 0.335 mmol) and cyanogen bromide (0.036 g, 0.335 mmol) in ethanol (16.8 mL) was added sodium hydroxide (0.067 g, 1.675 mmol) and the reaction was stirred at RT for 3 h. The reaction was neutralized with sat. NaHCO$_3$ and the solid filtered. The solid was redissolved and purified by HPLC to give 1-amino-7-fluoro-4-phenethyl-[1,2,4]triazolo[4,3-a]quinazolin-5(4H)-one, 2 TFA: ^{1}H NMR (400 MHz, DMSO-d_6): δ 8.29 (dd, J = 9.2, 4.2 Hz, 1H), 7.92 (dd, J = 8.5, 3.1 Hz, 1H), 7.82 (td, J = 8.6, 3.1 Hz, 1H), 7.34−7.24 (m, 4H), 7.22 (d, J = 7.0 Hz, 1H), 6.90 (s, 2H), 4.29 (dd, J = 9.5, 6.5 Hz, 2H), 3.06−2.98 (m, 2H); ^{19}F NMR (376 MHz, DMSO-d_6): δ −114.22; HRMS (ES-API) m/z: calcd for C$_{17}$H$_{15}$FN$_5$O (M + H), 324.1255; found, 324.1264.

7-Fluoro-1-methyl-4-phenethyl-[1,2,4]triazolo[4,3-a]quinazolin-5(4H)-one (17). 6-Fluoro-3-phenethyl-2-thioxo-2,3-dihydroquinazolin-4(1H)-one was synthesized according to General Procedure A. 6-Fluoro-2-hydrazineyl-3-phenethylquinazolin-4(3H)-one was synthesized according to General Procedure E. Then, 6-fluoro-2-hydrazinyl-3-phenethylquinazolin-4(3H)-one (0.1 g, 0.335 mmol) was stirred in Ac$_2$O (16.8 mL) at 100 °C for 5 h. The reaction was concentrated, filtered, and washed with water. The solid was dried and crystallized from EtOH to give 7-fluoro-1-methyl-4-phenethyl-[1,2,4]triazolo[4,3-a]quinazolin-5(4H)-one (0.0453 g, 42%): ^{1}H NMR (400 MHz, DMSO-d_6): δ 8.11 (dd, J = 9.2, 4.2 Hz, 1H), 7.95 (dd, J = 8.5, 3.1 Hz, 1H), 7.80 (ddd, J = 9.2, 8.0, 3.1 Hz, 1H), 7.29 (td, J = 9.0, 8.4, 6.1 Hz, 4H), 7.21 (td, J = 6.5, 2.2 Hz, 1H), 4.42−4.33 (m, 2H), 3.08−2.99 (m, 2H), 2.84 (s, 3H); ^{19}F NMR (376 MHz, DMSO-d_6): δ −114.29 (td, J = 8.2, 4.0 Hz).

7-Fluoro-4-phenethyl-[1,2,4]triazolo[4,3-a]quinazolin-5(4H)-one (18). 6-Fluoro-3-phenethyl-2-thioxo-2,3-dihydroquinazolin-4(1H)-one was synthesized according to General Procedure A. 6-Fluoro-2-hydrazineyl-3-phenethylquinazolin-4(3H)-one was synthesized according to General Procedure E. Then, 6-fluoro-2-hydrazinyl-3-phenethylquinazolin-4(3H)-one (0.1 g, 0.335 mmol) was stirred in formic acid (16.8 mL) at 100 °C for 5 h. The reaction was concentrated, redissolved, and purified by HPLC to give 7-fluoro-4-phenethyl-[1,2,4]triazolo[4,3-a]quinazolin-5(4H)-one, TFA: ^{1}H NMR (400 MHz, DMSO-d_6): δ 9.50 (s, 1H), 8.27 (dd, J = 8.8, 4.3 Hz, 1H), 7.89 (ddd, J = 11.0, 7.1, 3.9 Hz, 2H), 7.34−7.25 (m, 4H), 7.25−7.17 (m, 1H), 4.37 (dd, J = 9.2, 6.8 Hz, 2H), 3.09−3.01 (m, 2H); ^{19}F NMR (376 MHz, DMSO-d_6): δ −113.78 (td, J = 8.3, 4.1 Hz); HRMS (ES-API) m/z: calcd for C$_{17}$H$_{14}$FN$_4$O (M + H), 309.1146; found, 309.1155.

1-(Methylthio)-4-phenethyl-[1,2,4]triazolo[4,3-a]quinazolin-5(4H)-one (19). 3-Phenethyl-2-thioxo-2,3-dihydroquinazolin-4(1H)-one was synthesized according to General Procedure A. Then, 4-phenethyl-1-thioxo-2,4-dihydro-[1,2,4]triazolo[4,3-a]quinazolin-5(1H)-one was synthesized according to General Procedure D. Then, 1-(methylthio)-4-phenethyl-[1,2,4]triazolo[4,3-a]quinazolin-5(4H)-one was synthesized as follows: to a solution of 4-phenethyl-1-thioxo-2,4-dihydro-[1,2,4]triazolo[4,3-a]quinazolin-5(1H)-one (0.092 g, 0.223 mmol) in DMF (1.113 mL) was added K$_2$CO$_3$ (0.037 g, 0.267 mmol) and MeI (0.017 mL, 0.267 mmol). The reaction was quenched with methanol and concentrated. The reaction was stirred for 3 h and quenched with methanol. The crude mixture was concentrated and purified by HPLC to give 1-(methylthio)-4-phenethyl-[1,2,4]triazolo[4,3-a]quinazolin-5(4H)-one, TFA.

4-Ethyl-1-thioxo-2,4-dihydro-[1,2,4]triazolo[4,3-a]quinazolin-5(1H)-one (20). 3-Ethyl-2-thioxo-2,3-dihydroquinazolin-4(1H)-one was synthesized according to General Procedure A. Then, 4-ethyl-1-thioxo-2,4-dihydro-[1,2,4]triazolo[4,3-a]quinazolin-5(1H)-one, TFA, was synthesized according to General Procedure D: ^{1}H NMR (400 MHz, DMSO-d_6): δ 10.20 (d, J = 8.5 Hz, 1H), 8.20 (d, J = 7.8 Hz, 1H), 7.87 (t, J = 8.0 Hz, 1H), 7.59 (t, J = 7.7 Hz, 1H), 4.05 (q, J = 7.1

Hz, 2H), 1.23 (t, J = 7.2 Hz, 3H); HRMS (ES-API) m/z: calcd for C$_{11}$H$_{10}$N$_4$NaOS (M + Na), 269.0468; found, 269.0476.

4-Propyl-1-thioxo-2,4-dihydro-[1,2,4]triazolo[4,3-a]quinazolin-5(1H)-one (21). 4-Propyl-1-thioxo-2,4-dihydro-[1,2,4]triazolo[4,3-a]quinazolin-5(1H)-one was purchased from Enamine (Monmouth Jct., NJ).

4-Allyl-1-thioxo-2,4-dihydro-[1,2,4]triazolo[4,3-a]quinazolin-5(1H)-one (22). 4-Allyl-1-thioxo-2,4-dihydro-[1,2,4]triazolo[4,3-a]quinazolin-5(1H)-one was purchased from Enamine (Monmouth Jct., NJ).

4-Butyl-1-thioxo-2,4-dihydro-[1,2,4]triazolo[4,3-a]quinazolin-5(1H)-one (23). 4-Butyl-1-thioxo-2,4-dihydro-[1,2,4]triazolo[4,3-a]quinazolin-5(1H)-one was purchased from Enamine (Monmouth Jct., NJ).

4-Pentyl-1-thioxo-2,4-dihydro-[1,2,4]triazolo[4,3-a]quinazolin-5(1H)-one (24). 4-Pentyl-1-thioxo-2,4-dihydro-[1,2,4]triazolo[4,3-a]quinazolin-5(1H)-one was purchased Enamine (Monmouth Jct., NJ).

4-Isopentyl-1-thioxo-2,4-dihydro-[1,2,4]triazolo[4,3-a]quinazolin-5(1H)-one (25). 4-Isopentyl-1-thioxo-2,4-dihydro-[1,2,4]triazolo[4,3-a]quinazolin-5(1H)-one was purchased from Enamine (Monmouth Jct., NJ).

4-Isopropyl-1-thioxo-2,4-dihydro-[1,2,4]triazolo[4,3-a]quinazolin-5(1H)-one (26). 4-Isopropyl-1-thioxo-2,4-dihydro-[1,2,4]triazolo[4,3-a]quinazolin-5(1H)-one was purchased from ChemDiv (San Diego, CA).

1-Thioxo-4-(3,3,3-trifluoropropyl)-2,4-dihydro-[1,2,4]triazolo-[4,3-a]quinazolin-5(1H)-one (27). 2-Thioxo-3-(3,3,3-trifluoropropyl)-2,3-dihydroquinazolin-4(1H)-one was synthesized according to General Procedure B. Then, 1-thioxo-4-(3,3,3-trifluoropropyl)-2,4-dihydro-[1,2,4]triazolo[4,3-a]quinazolin-5(1H)-one, TFA, was synthesized according to General Procedure D: ^{1}H NMR (400 MHz, DMSO-d_6): δ 10.19 (d, J = 8.5 Hz, 1H), 8.21 (d, J = 7.8 Hz, 1H), 7.90 (t, J = 8.1 Hz, 1H), 7.61 (t, J = 7.7 Hz, 1H), 4.25 (t, J = 7.3 Hz, 2H), 2.72 (dt, J = 11.5, 7.4 Hz, 2H); ^{19}F NMR (376 MHz, DMSO-d_6): δ −64.31 (t, J = 11.3 Hz).

4-(3-Methoxypropyl)-1-thioxo-2,4-dihydro-[1,2,4]triazolo[4,3-a]quinazolin-5(1H)-one (28). 4-(3-Methoxypropyl)-1-thioxo-2,4-dihydro-[1,2,4]triazolo[4,3-a]quinazolin-5(1H)-one was purchased from Enamine (Monmouth Jct., NJ).

4-(3-Ethoxypropyl)-1-thioxo-2,4-dihydro-[1,2,4]triazolo[4,3-a]quinazolin-5(1H)-one (29). 4-(3-Ethoxypropyl)-1-thioxo-2,4-dihydro-[1,2,4]triazolo[4,3-a]quinazolin-5(1H)-one was purchased from Enamine (Monmouth Jct., NJ).

N-(sec-Butyl)-3-(5-oxo-1-thioxo-1,2-dihydro-[1,2,4]triazolo[4,3-a]quinazolin-4(5H)-yl)propenamide (30). N-(sec-Butyl)-3-(5-oxo-1-thioxo-1,2-dihydro-[1,2,4]triazolo[4,3-a]quinazolin-4(5H)-yl)-propenamide was purchased from ChemDiv (San Diego, CA).

N-Isopropyl-3-(5-oxo-1-thioxo-1,2-dihydro-[1,2,4]triazolo[4,3-a]quinazolin-4(5H)-yl)propenamide (31). N-Isopropyl-3-(5-oxo-1-thioxo-1,2-dihydro-[1,2,4]triazolo[4,3-a]quinazolin-4(5H)-yl)-propenamide was purchased from ChemDiv (San Diego, CA).

N-Isobutyl-3-(5-oxo-1-thioxo-1,2-dihydro-[1,2,4]triazolo[4,3-a]quinazolin-4(5H)-yl)propenamide (32). N-Isobutyl-3-(5-oxo-1-thioxo-1,2-dihydro-[1,2,4]triazolo[4,3-a]quinazolin-4(5H)-yl)-propenamide was purchased from ChemDiv (San Diego, CA).

4-(2,3-Dimethylphenyl)-1-thioxo-2,4-dihydro-[1,2,4]triazolo[4,3-a]quinazolin-5(1H)-one (33). 4-(2,3-Dimethylphenyl)-1-thioxo-2,4-dihydro-[1,2,4]triazolo[4,3-a]quinazolin-5(1H)-one was purchased from Enamine (Monmouth Jct., NJ).

4-(4-Fluorobenzyl)-1-thioxo-2,4-dihydro-[1,2,4]triazolo[4,3-a]quinazolin-5(1H)-one (34). 4-(4-Fluorobenzyl)-1-thioxo-2,4-dihydro-[1,2,4]triazolo[4,3-a]quinazolin-5(1H)-one was purchased from ChemDiv (San Diego, CA).

2-((Cyclopropyl(methyl)amino)methyl)-4-propyl-1-thioxo-2,4-dihydro-[1,2,4]triazolo[4,3-a]quinazolin-5(1H)-one (35). 2-((Cyclopropyl(methyl)amino)methyl)-4-propyl-1-thioxo-2,4-dihydro-[1,2,4]triazolo[4,3-a]quinazolin-5(1H)-one was purchased from Enamine (Monmouth Jct., NJ).

4-Methyl-2-((methyl(propyl)amino)methyl)-1-thioxo-2,4-dihydro-[1,2,4]triazolo[4,3-a]quinazolin-5(1H)-one (36). 4-Methyl-2-((methyl(propyl)amino)methyl)-1-thioxo-2,4-dihydro-[1,2,4]-

triazolo[4,3-*a*]quinazolin-5(1*H*)-one was purchased from Enamine (Monmouth Jct., NJ).

2-((Methyl(propyl)amino)methyl)-4-propyl-1-thioxo-2,4-dihydro-[1,2,4]triazolo[4,3-a]quinazolin(5(1H)-one (37). 2-((Methyl(propyl)amino)methyl)-4-propyl-1-thioxo-2,4-dihydro-[1,2,4]-triazolo[4,3-*a*]quinazolin-5(1*H*)-one was purchased from Enamine (Monmouth Jct., NJ).

2-(((Cyclopropylmethyl) (ethyl)amino)methyl)-4-propyl-1-thioxo-2,4-dihydro-[1,2,4]triazolo[4,3-a]quinazolin(1H)-one (38). 2-(((Cyclopropylmethyl) (ethyl)amino)methyl)-4-propyl-1-thioxo-2,4-dihydro-[1,2,4]triazolo[4,3-*a*]quinazolin-5(1*H*)-one was purchased from Enamine (Monmouth Jct., NJ).

2-(2-Oxo-2-phenylethyl)-4-propyl-1-thioxo-2,4-dihydro-[1,2,4]-triazolo[4,3-a]quinazolin-5(1H)-one (39). 2-(2-Oxo-2-phenylethyl)-4-propyl-1-thioxo-2,4-dihydro-[1,2,4]triazolo[4,3-*a*]quinazolin-5(1*H*)-one was purchased from ChemDiv (San Diego, CA).

7-Fluoro-4-phenethyl-1-thioxo-2,4-dihydro-[1,2,4]triazolo[4,3-a]quinazolin-5(1H)-one (40). 2-Amino-5-fluoro-*N*-phenethylbenzamide: To a solution of 2-amino-5-fluorobenzoic acid (250 mg, 1.61 mmol), phenethylamine (0.243 mL, 1.93 mmol), dimethylaminopyridine (100 mg, 0.81 mmol), and triethylamine (0.45 mL, 3.22 mmol) in anhydrous dichloromethane (5 mL) was added EDC·HCl (370 mg, 1.93 mmol) and stirred at RT for 18 h. Saturated aq NaHCO$_3$ solution and dichloromethane were added and stirred. The organic layer was separated, dried over Na$_2$SO$_4$, and evaporated under reduced pressure. The residue obtained was purified by silica-gel chromatography to afford the desired product as a white solid (200 mg, 48%). ^{1}H NMR (400 MHz, CDCl$_3$): δ 7.36 (t, *J* = 7.3 Hz, 2H), 7.27 (q, *J* = 6.7, 7.6 Hz, 3H), 6.96 (td, *J* = 2.9, 8.4 Hz, 1H), 6.89 (dd, *J* = 2.8, 9.2 Hz, 1H), 6.64 (dd, *J* = 4.6, 9.0 Hz, 1H), 6.01 (s, 1H), 5.24 (s, 2H), 3.69 (q, *J* = 6.6 Hz, 2H), 2.94 (t, *J* = 6.9 Hz, 2H); ^{19}F NMR (376 MHz, CDCl$_3$): δ −111.91; HRMS: (M + H) for C$_{16}$H$_{15}$N$_2$OF calcd, 259.1247; found, 259.1247.

6-Fluoro-3-phenethyl-2-thioxo-2,3-dihydroquinazolin-4(1*H*)-one: To a solution of 2-amino-5-fluoro-*N*-phenethylbenzamide (100 mg, 0.387 mmol) in anhydrous DMF (2 mL) at RT was added carbon disulfide (70 µL, 1.16 mmol) and DBU (127 µL, 0.851 mmol) sequentially. After stirring the reaction mixture for 18 h at RT, cold 1 N aq HCl was added with vigorous stirring. The precipitate was collected by filtration, washed with cold water and hexanes, and dried to give a white solid (110 mg, 95%). ^{1}H NMR (400 MHz, CDCl$_3$): δ 9.94 (s, 1H), 7.82 (dd, *J* = 2.9, 8.1 Hz, 1H), 7.40 (d, *J* = 7.7 Hz, 3H), 7.35 (t, *J* = 7.3 Hz, 1H), 7.27 (d, *J* = 4.9 Hz, 2H), 7.19−7.03 (m, 1H), 4.74 (dd, *J* = 6.4, 10.2 Hz, 2H), 3.11 (t, *J* = 8.3 Hz, 2H); ^{19}F NMR (376 MHz, CDCl$_3$): δ −114.59; HRMS: (M + H) for C$_{16}$H$_{13}$N$_2$OSF calcd, 301.0811; found, 301.0813.

6-Fluoro-2-hydrazineyl-3-phenethylquinazolin-4(3*H*)-one: Following the procedure mentioned for the synthesis of 2-hydrazineyl-3-phenethylquinazolin-4(3*H*)-one, 6-fluoro-3-phenethyl-2-thioxo-2,3-dihydroquinazolin-4(1*H*)-one (110 mg, 0.366 mmol) gave product 6-fluoro-2-hydrazineyl-3-phenethylquinazolin-4(3*H*)-one as a white solid (80 mg, 73%). ^{1}H NMR (400 MHz, CDCl$_3$): δ 7.81 (dt, *J* = 1.9, 8.5 Hz, 1H), 7.41−7.20 (m, 8H), 4.20 (t, *J* = 7.4 Hz, 2H), 3.04 (t, *J* = 7.4 Hz, 2H); ^{19}F NMR (376 MHz, CDCl$_3$): δ −117.99 (td, *J* = 4.8, 8.3 Hz); HRMS: (M + H) for C$_{16}$H$_{15}$N$_4$OF calcd, 299.1308; found, 299.1307.

7-Fluoro-4-phenethyl-1-thioxo-2,4-dihydro-[1,2,4]triazolo[4,3-*a*]-quinazolin-5(1*H*)-one: Following the procedure described for the synthesis of 4-phenethyl-1-thioxo-2,4-dihydro-[1,2,4]triazolo[4,3-*a*]-quinazolin-5(1*H*)-one, 6-fluoro-2-hydrazineyl-3-phenethylquinazolin-4(3*H*)-one (50 mg, 0.168 mmol) gave product 7-fluoro-4-phenethyl-1-thioxo-2,4-dihydro-[1,2,4]triazolo[4,3-*a*]quinazolin-5(1*H*)-one as a white solid (20 mg, 35%). ^{1}H NMR (400 MHz, DMSO-d_6): δ 14.16 (s, 1H), 10.31 (dd, *J* = 4.7, 9.3 Hz, 1H), 7.93 (dd, *J* = 3.1, 8.6 Hz, 1H), 7.83 (td, *J* = 3.1, 8.6 Hz, 1H), 7.27 (ddt, *J* = 7.3, 14.2, 19.9 Hz, 4H), 4.34−4.15 (m, 2H), 3.09−2.93 (m, 2H); ^{19}F NMR (376 MHz, DMSO-d_6): δ −112.99 (td, *J* = 4.7, 8.3 Hz); HRMS: (M + H) for C$_{17}$H$_{13}$N$_4$OSF calcd, 341.0872; found, 341.0871.

7-Bromo-4-phenethyl-1-thioxo-2,4-dihydro-[1,2,4]triazolo[4,3-a]quinazolin-5(1H)-one (41). 6-Bromo-3-phenethyl-2-thioxo-2,3-di-

hydroquinazolin-4(1*H*)-one was synthesized according to General Procedure A. Then, 7-bromo-4-phenethyl-1-thioxo-2,4-dihydro-[1,2,4]triazolo[4,3-*a*]quinazolin-5(1*H*)-one was synthesized according to General Procedure D: ^{1}H NMR (400 MHz, DMSO-d_6): δ 10.17 (d, *J* = 9.1 Hz, 1H), 8.25 (d, *J* = 2.4 Hz, 1H), 8.11 (dd, *J* = 9.0, 2.5 Hz, 1H), 7.34−7.17 (m, 5H), 4.25−4.17 (m, 2H), 3.02−2.94 (m, 2H); HRMS (ES-API) *m/z*: calcd for C$_{17}$H$_{14}$FN$_4$OS (M + H), 403.0046; found, 403.0046.

7-Iodo-4-phenethyl-1-thioxo-2,4-dihydro-[1,2,4]triazolo[4,3-a]quinazolin-5(1H)-one (42). 6-Iodo-3-phenethyl-2-thioxo-2,3-dihydroquinazolin-4(1*H*)-one was synthesized according to General Procedure A. Then, 7-iodo-4-phenethyl-1-thioxo-2,4-dihydro-[1,2,4]triazolo[4,3-*a*]quinazolin-5(1*H*)-one was synthesized according to General Procedure D: ^{1}H NMR (400 MHz, DMSO-d_6): δ 10.00 (d, *J* = 8.8 Hz, 1H), 8.41 (d, *J* = 2.1 Hz, 1H), 8.24 (dd, *J* = 8.9, 2.2 Hz, 1H), 7.32−7.18 (m, 5H), 4.24−4.16 (m, 2H), 3.02−2.93 (m, 2H).

7-Methyl-4-phenethyl-1-thioxo-2,4-dihydro-[1,2,4]triazolo[4,3-a]quinazolin-5(1H)-one (43). 6-Methyl-3-phenethyl-2-thioxo-2,3-dihydroquinazolin-4(1*H*)-one was synthesized according to General Procedure A. Then, 7-methyl-4-phenethyl-1-thioxo-2,4-dihydro-[1,2,4]triazolo[4,3-*a*]quinazolin-5(1*H*)-one was synthesized according to General Procedure D: ^{1}H NMR (400 MHz, DMSO-d_6): δ 10.06 (d, *J* = 8.6 Hz, 1H), 8.02−7.97 (m, 1Hl), 7.71 (dd, *J* = 8.8, 2.2 Hz, 1H), 7.33−7.16 (m, 5H), 4.26−4.18 (m, 2H), 3.03−2.94 (m, 2H), 2.44 (s, 3H).

N-(5-Oxo-4-phenethyl-1-thioxo-1,2,4,5-tetrahydro-[1,2,4]-triazolo[4,3-a]quinazolin-7-yl)acetamide (44). N-(4-Oxo-3-phenethyl-2-thioxo-1,2,3,4-tetrahydroquinazolin-6-yl)acetamide was synthesized according to General Procedure A. Then, N-(5-oxo-4-phenethyl-1-thioxo-1,2,4,5-tetrahydro-[1,2,4]triazolo[4,3-*a*]-quinazolin-7-yl)acetamide was synthesized according to General Procedure D: ^{1}H NMR (400 MHz, DMSO-d_6): δ 10.37 (s, 1H), 10.09 (d, *J* = 9.1 Hz, 1H), 8.51 (d, *J* = 2.6 Hz, 1H), 7.96 (dd, *J* = 9.1, 2.7 Hz, 1H), 7.26 (ddd, *J* = 19.6, 13.5, 7.3 Hz, 5H), 4.22 (dd, *J* = 9.4, 6.5 Hz, 2H), 2.99 (t, *J* = 7.9 Hz, 2H), 2.48 (t, *J* = 3.0 Hz, 2H), 2.08 (s, 3H); HRMS (ES-API) *m/z*: calcd for C$_{19}$H$_{18}$N$_5$O$_2$S (M + H), 380.1176; found, 380.1174.

7-(Dimethylamino)-4-phenethyl-1-thioxo-2,4-dihydro-[1,2,4]-triazolo[4,3-a]quinazolin-5(1H)-one (45). 6-(Dimethylamino)-3-phenethyl-2-thioxo-2,3-dihydroquinazolin-4(1*H*)-one was synthesized according to General Procedure A. Then, 7-(dimethylamino)-4-phenethyl-1-thioxo-2,4-dihydro-[1,2,4]triazolo[4,3-*a*]quinazolin-5(1*H*)-one, TFA, was synthesized according to General Procedure D: ^{1}H NMR (400 MHz, DMSO-d_6): δ 13.92 (s, 1H), 9.98 (d, *J* = 9.3 Hz, 1H), 7.33 (d, *J* = 3.1 Hz, 1H), 7.32−7.16 (m, 6H), 4.26−4.18 (m, 2H), 2.99 (s, 6H), 3.00−2.94 (m, 2H); HRMS (ES-API) *m/z*: calcd for C$_{19}$H$_{20}$N$_5$OS (M + H), 366.1383; found, 366.1388; purity (HPLC) 94.83%.

7-Morpholino-4-phenethyl-1-thioxo-2,4-dihydro-[1,2,4]triazolo-[4,3-a]quinazolin-5(1H)-one (46). 6-Morpholino-3-phenethyl-2-thioxo-2,3-dihydroquinazolin-4(1*H*)-one was synthesized according to General Procedure A. Then, 7-morpholino-4-phenethyl-1-thioxo-2,4-dihydro-[1,2,4]triazolo[4,3-*a*]quinazolin-5(1*H*)-one, TFA, was synthesized according to General Procedure D: ^{1}H NMR (400 MHz, DMSO-d_6): δ 13.97 (s, 1H), 10.02 (d, *J* = 9.3 Hz, 1H), 7.57 (d, *J* = 3.0 Hz, 1H), 7.53 (dd, *J* = 9.3, 3.0 Hz, 1H), 7.31−7.17 (m, 5H), 4.26−4.18 (m, 2H), 3.76 (t, *J* = 4.8 Hz, 4H), 3.22 (dd, *J* = 6.1, 3.6 Hz, 4H), 3.02−2.94 (m, 2H); HRMS (ES-API) *m/z*: calcd for C$_{21}$H$_{22}$N$_5$O$_2$S (M + H), 408.1489; found, 408.1490.

8-Fluoro-4-phenethyl-1-thioxo-2,4-dihydro-[1,2,4]triazolo[4,3-a]quinazolin-5(1H)-one (47). 7-Fluoro-3-phenethyl-2-thioxo-2,3-dihydroquinazolin-4(1*H*)-one was synthesized according to General Procedure A. Then, 8-fluoro-4-phenethyl-1-thioxo-2,4-dihydro-[1,2,4]triazolo[4,3-*a*]quinazolin-5(1*H*)-one, TFA, was synthesized according to General Procedure D: ^{1}H NMR (400 MHz, DMSO-d_6): δ 10.11 (dd, *J* = 11.4, 2.5 Hz, 1H), 8.27 (dd, *J* = 8.8, 6.3 Hz, 1H), 7.48 (td, *J* = 8.4, 2.6 Hz, 1H), 7.26 (ddt, *J* = 13.0, 11.5, 7.1 Hz, 5H), 4.25−4.16 (m, 2H), 3.02−2.94 (m, 2H); ^{19}F NMR (376 MHz, DMSO-d_6): δ −101.36 (dt, *J* = 11.9, 7.1 Hz); HRMS (ES-API) *m/z*: calcd for C$_{17}$H$_{14}$FN$_4$OS (M + H), 341.0867; found, 341.0882.

9-Fluoro-4-phenethyl-1-thioxo-2,4-dihydro-[1,2,4]triazolo[4,3-a]quinazolin-5(1H)-one **(48)**. 8-Fluoro-3-phenethyl-2-thioxo-2,3-di-hydroquinazolin-4(1H)-one was synthesized according to General Procedure A. Then, 9-fluoro-4-phenethyl-1-thioxo-2,4-dihydro-[1,2,4]triazolo[4,3-a]quinazolin-5(1H)-one, TFA, was synthesized according to General Procedure D: ^{1}H NMR (400 MHz, DMSO-d_6): δ 13.88 (s, 1H), 8.01 (d, J = 7.8 Hz, 1H), 7.83−7.73 (m, 1H), 7.62 (td, J = 8.0, 4.0 Hz, 1H), 7.25 (ddd, J = 18.6, 13.0, 7.3 Hz, 5H), 4.16 (dd, J = 9.2, 6.7 Hz, 2H), 3.02−2.94 (m, 2H); ^{19}F NMR (376 MHz, DMSO-d_6): δ −93.38 (dd, J = 11.6, 4.1 Hz); HRMS (ES-API) m/z: calcd for C$_{17}$H$_{14}$FN$_4$OS (M + H), 341.0867; found, 341.0859.

4-Phenethyl-1-thioxo-2,4-dihydropyrido[2,3-e][1,2,4]triazolo-[4,3-a]pyrimidin-5(1H)-one **(49)**. 3-Phenethyl-2-thioxo-2,3-dihydropyrido[3,2-d]pyrimidin-4(1H)-one was synthesized according to General Procedure A. Then, 4-phenethyl-1-thioxo-2,4-dihydropyrido[2,3-e][1,2,4]triazolo[4,3-a]pyrimidin-5(1H)-one, TFA, was synthesized according to General Procedure D.

4-Phenethyl-1-thioxo-2,4-dihydropyrido[4,3-e][1,2,4]triazolo-[4,3-a]pyrimidin-5(1H)-one **(50)**. 3-Phenethyl-2-thioxo-2,3-dihydropyrido[3,4-d]pyrimidin-4(1H)-one was synthesized according to General Procedure A. Then, 4-phenethyl-1-thioxo-2,4-dihydropyrido[4,3-e][1,2,4]triazolo[4,3-a]pyrimidin-5(1H)-one, TFA, was synthesized according to General Procedure D: ^{1}H NMR (400 MHz, DMSO-d_6): δ 11.36 (s, 1H), 8.82 (d, J = 5.0 Hz, 1H), 8.06 (d, J = 5.0 Hz, 1H), 7.33−7.22 (m, 4H), 7.20 (t, J = 7.1 Hz, 1H), 4.24−4.17 (m, 2H), 2.97 (t, J = 8.0 Hz, 2H).

6-Phenethyl-9-thioxo-8,9-dihydropyrido[3,2-e][1,2,4]triazolo-[4,3-a]pyrimidin-5(6H)-one **(51)**. 3-Phenethyl-2-thioxo-2,3-dihydropyrido[2,3-d]pyrimidin-4(1H)-one was synthesized according to General Procedure A. Then, 6-phenethyl-9-thioxo-8,9-dihydropyrido[3,2-e][1,2,4]triazolo[4,3-a]pyrimidin-5(6H)-one, TFA, was synthesized according to General Procedure D: ^{1}H NMR (400 MHz, DMSO-d_6): δ 13.84 (s, 1H), 8.83 (dd, J = 4.7, 1.9 Hz, 1H), 8.52 (dd, J = 7.8, 1.9 Hz, 1H), 7.63 (dd, J = 7.8, 4.8 Hz, 1H), 7.24 (ddt, J = 20.7, 14.0, 7.3 Hz, 5H), 4.23−4.14 (m, 2H), 2.97 (dd, J = 9.4, 6.4 Hz, 2H).

4-Benzyl-7-fluoro-1-thioxo-2,4-dihydro-[1,2,4]triazolo[4,3-a]-quinazolin-5(1H)-one **(52)**. 3-Benzyl-6-fluoro-2-thioxo-2,3-dihydroquinazolin-4(1H)-one was synthesized according to General Procedure A. Then, 4-benzyl-7-fluoro-1-thioxo-2,4-dihydro-[1,2,4]-triazolo[4,3-a]quinazolin-5(1H)-one was synthesized according to General Procedure D and purified by pouring into ice water and drops of acetic acid were added. The solid was filtered and recrystallized from dioxane to give 4-benzyl-7-fluoro-1-thioxo-2,4-dihydro-[1,2,4]-triazolo[4,3-a]quinazolin-5(1H)-one (0.0226 g, 25%): ^{1}H NMR (400 MHz, DMSO-d_6): δ 10.30 (dd, J = 9.4, 4.7 Hz, 1H), 7.95 (dd, J = 8.6, 3.1 Hz, 1H), 7.82 (ddd, J = 9.3, 7.9, 3.1 Hz, 1H), 7.43−7.36 (m, 2H), 7.30 (dd, J = 8.1, 6.2 Hz, 2H), 7.29−7.21 (m, 1H), 5.22 (s, 2H); ^{19}F NMR (376 MHz, DMSO-d_6): δ −113.06 (td, J = 8.4, 4.9 Hz); HRMS (ES-API) m/z: calcd for C$_{16}$H$_{12}$FN$_4$OS (M + H), 327.0710; found, 327.0716.

7-Fluoro-4-(3-phenylpropyl)-1-thioxo-2,4-dihydro-[1,2,4]-triazolo[4,3-a]quinazolin-5(1H)-one **(53)**. 6-Fluoro-3-(3-phenylpropyl)-2-thioxo-2,3-dihydroquinazolin-4(1H)-one was synthesized according to General Procedure A. Then, 7-fluoro-4-(3-phenylpropyl)-1-thioxo-2,4-dihydro-[1,2,4]triazolo[4,3-a]quinazolin-5(1H)-one, TFA, was synthesized according to General Procedure D: ^{1}H NMR (400 MHz, DMSO-d_6): δ 10.27 (dd, J = 9.3, 4.6 Hz, 1H), 7.90 (dd, J = 8.6, 3.1 Hz, 1H), 7.79 (dd, J = 8.6, 3.1 Hz, 1H), 7.25−7.14 (m, 4H), 7.10 (t, J = 7.0 Hz, 1H), 4.07 (t, J = 7.2 Hz, 2H), 2.67 (t, J = 7.7 Hz, 2H), 2.02 (p, J = 7.4 Hz, 2H); ^{19}F NMR (376 MHz, DMSO-d_6): δ −113.19 (td, J = 8.4, 4.9 Hz).

7-Chloro-4-propyl-1-thioxo-2,4-dihydro-[1,2,4]triazolo[4,3-a]-quinazolin-5(1H)-one **(54)**. 7-Chloro-4-propyl-1-thioxo-2,4-dihydro-[1,2,4]triazolo[4,3-a]quinazolin-5(1H)-one one was purchased from ChemDiv (San Diego, CA).

7-Chloro-1-thioxo-4-(3,3,3-trifluoropropyl)-2,4-dihydro-[1,2,4]-triazolo[4,3-a]quinazolin-5(1H)-one **(55)**. 6-Chloro-2-thioxo-3-(3,3,3-trifluoropropyl)-2,3-dihydroquinazolin-4(1H)-one was synthesized according to General Procedure B. Then, 7-chloro-1-thioxo-4-(3,3,3-trifluoropropyl)-2,4-dihydro-[1,2,4]triazolo[4,3-a]quinazolin-

5(1H)-one, TFA, was synthesized according to General Procedure D: ^{1}H NMR (400 MHz, DMSO-d_6): δ 10.23 (d, J = 9.1 Hz, 1H), 8.14 (d, J = 2.5 Hz, 1H), 8.00 (dd, J = 9.1, 2.5 Hz, 1H), 4.25 (t, J = 7.3 Hz, 2H), 2.72 (dt, J = 17.7, 9.2 Hz, 2H); ^{19}F NMR (376 MHz, DMSO-d_6): δ −64.33 (t, J = 11.3 Hz); HRMS (ES-API) m/z: calcd for C$_{12}$H$_9$ClF$_3$N$_4$OS (M + H), 349.0132; found, 349.0141; purity (HPLC) 91.99%.

7-Chloro-4-(3-isopropoxypropyl)-1-thioxo-2,4-dihydro-[1,2,4]-triazolo[4,3-a]quinazolin-5(1H)-one **(56)**. 7-Chloro-4-(3-isopropoxypropyl)-1-thioxo-2,4-dihydro-[1,2,4]triazolo[4,3-a]quinazolin-5(1H)-one was purchased from ChemDiv (San Diego, CA).

3-(7-Chloro-5-oxo-1-thioxo-1,2-dihydro-[1,2,4]triazolo[4,3-a]-quinazolin-4(5H)-yl)-N-isopropylpropanamide **(57)**. 3-(7-Chloro-5-oxo-1-thioxo-1,2-dihydro-[1,2,4]triazolo[4,3-a]quinazolin-4(5H)-yl)-N-isopropylpropanamide one was purchased from ChemDiv (San Diego, CA).

N-Isopropyl-3-(7-methyl-5-oxo-1-thioxo-1,2-dihydro-[1,2,4]-triazolo[4,3-a]quinazolin-4(5H)-yl)propanamide **(58)**. N-Isopropyl-3-(7-methyl-5-oxo-1-thioxo-1,2-dihydro-[1,2,4]triazolo[4,3-a]-quinazolin-4(5H)-yl)propanamide one was purchased from ChemDiv (San Diego, CA). Purity (HPLC) 93.49%.

N-Isopropyl-5-oxo-4-propyl-1-thioxo-1,2,4,5-tetrahydro-[1,2,4]-triazolo[4,3-a]quinazoline-8-carboxamide **(59)**. N-Isopropyl-5-oxo-4-propyl-1-thioxo-1,2,4,5-tetrahydro-[1,2,4]triazolo[4,3-a]-quinazoline-8-carboxamide one was purchased from ChemDiv (San Diego, CA).

N-Cyclopentyl-4-isopentyl-5-oxo-1-thioxo-1,2,4,5-tetrahydro-[1,2,4]triazolo[4,3-a]quinazoline-8-carboxamide **(60)**. N-Cyclopentyl-4-isopentyl-5-oxo-1-thioxo-1,2,4,5-tetrahydro-[1,2,4]triazolo[4,3-a]quinazoline-8-carboxamideone was purchased from ChemDiv (San Diego, CA).

N-Cyclopentyl-4-methyl-5-oxo-1-thioxo-1,2,4,5-tetrahydro-[1,2,4]triazolo[4,3-a]quinazoline-8-carboxamide **(61)**. N-Cyclopentyl-4-methyl-5-oxo-1-thioxo-1,2,4,5-tetrahydro-[1,2,4]triazolo[4,3-a]-quinazoline-8-carboxamide one was purchased from ChemDiv (San Diego, CA).

6-Fluoro-N-methyl-4-oxo-3-phenethyl-3,4-dihydroquinazoline-1(2H)-carbothioamide **(62)**. 6-Fluoro-3-phenethyl-2-thioxo-2,3-dihydroquinazolin-4(1H)-one was synthesized according to General Procedure A. Then, 6-fluoro-3-phenethyl-2,3-dihydroquinazolin-4(1H)-one was synthesized as follows: to a solution of 6-fluoro-3-phenethyl-2-thioxo-2,3-dihydroquinazolin-4(1H)-one (0.2 g, 0.666 mmol) and nickel(II)chloride (0.604 g, 4.66 mmol) in MeOH (5 mL) was added sodium borohydride (0.529 g, 13.98 mmol) carefully. The reaction was stirred at RT for 30 min. The reaction was then filtered through Celite and the solid washed with MeOH. The filtrate was taken up in EtOAc and washed with water. The organics were dried over MgSO$_4$, filtered, and concentrated. The product was recrystallized from EtOH.

6-Fluoro-N-methyl-4-oxo-3-phenethyl-3,4-dihydroquinazoline-1(2H)-carbothioamide, TFA, was synthesized as follows: to a solution of 6-fluoro-3-phenethyl-2,3-dihydroquinazolin-4(1H)-one (0.05 g, 0.185 mmol) in DCM (0.462 mL) was added 1,1′-thiocarbonyldiimidazole (0.049 g, 0.277 mmol) and the reaction was stirred for 2 h at RT. Methylamine hydrochloride (0.125 g, 1.850 mmol) and triethylamine (0.284 mL, 2.035 mmol) were added, and the reaction was stirred for 24 h. The reaction was concentrated under a stream of N$_2$ and purified by HPLC: ^{1}H NMR (400 MHz, DMSO-d_6): δ 8.42 (s, 1H), 7.51 (d, J = 8.8 Hz, 1H), 7.41 (d, J = 6.3 Hz, 2H), 7.19 (dq, J = 14.0, 7.2 Hz, 4H), 5.43 (s, 2H), 3.66 (t, J = 7.3 Hz, 2H), 2.93 (d, J = 4.2 Hz, 3H), 2.83 (t, J = 7.4 Hz, 2H); ^{19}F NMR (376 MHz, DMSO-d_6): δ −115.99; HRMS (ES-API) m/z: calcd for C$_{18}$H$_{18}$F$_3$N$_3$NaOS (M + Na), 366.1047; found, 366.1052.

4-Ethyl-7-fluoro-1-thioxo-2,4-dihydro-[1,2,4]triazolo[4,3-a]-quinazolin-5(1H)-one **(63)**. 3-Ethyl-6-fluoro-2-thioxo-2,3-dihydroquinazolin-4(1H)-one was synthesized according to General Procedure A. Then, 4-ethyl-7-fluoro-1-thioxo-2,4-dihydro-[1,2,4]triazolo[4,3-a]-quinazolin-5(1H)-one was synthesized according to General Procedure D: ^{1}H NMR (400 MHz, DMSO-d_6): δ 10.28 (dd, J = 9.3, 4.7 Hz, 1H), 7.91 (dd, J = 8.6, 3.1 Hz, 1H), 7.79 (ddd, J = 9.3, 8.0, 3.1 Hz, 1H), 4.06 (q, J = 7.1 Hz, 2H), 1.24 (t, J = 7.1 Hz, 3H);

^{19}F NMR (376 MHz, DMSO-d_6): δ −113.15 (td, J = 8.5, 4.8 Hz); HRMS (ES-API) m/z: calcd for $C_{11}H_{10}FN_4OS$ (M + H), 265.0554; found, 265.0557; purity (HPLC) 91.89%.

7-Fluoro-4-propyl-1-thioxo-2,4-dihydro-[1,2,4]triazolo[4,3-a]-quinazolin-5(1H)-one (64). 7-Fluoro-4-propyl-1-thioxo-2,4-dihydro-[1,2,4]triazolo[4,3-a]quinazolin-5(1H)-one was purchased from ChemDiv (San Diego, CA).

7-Fluoro-1-thioxo-4-(3,3,3-trifluoropropyl)-2,4-dihydro-[1,2,4]-triazolo[4,3-a]quinazolin-5(1H)-one (65). 6-Fluoro-2-thioxo-3-(3,3,3-trifluoropropyl)-2,3-dihydroquinazolin-4(1H)-one was synthesized according to General Procedure B. Then, 7-fluoro-1-thioxo-4-(3,3,3-trifluoropropyl)-2,4-dihydro-[1,2,4]triazolo[4,3-a]quinazolin-5(1H)-one, TFA salt, was synthesized according to General Procedure D: ^{1}H NMR (400 MHz, DMSO-d_6): δ 10.27 (d, J = 6.5 Hz, 1H), 7.93 (dd, J = 8.6, 3.0 Hz, 1H), 7.82 (td, J = 9.3, 8.7, 3.1 Hz, 1H), 4.26 (t, J = 7.2 Hz, 2H), 2.72 (dtd, J = 18.6, 11.3, 7.7 Hz, 2H); ^{19}F NMR (376 MHz, DMSO-d_6): δ −64.33 (t, J = 11.3 Hz), −112.81; HRMS (ES-API) m/z: calcd for $C_{12}H_8F_4N_4NaOS$ (M + Na), 355.0247; found, 355.0245.

7-Fluoro-4-(3-hydroxypropyl)-1-thioxo-2,4-dihydro-[1,2,4]-triazolo[4,3-a]quinazolin-5(1H)-one (66). 6-Fluoro-3-(3-hydroxypropyl)-2-thioxo-2,3-dihydroquinazolin-4(1H)-one was synthesized according to General Procedure B. Then, 7-fluoro-4-(3-hydroxypropyl)-1-thioxo-2,4-dihydro-[1,2,4]triazolo[4,3-a]quinazolin-5(1H)-one, TFA salt, was synthesized according to General Procedure D: ^{1}H NMR (400 MHz, DMSO-d_6): δ 10.28 (dd, J = 9.4, 4.6 Hz, 1H), 7.90 (dd, J = 8.6, 3.1 Hz, 1H), 7.78 (td, J = 8.5, 3.0 Hz, 1H), 4.48 (t, J = 5.1 Hz, 1H), 4.08 (t, J = 7.4 Hz, 2H), 3.47 (q, J = 5.8 Hz, 2H), 1.89−1.77 (m, 2H); ^{19}F NMR (376 MHz, DMSO-d_6): δ −113.18 (q, J = 7.4 Hz); HRMS (ES-API) m/z: calcd for $C_{12}H_{12}FN_4O_2S$ (M + H), 294.0660; found, 294.0664.

4-(2-Aminoethyl)-7-fluoro-1-thioxo-2,4-dihydro-[1,2,4]triazolo-[4,3-a]quinazolin-5(1H)-one (67). tert-Butyl (2-(6-fluoro-4-oxo-2-thioxo-1,4-dihydroquinazolin-3(2H)-yl)ethyl)carbamate was synthesized according to General Procedure C. Then, tert-butyl (2-(7-fluoro-5-oxo-1-thioxo-1,2-dihydro-[1,2,4]triazolo[4,3-a]quinazolin-4(5H)-yl)ethyl)carbamate was synthesized according to General Procedure D. Then, 4-(2-aminoethyl)-7-fluoro-1-thioxo-2,4-dihydro-[1,2,4]-triazolo[4,3-a]quinazolin-5(1H)-one, di-TFA salt, was synthesized by treating tert-butyl (2-(7-fluoro-5-oxo-1-thioxo-1,2-dihydro-[1,2,4]-triazolo[4,3-a]quinazolin-4(5H)-yl)ethyl)carbamate (0.112 g, 0.295 mmol) in DCM (1.230 mL) and MeOH (0.246 mL) with TFA (0.989 mL, 12.84 mmol). The reaction was stirred at RT for 3 h, then blown down, redissolved, and purified by HPLC: ^{1}H NMR (400 MHz, DMSO-d_6): δ 10.31 (dd, J = 9.3, 4.6 Hz, 1H), 7.95 (dd, J = 8.5, 3.1 Hz, 1H), 7.85 (ddd, J = 9.2, 7.6, 3.2 Hz, 3H), 4.32 (t, J = 5.8 Hz, 2H), 3.20 (t, J = 6.0 Hz, 2H); ^{19}F NMR (376 MHz, DMSO-d_6): δ −112.75 (td, J = 8.3, 4.7 Hz); HRMS (ES-API) m/z: calcd for $C_{11}H_{10}FN_5NaOS$ (M + Na), 302.0482; found, 302.0493.

4-(3-Aminopropyl)-7-fluoro-1-thioxo-2,4-dihydro-[1,2,4]triazolo-[4,3-a]quinazolin-5(1H)-one (68). tert-Butyl (3-(6-fluoro-4-oxo-2-thioxo-1,4-dihydroquinazolin-3(2H)-yl)propyl)carbamate was synthesized according to General Procedure C. Then, tert-butyl (3-(7-fluoro-5-oxo-1-thioxo-1,2-dihydro-[1,2,4]triazolo[4,3-a]quinazolin-4(5H)-yl)propyl)carbamate was synthesized according to General Procedure D. Then, 4-(3-aminopropyl)-7-fluoro-1-thioxo-2,4-dihydro-[1,2,4]-triazolo[4,3-a]quinazolin-5(1H)-one, di-TFA salt, was synthesized by treating a solution of tert-butyl (3-(7-fluoro-5-oxo-1-thioxo-1,2-dihydro-[1,2,4]triazolo[4,3-a]quinazolin-4(5H)-yl)propyl)carbamate (0.056 g, 0.142 mmol) in DCM (0.593 mL), MeOH (0.119 mL) was added to TFA (0.477 mL, 6.19 mmol), and the reaction stirred at RT for 3 h. The reaction was then concentrated, and the product was purified by ISCO (DCM/MeOH +3.3% NH$_4$OH, 0−100%): ^{1}H NMR (400 MHz, DMSO-d_6): δ 10.30 (dd, J = 9.4, 4.7 Hz, 1H), 7.92 (dd, J = 8.5, 3.1 Hz, 1H), 7.83 (ddd, J = 9.3, 7.9, 3.1 Hz, 1H), 7.65 (s, 3H), 4.10 (t, J = 6.8 Hz, 2H), 2.89 (q, J = 8.4, 7.3 Hz, 2H), 2.00 (p, J = 7.0 Hz, 2H); ^{19}F NMR (376 MHz, DMSO-d_6): δ −113.06 (td, J = 8.3, 4.8 Hz); HRMS (ES-API) m/z: calcd for $C_{12}H_{13}FN_5OS$ (M + H), 294.0819; found, 294.0825.

4-(3-Aminopropyl)-9-fluoro-1-thioxo-2,4-dihydro-[1,2,4]triazolo-[4,3-a]quinazolin-5(1H)-one (69). tert-Butyl (3-(8-fluoro-4-oxo-2-thioxo-1,4-dihydroquinazolin-3(2H)-yl)propyl)carbamate was synthesized according to General Procedure A. Then, tert-butyl (3-(9-fluoro-5-oxo-1-thioxo-1,2-dihydro-[1,2,4]triazolo[4,3-a]quinazolin-4(5H)-yl)propyl)carbamate was synthesized according to General Procedure D. Then, 4-(3-aminopropyl)-9-fluoro-1-thioxo-2,4-dihydro-[1,2,4]-triazolo[4,3-a]quinazolin-5(1H)-one was synthesized as follows: tert-butyl (3-(9-fluoro-5-oxo-1-thioxo-1,2-dihydro-[1,2,4]triazolo[4,3-a]-quinazolin-4(5H)-yl)propyl)carbamate (0.170 g, 0.432 mmol) was dissolved in HCl in dioxane (1.512 mL, 6.05 mmol) and the solution stirred at RT for 5 h. The reaction was quenched with triethylamine (0.843 mL, 6.05 mmol), filtered, and concentrated. The product was purified by ISCO (EtOAc/hexanes, 0−100%) to give 4-(3-aminopropyl)-9-fluoro-1-thioxo-2,4-dihydro-[1,2,4]triazolo[4,3-a]-quinazolin-5(1H)-one, di-TFA salt: ^{19}F NMR (376 MHz, DMSO-d_6): δ −93.31 (dd, J = 11.6, 4.2 Hz).

4-(2-(Dimethylamino)ethyl)-7-fluoro-1-thioxo-2,4-dihydro-[1,2,4]triazolo[4,3-a]quinazolin-5(1H)-one (70). 3-(2-(Dimethylamino)ethyl)-6-fluoro-2-thioxo-2,3-dihydroquinazolin-4(1H)-one was synthesized according to General Procedure B. Then, 4-(2-(dimethylamino)ethyl)-7-fluoro-1-thioxo-2,4-dihydro-[1,2,4]-triazolo[4,3-a]quinazolin-5(1H)-one, di-TFA salt, was synthesized according to General Procedure D: ^{1}H NMR (400 MHz, DMSO-d_6): δ 10.30 (dd, J = 9.3, 4.6 Hz, 1H), 9.10 (s, 1H), 7.95 (dd, J = 8.5, 3.1 Hz, 1H), 7.86 (td, J = 8.5, 3.1 Hz, 1H), 4.40 (t, J = 5.6 Hz, 2H), 3.50−3.43 (m, 2H), 2.85 (s, 6H); ^{19}F NMR (376 MHz, DMSO-d_6): δ −112.62 (q, J = 7.5 Hz); HRMS (ES-API) m/z: calcd for $C_{13}H_{15}FN_5OS$ (M + H), 308.0976; found, 308.0989.

4-(1-(Dimethylamino)propan-2-yl)-7-fluoro-1-thioxo-2,4-dihydro-[1,2,4]triazolo[4,3-a]quinazolin-5(1H)-one (71). 3-(1-(Dimethylamino)propan-2-yl)-6-fluoro-2-thioxo-2,3-dihydroquinazolin-4(1H)-one was synthesized according to General Procedure B. Then, 4-(1-(dimethylamino)propan-2-yl)-7-fluoro-1-thioxo-2,4-dihydro-[1,2,4]triazolo[4,3-a]quinazolin-5(1H)-one, di-TFA salt, was synthesized according to General Procedure D: ^{1}H NMR (400 MHz, DMSO-d_6): δ 10.34 (dd, J = 9.3, 4.6 Hz, 1H), 9.24 (s, 1H), 7.94 (dd, J = 8.6, 3.1 Hz, 1H), 7.85 (td, J = 9.2, 8.7, 3.1 Hz, 1H), 4.05 (t, J = 12.3 Hz, 1H), 3.35 (s, 2H), 2.80 (d, J = 17.7 Hz, 6H), 1.52 (d, J = 6.8 Hz, 3H); ^{19}F NMR (376 MHz, DMSO-d_6): δ −112.68 (q, J = 7.8 Hz); HRMS (ES-API) m/z: calcd for $C_{14}H_{17}FN_5OS$ (M + H), 322.1132; found, 322.1139.

N-(2-(7-Fluoro-5-oxo-1-thioxo-1,2-dihydro-[1,2,4]triazolo[4,3-a]-quinazolin-4(5H)-yl)ethyl)acetamide (72). N-(2-(6-Fluoro-4-oxo-2-thioxo-1,4-dihydroquinazolin-3(2H)-yl)ethyl)acetamide was synthesized according to General Procedure B. Then, N-(2-(7-fluoro-5-oxo-1-thioxo-1,2-dihydro-[1,2,4]triazolo[4,3-a]quinazolin-4(5H)-yl)-ethyl)acetamide, TFA salt, was synthesized according to General Procedure D: ^{1}H NMR (400 MHz, DMSO-d_6): δ 10.30 (dd, J = 9.3, 4.6 Hz, 1H), 7.92 (dd, J = 8.6, 3.0 Hz, 1H), 7.88−7.76 (m, 2H), 4.08 (t, J = 5.8 Hz, 2H), 3.39 (q, J = 6.1 Hz, 2H), 1.64 (s, 3H); ^{19}F NMR (376 MHz, DMSO-d_6): δ −113.00 (q, J = 7.6, 6.7 Hz); HRMS (ES-API) m/z: calcd for $C_{13}H_{13}FN_5O_2S$ (M + H), 322.0769; found, 322.0780.

N-(3-(7-Fluoro-5-oxo-1-thioxo-1,2-dihydro-[1,2,4]triazolo[4,3-a]-quinazolin-4(5H)-yl)propyl)acetamide (73). tert-Butyl (3-(6-fluoro-4-oxo-2-thioxo-1,4-dihydroquinazolin-3(2H)-yl)propyl)carbamate was synthesized according to General Procedure C.

3-(3-Aminopropyl)-6-fluoro-2-thioxo-2,3-dihydroquinazolin-4(1H)-one: TFA (1.476 mL, 19.15 mmol) was added to a solution of crude tert-butyl (3-(6-fluoro-4-oxo-2-thioxo-1,4-dihydroquinazolin-3(2H)-yl)propyl)carbamate (0.1556 g, 0.440 mmol) in DCM (2.201 mL), and the reaction was stirred at RT for 2 h. The reaction was then blown down, the residue dissolved in MeOH, gravity filtered through a PL-HCO$_3$ SPE cartridge, and concentrated. The crude product was used without further purification.

N-(3-(6-Fluoro-4-oxo-2-thioxo-1,4-dihydroquinazolin-3(2H)-yl)-propyl)acetamide: to a solution of 3-(3-aminopropyl)-6-fluoro-2-thioxo-2,3-dihydroquinazolin-4(1H)-one (0.05 g, 0.197 mmol) in pyridine (0.6 mL) was added acetyl chloride (0.021 mL, 0.296 mmol)

and the reaction stirred at 0 °C for 2 h. The reaction was then cooled to RT and poured into ice water and filtered, and the solid was washed with water and Et$_2$O and dried. The crude product was used without further purification.

N-(3-(7-Fluoro-5-oxo-1-thioxo-1,2-dihydro-[1,2,4]triazolo[4,3-a]-quinazolin-4(5*H*)-yl)propyl)acetamide, TFA salt, was synthesized according to General Procedure D: ^{1}H NMR (400 MHz, DMSO-d_6): δ 10.29 (dd, *J* = 9.4, 4.7 Hz, 1H), 7.91 (dd, *J* = 8.6, 3.1 Hz, 1H), 7.86−7.75 (m, 2H), 4.02 (dd, *J* = 8.2, 6.3 Hz, 2H), 3.09 (q, *J* = 6.6 Hz, 2H), 1.82 (p, *J* = 7.2 Hz, 2H), 1.76 (s, 3H); ^{19}F NMR (376 MHz, DMSO-d_6): δ −113.17 (td, *J* = 8.2, 4.5 Hz); HRMS (ES-API) *m/z*: calcd for C$_{17}$H$_{18}$F$_3$N$_4$OS (M + H), 336.0925; found, 336.0929; purity (HPLC) 90.11%.

N-(3-(7-Fluoro-5-oxo-1-thioxo-1,2-dihydro-[1,2,4]triazolo[4,3-a]-quinazolin-4(5H)-yl)propyl)benzamide (**74**). *N*-(3-(7-Fluoro-5-oxo-1-thioxo-1,2-dihydro-[1,2,4]triazolo[4,3-a]quinazolin-4(5*H*)-yl)-propyl)benzamide, TFA salt, was synthesized according to General Procedure F: ^{1}H NMR (400 MHz, DMSO-d_6): δ 10.31 (dd, *J* = 9.3, 4.7 Hz, 1H), 8.46 (t, *J* = 5.7 Hz, 1H), 7.91 (dd, *J* = 8.6, 3.1 Hz, 1H), 7.85−7.78 (m, 3H), 7.54−7.49 (m, 1H), 7.48−7.42 (m, 2H), 4.11 (dd, *J* = 8.1, 6.6 Hz, 2H), 3.36 (q, *J* = 6.6 Hz, 2H), 1.99 (p, *J* = 6.9 Hz, 2H); ^{19}F NMR (376 MHz, DMSO-d_6): δ −113.15 (td, *J* = 8.2, 4.6 Hz); HRMS (ES-API) *m/z*: calcd for C$_{19}$H$_{17}$FN$_5$O$_2$S (M + H), 398.1082; found, 398.1063.

N-(2-(7-Fluoro-5-oxo-1-thioxo-1,2-dihydro-[1,2,4]triazolo[4,3-a]-quinazolin-4(5H)-yl)ethyl)methanesulfonamide (**75**). *N*-(2-(6-Fluoro-4-oxo-2-thioxo-1,4-dihydroquinazolin-3(2*H*)-yl)ethyl)-methanesulfonamide was synthesized according to General Procedure C. Then, *N*-(2-(7-fluoro-5-oxo-1-thioxo-1,2-dihydro-[1,2,4]triazolo-[4,3-a]quinazolin-4(5*H*)-yl)ethyl)methanesulfonamide, TFA salt, was synthesized according to General Procedure D: ^{1}H NMR (400 MHz, DMSO-d_6): δ 10.30 (dd, *J* = 9.3, 4.7 Hz, 1H), 7.93 (dd, *J* = 8.6, 3.1 Hz, 1H), 7.81 (ddd, *J* = 9.3, 8.0, 3.1 Hz, 1H), 7.17 (t, *J* = 6.4 Hz, 1H), 4.18 (t, *J* = 6.2 Hz, 2H), 3.36 (q, *J* = 6.2 Hz, 2H), 2.88 (s, 3H); ^{19}F NMR (376 MHz, DMSO-d_6): δ −112.99 (td, *J* = 8.3, 4.7 Hz); HRMS (ES-API) *m/z*: calcd for C$_{12}$H$_{13}$FN$_5$O$_3$S$_2$ (M + H), 358.0438; found, 358.0441.

N-(3-(7-Fluoro-5-oxo-1-thioxo-1,2-dihydro-[1,2,4]triazolo[4,3-a]-quinazolin-4(5H)-yl)propyl)methanesulfonamide (**76**). *N*-(3-(7-Fluoro-5-oxo-1-thioxo-1,2-dihydro-[1,2,4]triazolo[4,3-a]quinazolin-4(5*H*)-yl)propyl)methanesulfonamide was synthesized by treating 4-(3-aminopropyl)-7-fluoro-1-thioxo-2,4-dihydro-[1,2,4]triazolo[4,3-a]-quinazolin-5(1*H*)-one (0.05 g, 0.170 mmol) in DCM (0.852 mL) at RT with methanesulfonyl chloride (0.015 mL, 0.188 mmol) and triethylamine (0.029 mL, 0.205 mmol). The reaction was stirred at RT for 2 h, concentrated, and purified by HPLC: ^{1}H NMR (400 MHz, DMSO-d_6): δ 10.29 (dd, *J* = 9.3, 4.7 Hz, 1H), 7.92 (dd, *J* = 8.6, 3.1 Hz, 1H), 7.81 (ddd, *J* = 9.3, 8.0, 3.2 Hz, 1H), 7.00 (t, *J* = 5.9 Hz, 1H), 4.07 (t, *J* = 7.1 Hz, 2H), 3.02 (q, *J* = 6.7 Hz, 2H), 2.86 (s, 3H), 1.89 (p, *J* = 7.1 Hz, 2H); ^{19}F NMR (376 MHz, DMSO-d_6): δ −113.18 (td, *J* = 8.3, 5.0 Hz); HRMS (ES-API) *m/z*: calcd for C$_{13}$H$_{15}$FN$_5$O$_3$S$_2$ (M + H), 372.0595; found, 372.0601; purity (HPLC) 94.02%.

(2-(7-Fluoro-5-oxo-1-thioxo-1,2-dihydro-[1,2,4]triazolo[4,3-a]-quinazolin-4(5H)-yl)ethyl)phosphonic Acid (**77**). (2-(7-Fluoro-5-oxo-1-thioxo-1,2-dihydro-[1,2,4]triazolo[4,3-a]quinazolin-4(5*H*)-yl)-ethyl)phosphonic acid was synthesized by treating a solution of diethyl (2-(7-(fluoro-5-oxo-1-thioxo-1,2-dihydro-[1,2,4]triazolo[4,3-a]quinazolin-4(5*H*)-yl)ethyl)phosphonate (0.111 g, 0.277 mmol) in DCM (4.62 mL) at 0 °C with bromotrimethylsilane (0.216 mL, 1.663 mmol) dropwise (fast). The reaction was then warmed to RT, and the solution was stirred for 8 h. The reaction was concentrated, redissolved, and purified by HPLC: ^{1}H NMR (400 MHz, DMSO-d_6): δ 10.27 (dd, *J* = 9.3, 4.6 Hz, 1H), 7.90 (dd, *J* = 8.7, 3.1 Hz, 1H), 7.79 (td, *J* = 8.5, 3.1 Hz, 1H), 4.24−4.14 (m, 2H), 2.06−1.93 (m, 2H); ^{19}F NMR (376 MHz, DMSO-d_6): δ −113.10 (q, *J* = 7.5 Hz); ^{31}P NMR (162 MHz, DMSO-d_6): δ 20.70.

Diethyl (2-(7-Fluoro-5-oxo-1-thioxo-1,2-dihydro-[1,2,4]triazolo-[4,3-a]quinazolin-4(5H)-yl)ethyl)phosphonate (**78**). Diethyl (2-(6-fluoro-4-oxo-2-thioxo-1,4-dihydroquinazolin-3(2*H*)-yl)ethyl)-

phosphonate was synthesized according to General Procedure B. Then, diethyl (2-(7-fluoro-5-oxo-1-thioxo-1,2-dihydro-[1,2,4]triazolo-[4,3-a]quinazolin-4(5*H*)-yl)ethyl)phosphonate, TFA salt, was synthesized according to General Procedure D: ^{1}H NMR (400 MHz, DMSO-d_6): δ 10.32 (d, *J* = 7.3 Hz, 1H), 7.92 (dd, *J* = 8.5, 3.1 Hz, 1H), 7.80 (ddd, *J* = 9.1, 7.9, 3.1 Hz, 1H), 4.25−4.15 (m, 2H), 4.00 (dqd, *J* = 8.1, 7.0, 3.5 Hz, 4H), 3.26 (s, 1H), 2.28−2.15 (m, 2H), 1.22 (t, *J* = 7.0 Hz, 6H); ^{19}F NMR (376 MHz, DMSO-d_6): δ −113.07; ^{31}P NMR (162 MHz, DMSO-d_6): δ 26.69; HRMS (ES-API) *m/z*: calcd for C$_{15}$H$_{19}$FN$_4$O$_4$PS (M + H), 401.0843; found, 401.0856.

4-(Cyclopropylmethyl)-7-fluoro-1-thioxo-2,4-dihydro-[1,2,4]-triazolo[4,3-a]quinazolin-5(1H)-one (**79**). 3-(Cyclopropylmethyl)-6-fluoro-2-thioxo-2,3-dihydroquinazolin-4(1*H*)-one was synthesized according to General Procedure B. Then, 4-(cyclopropylmethyl)-7-fluoro-1-thioxo-2,4-dihydro-[1,2,4]triazolo[4,3-a]quinazolin-5(1*H*)-one, TFA salt, was synthesized according to General Procedure D: ^{1}H NMR (400 MHz, DMSO-d_6): δ 10.29 (dd, *J* = 9.3, 4.7 Hz, 1H), 7.92 (dd, *J* = 8.6, 3.0 Hz, 1H), 7.80 (ddd, *J* = 9.3, 7.9, 3.1 Hz, 1H), 3.92 (d, *J* = 7.1 Hz, 2H), 1.27 (s, 1H), 0.49−0.37 (m, 4H); ^{19}F NMR (376 MHz, DMSO-d_6): δ −113.02 (td, *J* = 8.3, 4.7 Hz); HRMS (ES-API) *m/z*: calcd for C$_{13}$H$_{12}$FN$_4$OS (M + H), 291.0710; found, 291.0720.

7-Fluoro-4-(trans-2-methylcyclopropyl)-1-thioxo-2,4-dihydro-[1,2,4]triazolo[4,3-a]quinazolin-5(1H)-one (**80**). 6-Fluoro-3-(*trans*-2-methylcyclopropyl)-2-thioxo-2,3-dihydroquinazolin-4(1*H*)-one was synthesized according to General Procedure B. Then, 7-fluoro-4-(*trans*-2-methylcyclopropyl)-1-thioxo-2,4-dihydro-[1,2,4]triazolo[4,3-a]quinazolin-5(1*H*)-one, TFA salt, was synthesized according to General Procedure D: ^{1}H NMR (400 MHz, DMSO-d_6): δ 13.99 (s, 1H), 10.26 (dd, *J* = 9.3, 4.6 Hz, 1H), 7.86 (dd, *J* = 8.8, 3.1 Hz, 1H), 7.76 (ddd, *J* = 10.7, 8.2, 3.0 Hz, 1H), 2.56 (dt, *J* = 7.3, 3.5 Hz, 1H), 1.27−1.19 (m, 1H), 1.15 (d, *J* = 6.0 Hz, 3H), 1.07 (dt, *J* = 9.6, 4.8 Hz, 1H), 0.90 (q, *J* = 6.6 Hz, 1H); ^{19}F NMR (376 MHz, DMSO-d_6): δ −113.28 (q, *J* = 7.3, 6.8 Hz); HRMS (ES-API) *m/z*: calcd for C$_{13}$H$_{12}$FN$_4$OS (M + H), 291.0710; found, 291.0717.

4-(2-Chlorophenethyl)-7-fluoro-1-thioxo-2,4-dihydro-[1,2,4]-triazolo[4,3-a]quinazolin-5(1H)-one (**81**). 3-(2-Chlorophenethyl)-6-fluoro-2-thioxo-2,3-dihydroquinazolin-4(1*H*)-one was synthesized according to General Procedure B. Then, 4-(2-chlorophenethyl)-7-fluoro-1-thioxo-2,4-dihydro-[1,2,4]triazolo[4,3-a]quinazolin-5(1*H*)-one, TFA salt, was synthesized according to General Procedure D: ^{1}H NMR (400 MHz, DMSO-d_6): δ 10.28 (s, 1H), 7.88 (dd, *J* = 8.6, 2.9 Hz, 1H), 7.80 (t, *J* = 8.7 Hz, 1H), 7.39 (dd, *J* = 5.6, 3.7 Hz, 1H), 7.36−7.29 (m, 1H), 7.23 (dd, *J* = 5.9, 3.5 Hz, 2H), 4.27 (t, *J* = 7.5 Hz, 2H), 3.13 (t, *J* = 7.3 Hz, 2H); ^{19}F NMR (376 MHz, DMSO-d_6): δ −112.98; HRMS (ES-API) *m/z*: calcd for C$_{17}$H$_{13}$ClFN$_4$OS (M + H), 375.0477; found, 375.0481.

4-(4-Chlorophenethyl)-7-fluoro-1-thioxo-2,4-dihydro-[1,2,4]-triazolo[4,3-a]quinazolin-5(1H)-one (**82**). 3-(4-Chlorophenethyl)-6-fluoro-2-thioxo-2,3-dihydroquinazolin-4(1*H*)-one was synthesized according to General Procedure B. Then, 4-(4-chlorophenethyl)-7-fluoro-1-thioxo-2,4-dihydro-[1,2,4]triazolo[4,3-a]quinazolin-5(1*H*)-one, TFA salt, was synthesized according to General Procedure D: ^{1}H NMR (400 MHz, DMSO-d_6): δ 10.28 (dd, *J* = 9.4, 4.6 Hz, 1H), 7.89 (dd, *J* = 8.6, 3.1 Hz, 1H), 7.80 (ddd, *J* = 9.3, 7.9, 3.1 Hz, 1H), 7.32 (d, *J* = 8.5 Hz, 2H), 7.27 (d, *J* = 8.5 Hz, 2H), 4.21 (t, *J* = 7.7 Hz, 2H), 2.98 (t, *J* = 7.6 Hz, 2H); ^{19}F NMR (376 MHz, DMSO-d_6): δ −113.00 (td, *J* = 8.4, 5.0 Hz); HRMS (ES-API) *m/z*: calcd for C$_{17}$H$_{13}$Cl FN$_4$OS (M + H), 375.0477; found, 375.0480.

7-Fluoro-4-(2-(pyridin-2-yl)ethyl)-1-thioxo-2,4-dihydro-[1,2,4]-triazolo[4,3-a]quinazolin-5(1H)-one (**83**). 6-Fluoro-3-(2-(pyridin-2-yl)ethyl)-2-thioxo-2,3-dihydroquinazolin-4(1*H*)-one was synthesized according to General Procedure B. Then, 7-fluoro-4-(2-(pyridin-2-yl)ethyl)-1-thioxo-2,4-dihydro-[1,2,4]triazolo[4,3-a]quinazolin-5(1*H*)-one, TFA salt, was synthesized according to General Procedure D: ^{1}H NMR (400 MHz, DMSO-d_6): δ 10.29 (dd, *J* = 9.4, 4.6 Hz, 1H), 8.46 (d, *J* = 5.0 Hz, 1H), 7.88 (dd, *J* = 8.6, 3.0 Hz, 1H), 7.80 (td, *J* = 8.6, 3.1 Hz, 1H), 7.76−7.73 (m, 1H), 7.36 (d, *J* = 7.7 Hz, 1H), 7.29−7.24 (m, 1H), 4.38 (t, *J* = 7.6 Hz, 2H), 3.20−3.11 (m, 2H); ^{19}F NMR (376 MHz, DMSO-d_6): δ −112.97 to −113.04

(m); HRMS (ES-API) m/z: calcd for $C_{16}H_{13}FN_5OS$ (M + H), 342.0819; found, 342.0818; purity (HPLC) 94.92%.

7-Fluoro-4-(2-(pyridin-3-yl)ethyl)-1-thioxo-2,4-dihydro-[1,2,4]-triazolo[4,3-a]quinazolin-5(1H)-one (84). 6-Fluoro-3-(2-(pyridin-3-yl)ethyl)-2-thioxo-2,3-dihydroquinazolin-4(1H)-one was synthesized according to General Procedure B. Then, 7-fluoro-4-(2-(pyridin-3-yl)ethyl)-1-thioxo-2,4-dihydro-[1,2,4]triazolo[4,3-a]quinazolin-5(1H)-one was synthesized according to General Procedure D: ^{1}H NMR (400 MHz, DMSO-d_6): δ 10.30 (dd, J = 9.3, 4.7 Hz, 1H), 8.56 (d, J = 2.2 Hz, 1H), 8.50 (dd, J = 4.9, 1.6 Hz, 1H), 7.92−7.85 (m, 2H), 7.82 (td, J = 8.6, 3.1 Hz, 1H), 7.46 (dd, J = 7.9, 5.0 Hz, 1H), 4.29 (t, J = 7.2 Hz, 2H), 3.08 (t, J = 7.2 Hz, 2H); ^{19}F NMR (376 MHz, DMSO-d_6): δ −113.00 (td, J = 8.2, 4.6 Hz); HRMS (ES-API) m/z: calcd for $C_{16}H_{13}FN_5OS$ (M + H), 342.0819; found, 342.0811.

7-Fluoro-4-(2-(pyridin-4-yl)ethyl)-1-thioxo-2,4-dihydro-[1,2,4]-triazolo[4,3-a]quinazolin-5(1H)-one (85). 6-Fluoro-3-(2-(pyridin-4-yl)ethyl)-2-thioxo-2,3-dihydroquinazolin-4(1H)-one was synthesized according to General Procedure B. Then, 7-fluoro-4-(2-(pyridin-4-yl)ethyl)-1-thioxo-2,4-dihydro-[1,2,4]triazolo[4,3-a]quinazolin-5(1H)-one, TFA salt, was synthesized according to General Procedure D: ^{1}H NMR (400 MHz, DMSO-d_6): δ 10.30 (dd, J = 9.3, 4.7 Hz, 1H), 8.65−8.59 (m, 2H), 7.91−7.77 (m, 2H), 7.66 (d, J = 5.6 Hz, 2H), 4.34 (t, J = 7.1 Hz, 2H), 3.17 (t, J = 7.1 Hz, 2H); ^{19}F NMR (376 MHz, DMSO-d_6): δ −112.98 (td, J = 8.2, 4.7 Hz); HRMS (ES-API) m/z: calcd for $C_{16}H_{13}FN_5OS$ (M + H), 342.0819; found, 342.0825.

tert-Butyl 3-(2-(7-fluoro-5-oxo-1-thioxo-1,2-dihydro-[1,2,4]-triazolo[4,3-a]quinazolin-4(5H)-yl)ethyl)azetidine-1-carboxylate (86). *tert*-Butyl 3-(2-(6-fluoro-4-oxo-2-thioxo-1,4-dihydroquinazolin-3(2H)-yl)ethyl)azetidine-1-carboxylate was synthesized according to General Procedure B. Then, *tert*-butyl 3-(2-(7-fluoro-5-oxo-1-thioxo-1,2-dihydro-[1,2,4]triazolo[4,3-a]quinazolin-4(5H)-yl)ethyl)-azetidine-1-carboxylate, TFA salt, was synthesized according to General Procedure D: ^{1}H NMR (400 MHz, DMSO-d_6): δ 10.28 (dd, J = 9.3, 4.6 Hz, 1H), 7.90 (dd, J = 8.6, 3.1 Hz, 1H), 7.79 (ddd, J = 9.3, 7.9, 3.1 Hz, 1H), 3.98 (t, J = 6.8 Hz, 2H), 3.84 (s, 2H), 3.47 (s, 2H), 2.59−2.49 (m, 1H), 1.95 (q, J = 7.1 Hz, 2H), 1.33 (s, 8H); ^{19}F NMR (376 MHz, DMSO-d_6): δ −113.14 (q, J = 7.5 Hz); HRMS (ES-API) m/z: calcd for $C_{19}H_{22}FN_5NaO_3S$ (M + Na), 442.1320; found, 442.1332.

7-Fluoro-4-(2-(1-methylpyrrolidin-2-yl)ethyl)-1-thioxo-2,4-dihydro-[1,2,4]triazolo[4,3-a]quinazolin-5(1H)-one (87). 6-Fluoro-3-(2-(1-methylpyrrolidin-2-yl)ethyl)-2-thioxo-2,3-dihydroquinazolin-4(1H)-one was synthesized according to General Procedure B. Then, 7-fluoro-4-(2-(1-methylpyrrolidin-2-yl)ethyl)-1-thioxo-2,4-dihydro-[1,2,4]triazolo[4,3-a]quinazolin-5(1H)-one, di-TFA salt, was synthesized according to General Procedure D: ^{1}H NMR (400 MHz, DMSO-d_6): δ 10.30 (dd, J = 9.3, 4.6 Hz, 1H), 9.43 (s, 1H), 7.92 (dd, J = 8.5, 3.1 Hz, 1H), 7.83 (td, J = 8.5, 3.1 Hz, 1H), 4.11 (dp, J = 28.3, 7.4 Hz, 2H), 3.51 (d, J = 11.9 Hz, 1H), 3.01 (d, J = 10.1 Hz, 1H), 2.73 (s, 3H), 2.65 (d, J = 10.2 Hz, 1H), 2.43−2.25 (m, 1H), 2.04−1.79 (m, 3H), 1.72 (dq, J = 16.0, 8.5 Hz, 1H); ^{19}F NMR (376 MHz, DMSO-d_6): δ −112.96 (dt, J = 12.5, 6.1 Hz); HRMS (ES-API) m/z: calcd for $C_{16}H_{18}FN_5NaOS$ (M + Na), 370.1108; found, 370.1121.

7-Fluoro-4-(2-(piperidin-1-yl)ethyl)-1-thioxo-2,4-dihydro-[1,2,4]-triazolo[4,3-a]quinazolin-5(1H)-one (88). 6-Fluoro-3-(2-(piperidin-1-yl)ethyl)-2-thioxo-2,3-dihydroquinazolin-4(1H)-one was synthesized according to General Procedure B. Then, 7-fluoro-4-(2-(piperidin-1-yl)ethyl)-1-thioxo-2,4-dihydro-[1,2,4]triazolo[4,3-a]-quinazolin-5(1H)-one, di-TFA salt, was synthesized according to General Procedure D: ^{1}H NMR (400 MHz, DMSO-d_6): δ 10.31 (dd, J = 9.3, 4.6 Hz, 1H), 8.78 (s, 1H), 7.96 (dd, J = 8.5, 3.0 Hz, 1H), 7.86 (td, J = 8.6, 3.0 Hz, 1H), 4.41 (t, J = 6.1 Hz, 2H), 3.61 (s, 2H), 3.44 (s, 2H), 2.96 (s, 3H), 1.89−1.28 (m, 5H); ^{19}F NMR (376 MHz, DMSO-d_6): δ −112.56 (q, J = 7.4 Hz); HRMS (ES-API) m/z: calcd for $C_{16}H_{19}FN_5OS$ (M + H), 348.1289; found, 348.1305.

4-(2-(4,4-Difluoropiperidin-1-yl)ethyl)-7-fluoro-1-thioxo-2,4-di-hydro-[1,2,4]triazolo[4,3-a]quinazolin-5(1H)-one (89). 3-(2-(4,4-Difluoropiperidin-1-yl)ethyl)-6-fluoro-2-thioxo-2,3-dihydroquinazo-lin-4(1H)-one was synthesized according to General Procedure B.

Then, 4-(2-(4,4-difluoropiperidin-1-yl)ethyl)-7-fluoro-1-thioxo-2,4-di-hydro-[1,2,4]triazolo[4,3-a]quinazolin-5(1H)-one, di-TFA salt, was synthesized according to General Procedure D: ^{19}F NMR (376 MHz, DMSO-d_6): δ −95.47 (d, J = 213.5 Hz), −100.80 (d, J = 228.4 Hz), −112.68; HRMS (ES-API) m/z: calcd for $C_{16}H_{16}F_3N_5NaOS$ (M + Na), 406.0920; found, 406.0937.

7-Fluoro-4-(2-morpholinoethyl)-1-thioxo-2,4-dihydro-[1,2,4]-triazolo[4,3-a]quinazolin-5(1H)-one (90). 6-Fluoro-3-(2-morpholi-noethyl)-2-thioxo-2,3-dihydroquinazolin-4(1H)-one was synthesized according to General Procedure B. Then, 7-fluoro-4-(2-morpholi-noethyl)-1-thioxo-2,4-dihydro-[1,2,4]triazolo[4,3-a]quinazolin-5(1H)-one, di-TFA salt, was synthesized according to General Procedure D: ^{1}H NMR (400 MHz, DMSO-d_6): δ 10.31 (dd, J = 9.4, 4.5 Hz, 1H), 9.48 (s, 1H), 7.95 (dd, J = 8.6, 3.1 Hz, 1H), 7.86 (t, J = 8.9 Hz, 1H), 4.41 (s, 2H), 3.98 (s, 2H), 3.57 (dd, J = 25.5, 15.2 Hz, 2H), 3.35 (s, 4H), 3.18 (s, 2H); ^{19}F NMR (376 MHz, DMSO-d_6): δ −112.55; HRMS (ES-API) m/z: calcd for $C_{15}H_{17}FN_5O_2S$ (M + H), 350.1082; found, 350.1091.

7-Fluoro-4-(2-(4-methylpiperazin-1-yl)ethyl)-1-thioxo-2,4-dihy-dro-[1,2,4]triazolo[4,3-a]quinazolin-5(1H)-one (91). 6-Fluoro-3-(2-(4-methylpiperazin-1-yl)ethyl)-2-thioxo-2,3-dihydroquinazolin-4(1H)-one was synthesized according to General Procedure B. Then, 7-fluoro-4-(2-(4-methylpiperazin-1-yl)ethyl)-1-thioxo-2,4-dihydro-[1,2,4]triazolo[4,3-a]quinazolin-5(1H)-one, di-TFA salt, was synthe-sized according to General Procedure D: HRMS (ES-API) m/z: calcd for $C_{17}H_{18}F_3N_4OS$ (M + H), 363.1398; found, 363.1384.

tert-Butyl 4-(2-(7-fluoro-5-oxo-1-thioxo-1,2-dihydro-[1,2,4]-triazolo[4,3-a]quinazolin-4(5H)-yl)ethyl)piperazine-1-carboxylate (92). *tert*-Butyl 4-(2-(6-fluoro-4-oxo-2-thioxo-1,4-dihydroquinazolin-3(2H)-yl)ethyl)piperazine-1-carboxylate was synthesized according to General Procedure B. Then, *tert*-butyl 4-(2-(7-fluoro-5-oxo-1-thioxo-1,2-dihydro-[1,2,4]triazolo[4,3-a]quinazolin-4(5H)-yl)ethyl)-piperazine-1-carboxylate, di-TFA salt, was synthesized according to General Procedure D: HRMS (ES-API) m/z: calcd for $C_{20}H_{26}FN_6O_3S$ (M + H), 449.1766; found, 449.1786.

4-(2-(4,4-Difluorocyclohexyl)ethyl)-7-fluoro-1-thioxo-2,4-dihy-dro-[1,2,4]triazolo[4,3-a]quinazolin-5(1H)-one (93). 3-(2-(4,4-Difluorocyclohexyl)ethyl)-6-fluoro-2-thioxo-2,3-dihydroquinazolin-4(1H)-one was synthesized according to General Procedure B. Then, 4-(2-(4,4-difluorocyclohexyl)ethyl)-7-fluoro-1-thioxo-2,4-dihydro-[1,2,4]triazolo[4,3-a]quinazolin-5(1H)-one, TFA salt, was synthe-sized according to General Procedure D: ^{1}H NMR (400 MHz, DMSO-d_6): δ 10.28 (dd, J = 9.4, 4.6 Hz, 1H), 7.91 (dd, J = 8.7, 3.0 Hz, 1H), 7.84−7.74 (m, 1H), 4.05 (t, J = 7.4 Hz, 2H), 1.96 (d, J = 10.9 Hz, 2H), 1.88−1.58 (m, 6H), 1.46 (s, 1H), 1.16 (q, J = 12.3 Hz, 2H); ^{19}F NMR (376 MHz, DMSO-d_6): δ −89.54 (d, J = 231.6 Hz), −99.44 (d, J = 231.4 Hz), −113.14 (q, J = 7.1, 6.2 Hz); HRMS (ES-API) m/z: calcd for $C_{17}H_{18}F_3N_4OS$ (M + H), 383.1148; found, 383.1166.

1-Amino-N-(3-(7-fluoro-5-oxo-1-thioxo-1,2-dihydro-[1,2,4]-triazolo[4,3-a]quinazolin-4(5H)-yl)propyl)-3,6,9,12-tetraoxapenta-decan-15-amide (94). To a solution of **95** (0.025 g, 0.039 mmol) in DCM (0.195 mL) was added TFA (0.066 mL, 0.858 mmol) and the reaction stirred at RT overnight. The reaction was then blown down and redissolved. The crude material was purified by RP-ISCO (H_2O/MeCN + 0.2% NH_4OH, 10−100%) to give 1-amino-*N*-(3-(7-fluoro-5-oxo-1-thioxo-1,2-dihydro-[1,2,4]triazolo[4,3-a]quinazolin-4(5H)-yl)propyl)-3,6,9,12-tetraoxapentadecan-15-amide, di-TFA salt: ^{1}H NMR (400 MHz, CD_2Cl_2): δ 13.38 (s, 1H), 10.25 (dd, J = 9.3, 4.6 Hz, 1H), 8.04 (s, 3H), 7.95 (dd, J = 8.3, 3.0 Hz, 1H), 7.45 (ddd, J = 9.4, 7.5, 3.1 Hz, 1H), 7.40 (s, 1H), 5.53 (s, 1H), 4.21 (t, J = 6.7 Hz, 2H), 3.89−3.55 (m, 16H), 3.27 (d, J = 22.8 Hz, 4H), 2.57 (s, 2H), 2.01 (s, 2H); ^{19}F NMR (376 MHz, CD_2Cl_2): δ −112.54 (td, J = 7.9, 4.4 Hz).

tert-Butyl (19-(7-fluoro-5-oxo-1-thioxo-1,2-dihydro-[1,2,4]-triazolo[4,3-a]quinazolin-4(5H)-yl)-15-oxo-3,6,9,12-tetraoxa-16-azanonadecyl)carbamate (95). *tert*-Butyl (19-(7-fluoro-5-oxo-1-thioxo-1,2-dihydro-[1,2,4]triazolo[4,3-a]quinazolin-4(5H)-yl)-15-oxo-3,6,9,12-tetraoxa-16-azanonadecyl)carbamate, TFA salt, was synthesized according to General Procedure F.

(S)-22-Amino-1-(7-fluoro-5-oxo-1-thioxo-1,2-dihydro-[1,2,4]-triazolo[4,3-a]quinazolin-4(5H)-yl)-5,21-dioxo-8,11,14,17-tetraoxa-4,20-diazapentacosan-25-oic Acid (96) and tert-Butyl (S)-22-Amino-1-(7-fluoro-5-oxo-1-thioxo-1,2-dihydro-[1,2,4]triazolo[4,3-a]quinazolin-4(5H)-yl)-5,21-dioxo-8,11,14,17-tetraoxa-4,20-diazapentacosan-25-oate (97). tert-Butyl (S)-22-((tert-butoxycarbonyl)-amino)-1-(7-fluoro-5-oxo-1-thioxo-1,2-dihydro-[1,2,4]-triazolo[4,3-a]-quinazolin-4(5H)-yl)-5,21-dioxo-8,11,14,17-tetraoxa-4,20-diazapenta-cosan-25-oate: To a solution of 95 (0.04 g, 0.074 mmol) in DMF (0.190 mL) was added a solution of (S)-5-(tert-butoxy)-2-((tert-butoxycarbonyl)amino)-5-oxopentanoic acid (Boc-L-Glu-γ-t-Bu-ester, 0.067 g, 0.222 mmol) and COMU (0.063 g, 0.148 mmol) followed by DIPEA (0.013 mL, 0.074 mmol). The reaction was then stirred overnight at RT. The reaction was quenched with water and concentrated. The product was purified by RP-ISCO (H$_2$O/MeCN + 3.3% NH$_4$OH, 10−75%) to give the protected amino acid intermediate (0.0245 g, 40%): MS (ES-API) found (M + H), 826.2 and (M + Na), 848.1.

Compounds 96 and 97 were then prepared according to the following method. TFA (0.022 mL, 0.291 mmol) and triisopropylsilane (5.95 μL, 0.029 mmol) were added to a solution of the protected amino acid intermediate (0.012 g, 0.015 mmol) in DCM (0.145 mL). The reaction was stirred at RT for 2 h and concentrated. The mixture of products was purified by HPLC to give 96 (2 TFA) and 97 (2 TFA): 96: HRMS (ES-API) m/z: calcd for C$_{28}$H$_{41}$FN$_7$O$_9$S (M + H), 670.2665; found, 670.2672. 97: ^{1}H NMR (400 MHz, dmso): δ 10.29 (dd, J = 9.3, 4.7 Hz, 1H), 8.47 (t, J = 5.7 Hz, 1H), 8.07 (s, 3H), 7.91 (dd, J = 8.6, 3.1 Hz, 1H), 7.86 (s, 1H), 7.83−7.76 (m, 1H), 4.02 (t, J = 7.3 Hz, 2H), 3.72 (s, 1H), 3.56 (t, J = 6.5 Hz, 2H), 3.46−3.39 (m, 9H), 3.26−3.15 (m, 2H), 3.11 (q, J = 6.7 Hz, 2H), 2.27 (t, J = 7.2 Hz, 3H), 1.85 (dt, J = 23.5, 7.2 Hz, 3H), 1.37 (s, 9H); ^{19}F NMR (376 MHz, dmso): δ −113.13 (dd, J = 8.2, 4.8 Hz); HRMS (ES-API) m/z: calcd for C$_{32}$H$_{49}$FN$_7$O$_9$S (M + H), 726.3291; found, 726.3284.

3-(2-(2-(2-Aminoethoxy)ethoxy)ethoxy)-N-(3-(7-fluoro-5-oxo-1-thioxo-1,2-dihydro-[1,2,4]triazolo[4,3-a]quinazolin-4(5H)-yl)-propyl)propenamide (98). To a solution of 99 (0.1496 g, 0.251 mmol) in HCl in dioxane (0.627 mL, 2.507 mmol) was added triisopropylsilane (0.079 g, 0.501 mmol), and the solution was stirred at RT for 2 h and then concentrated. The product was purified by HPLC to give 3-(2-(2-(2-aminoethoxy)ethoxy)ethoxy)-N-(3-(7-fluoro-5-oxo-1-thioxo-1,2-dihydro-[1,2,4]triazolo[4,3-a]quinazolin-4(5H)-yl)propyl)propenamide, di-TFA salt: HRMS (ES-API) m/z: calcd for C$_{21}$H$_{30}$FN$_6$O$_5$S (M + H), 497.1977; found, 497.1973.

tert-Butyl (16-(7-fluoro-5-oxo-1-thioxo-1,2-dihydro-[1,2,4]-triazolo[4,3-a]quinazolin-4(5H)-yl)-12-oxo-3,6,9-trioxa-13-azahexadecyl)carbamate (99). tert-Butyl (16-(7-fluoro-5-oxo-1-thioxo-1,2-dihydro-[1,2,4]triazolo[4,3-a]quinazolin-4(5H)-yl)-12-oxo-3,6,9-trioxa-13-azahexadecyl)carbamate, TFA salt, was synthesized according to General Procedure F: HRMS (ES-API) m/z: calcd for C$_{26}$H$_{37}$FN$_6$NaO$_7$S (M + Na), 619.2321; found, 619.2330.

6-Amino-N-(3-(7-fluoro-5-oxo-1-thioxo-1,2-dihydro-[1,2,4]-triazolo[4,3-a]quinazolin-4(5H)-yl)propyl)hexanamide (100). Triisopropylsilane (0.031 g, 0.193 mmol) was added to a solution of 101 (0.049 g, 0.097 mmol) in HCl in dioxane (0.242 mL, 0.967 mmol), and the solution was stirred at RT for 2 h. The reaction was concentrated and purified by HPLC to give 6-amino-N-(3-(7-fluoro-5-oxo-1-thioxo-1,2-dihydro-[1,2,4]triazolo[4,3-a]quinazolin-4(5H)-yl)propyl)hexanamide, di-TFA salt: ^{1}H NMR (400 MHz, dmso): δ 10.29 (dd, J = 9.3, 4.7 Hz, 1H), 7.91 (dd, J = 8.6, 3.1 Hz, 1H), 7.81 (td, J = 7.9, 2.9 Hz, 2H), 7.61 (s, 3H), 4.02 (t, J = 7.4 Hz, 2H), 3.11 (q, J = 6.6 Hz, 2H), 2.75 (h, J = 6.0 Hz, 2H), 2.03 (t, J = 7.3 Hz, 2H), 1.82 (p, J = 7.2 Hz, 2H), 1.55−1.41 (m, 4H), 1.31−1.19 (m, 2H); ^{19}F NMR (376 MHz, dmso): δ −113.13 (td, J = 8.3, 4.8 Hz); HRMS (ES-API) m/z: calcd for C$_{18}$H$_{23}$FN$_6$NaO$_2$S (M + Na), 430.1506; found, 430.1512.

tert-Butyl (6-((3-(7-fluoro-5-oxo-1-thioxo-1,2-dihydro-[1,2,4]-triazolo[4,3-a]quinazolin-4(5H)-yl)propyl)amino)-6-oxohexyl)-carbamate (101). tert-Butyl (6-((3-(7-fluoro-5-oxo-1-thioxo-1,2-dihydro-[1,2,4]triazolo[4,3-a]quinazolin-4(5H)-yl)propyl)amino)-6-oxohexyl)carbamate was synthesized according to General Procedure F: ^{1}H NMR (400 MHz, DMSO-d$_6$): δ 10.29 (dd, J = 9.3, 4.7 Hz, 1H), 7.91 (dd, J = 8.5, 3.1 Hz, 1H), 7.80 (ddd, J = 9.1, 7.8, 2.8 Hz, 2H), 6.73 (t, J = 5.6 Hz, 1H), 4.02 (dd, J = 8.3, 6.3 Hz, 2H), 3.10 (q, J = 6.6 Hz, 2H), 2.86 (q, J = 6.6 Hz, 2H), 2.00 (t, J = 7.4 Hz, 2H), 1.82 (p, J = 7.0 Hz, 2H), 1.44 (p, J = 7.4 Hz, 2H), 1.37−1.27 (m, 11H), 1.24−1.11 (m, 2H); ^{19}F NMR (376 MHz, DMSO-d$_6$): δ −113.19; HRMS (ES-API) m/z: calcd for C$_{23}$H$_{31}$FN$_6$NaO$_4$S (M + Na), 529.2004; found, 529.1994.

tert-Butyl (R)-4-((tert-butoxycarbonyl)amino)-5-((3-(7-fluoro-5-oxo-1-thioxo-1,2-dihydro-[1,2,4]triazolo[4,3-a]quinazolin-4(5H)-yl)propyl)amino)-5-oxopentanoate (102). tert-Butyl (R)-4-((tert-butoxycarbonyl)amino)-5-((3-(7-fluoro-5-oxo-1-thioxo-1,2-dihydro-[1,2,4]triazolo[4,3-a]quinazolin-4(5H)-yl)propyl)amino)-5-oxopen-tanoate, TFA salt, was synthesized according to General Procedure F: ^{1}H NMR (400 MHz, DMSO-d$_6$): δ 10.29 (dd, J = 9.3, 4.7 Hz, 1H), 7.90 (dd, J = 8.6, 3.1 Hz, 1H), 7.85−7.76 (m, 2H), 6.82 (d, J = 8.2 Hz, 1H), 4.03 (t, J = 7.2 Hz, 2H), 3.90−3.80 (m, 1H), 3.12 (dp, J = 20.2, 6.6 Hz, 2H), 2.18 (t, J = 7.7 Hz, 2H), 1.83 (dt, J = 13.7, 6.5 Hz, 3H), 1.66 (dt, J = 14.3, 7.6 Hz, 1H), 1.36 (s, 9H), 1.35 (s, 9H); ^{19}F NMR (376 MHz, DMSO-d$_6$): δ −113.21 (t, J = 6.8 Hz); HRMS (ES-API) m/z: calcd for C$_{26}$H$_{35}$FN$_6$NaO$_6$S (M + Na), 601.2215; found, 601.2214.

tert-Butyl (S)-4-((tert-butoxycarbonyl)amino)-5-((3-(7-fluoro-5-oxo-1-thioxo-1,2-dihydro-[1,2,4]triazolo[4,3-a]quinazolin-4(5H)-yl)propyl)amino)-5-oxopentanoate (103). tert-Butyl (S)-4-((tert-butoxycarbonyl)amino)-5-((3-(7-fluoro-5-oxo-1-thioxo-1,2-dihydro-[1,2,4]triazolo[4,3-a]quinazolin-4(5H)-yl)propyl)amino)-5-oxopen-tanoate, TFA salt, was synthesized according to General Procedure F: ^{19}F NMR (376 MHz, DMSO-d$_6$): δ −113.15 (d, J = 11.0 Hz); HRMS (ES-API) m/z: calcd for C$_{26}$H$_{35}$FN$_6$NaO$_6$S (M + Na), 601.2215; found, 601.2216.

tert-Butyl (S)-4-Amino-5-((3-(7-fluoro-5-oxo-1-thioxo-1,2-dihydro-[1,2,4]quinazolin-4(5H)-yl)propyl)amino)-5-oxopentanoate (104) and (S)-4-Amino-5-((3-(7-fluoro-5-oxo-1-thioxo-1,2-dihydro-[1,2,4]triazolo[4,3-a]quinazolin-4(5H)-yl)propyl)-amino)-5-oxopentanoic Acid (105). TFA (0.041 mL, 0.532 mmol) and triisopropylsilane (10.90 μL, 0.053 mmol) were added to a solution of 103 (0.0154 g, 0.027 mmol) in DCM (0.266 mL). The reaction was stirred at RT for 2 h and concentrated. The products were purified by HPLC to give tert-butyl (S)-4-amino-5-((3-(7-fluoro-5-oxo-1-thioxo-1,2-dihydro-[1,2,4]triazolo[4,3-a]quinazolin-4(5H)-yl)propyl)amino)-5-oxopentanoate, di-TFA salt, and (S)-4-amino-5-((3-(7-fluoro-5-oxo-1-thioxo-1,2-dihydro-[1,2,4]triazolo[4,3-a]-quinazolin-4(5H)-yl)propyl)amino)-5-oxopentanoic acid; 104: ^{1}H NMR (400 MHz, DMSO-d$_6$): δ 10.30 (dd, J = 9.3, 4.8 Hz, 1H), 8.25 (s, 3H), 8.01 (t, J = 5.7 Hz, 1H), 7.91 (dd, J = 8.6, 3.1 Hz, 1H), 7.82 (ddd, J = 9.3, 8.0, 3.1 Hz, 1H), 4.07−3.99 (m, 2H), 3.92 (t, J = 6.3 Hz, 1H), 3.13 (q, J = 6.7 Hz, 2H), 2.22 (ddt, J = 22.8, 15.3, 7.4 Hz, 2H), 1.95 (q, J = 7.4 Hz, 2H), 1.85 (p, J = 7.1 Hz, 2H), 1.45 (s, 9H); ^{19}F NMR (376 MHz, DMSO-d$_6$): δ −113.12 (dt, J = 7.8, 4.1 Hz); HRMS (ES-API) m/z: calcd for C$_{21}$H$_{28}$FN$_6$O$_4$S (M + H), 479.1871; found, 479.1866. 105: ^{1}H NMR (400 MHz, DMSO-d$_6$): δ 10.31 (dd, J = 9.3, 4.7 Hz, 1H), 8.26 (s, 3H), 8.02 (t, J = 5.7 Hz, 1H), 7.92 (dd, J = 8.5, 3.1 Hz, 1H), 7.83 (ddd, J = 9.3, 8.0, 3.1 Hz, 1H), 4.05 (dd, J = 8.1, 6.4 Hz, 2H), 3.93 (t, J = 6.6 Hz, 1H), 3.15 (q, J = 6.7 Hz, 2H), 2.54 (s, 0H), 2.24 (ddt, J = 23.0, 15.4, 7.5 Hz, 2H), 1.97 (q, J = 7.4 Hz, 2H), 1.86 (p, J = 7.2 Hz, 2H), 1.46 (s, 9H); ^{19}F NMR (376 MHz, DMSO-d$_6$): δ −113.10 (td, J = 8.2, 4.8 Hz); HRMS (ES-API) m/z: calcd for C$_{17}$H$_{20}$FN$_6$O$_4$S (M + H), 423.1245; found, 423.1232.

4-((3-(7-Fluoro-5-oxo-1-thioxo-1,2-dihydro-[1,2,4]triazolo[4,3-a]quinazolin-4(5H)-yl)propyl)amino)-4-oxobutanoic Acid (106). 4-((3-(7-Fluoro-5-oxo-1-thioxo-1,2-dihydro-[1,2,4]triazolo[4,3-a]-quinazolin-4(5H)-yl)propyl)amino)-4-oxobutanoic acid, TFA salt, was synthesized according to General Procedure F: ^{1}H NMR (400 MHz, DMSO-d$_6$): δ 10.34 (s, 1H), 7.92 (dd, J = 8.6, 3.1 Hz, 1H), 7.86 (t, J = 5.6 Hz, 1H), 7.80 (ddd, J = 9.3, 8.0, 3.1 Hz, 1H), 4.05 (t, J = 7.3 Hz, 2H), 3.12 (q, J = 6.7 Hz, 2H), 2.45−2.37 (m, 2H), 2.32−2.24 (m, 3H), 1.84 (p, J = 7.1 Hz, 2H); ^{19}F NMR (376 MHz, DMSO-d$_6$): δ −113.28; HRMS (ES-API) m/z: calcd for C$_{16}$H$_{17}$FN$_5$O$_4$S (M + H), 394.0980; found, 394.0979.

W

N-(3-(7-Fluoro-5-oxo-1-thioxo-1,2-dihydro-[1,2,4]triazolo[4,3-a]quinazolin-4(5H)-yl)propyl)-4-sulfamoylbutanamide (**107**). *N*-(3-(7-Fluoro-5-oxo-1-thioxo-1,2-dihydro-[1,2,4]triazolo[4,3-*a*]quinazolin-4(5H)-yl)propyl)-4-sulfamoylbutanamide, TFA salt, was synthesized according to General Procedure F: ^{1}H NMR (400 MHz, DMSO-d_6): δ 10.31 (dd, J = 9.3, 4.7 Hz, 1H), 7.93 (dd, J = 8.6, 3.1 Hz, 1H), 7.87 (t, J = 5.6 Hz, 1H), 7.85–7.78 (m, 1H), 6.75 (s, 2H), 4.05 (dd, J = 8.1, 6.3 Hz, 2H), 3.13 (q, J = 6.6 Hz, 2H), 3.00–2.92 (m, 2H), 2.20 (t, J = 7.4 Hz, 2H), 1.94–1.81 (m, 4H); ^{19}F NMR (376 MHz, DMSO-d_6): δ −113.14; HRMS (ES-API) *m/z*: calcd for $C_{16}H_{20}FN_6O_4S_2$ (M + H), 443.0966; found, 443.0977.

N-(3-(7-Fluoro-5-oxo-1-thioxo-1,2-dihydro-[1,2,4]triazolo[4,3-a]quinazolin-4(5H)-yl)propyl)cyclopentanecarboxamide (**108**). *N*-(3-(7-Fluoro-5-oxo-1-thioxo-1,2-dihydro-[1,2,4]triazolo[4,3-*a*]quinazolin-4(5H)-yl)propyl)cyclopentanecarboxamide, TFA salt, was synthesized according to General Procedure F: ^{1}H NMR (400 MHz, DMSO-d_6): δ 10.29 (dd, J = 9.3, 4.7 Hz, 1H), 7.91 (dd, J = 8.6, 3.1 Hz, 1H), 7.80 (ddd, J = 9.3, 8.0, 3.1 Hz, 1H), 7.75 (t, J = 5.6 Hz, 1H), 4.02 (dd, J = 8.2, 6.5 Hz, 2H), 3.10 (q, J = 6.6 Hz, 2H), 1.82 (p, J = 7.0 Hz, 2H), 1.73–1.63 (m, 2H), 1.63–1.51 (m, 4H), 1.50–1.40 (m, 2H); ^{19}F NMR (376 MHz, DMSO-d_6): δ −113.19 (td, J = 8.2, 4.6 Hz); HRMS (ES-API) *m/z*: calcd for $C_{18}H_{21}FN_5O_2S$ (M + H), 390.1395; found, 390.1387.

trans-4-(*tert*-Butyl)-*N*-(3-(7-fluoro-5-oxo-1-thioxo-1,2-dihydro-[1,2,4]triazolo[4,3-a]quinazolin-4(5H)-yl)propyl)cyclohexane-1-carboxamide (**109**). *trans*-4-(*tert*-Butyl)-*N*-(3-(7-fluoro-5-oxo-1-thioxo-1,2-dihydro-[1,2,4]triazolo[4,3-*a*]quinazolin-4(5H)-yl)propyl)cyclohexane-1-carboxamide, TFA salt, was synthesized according to General Procedure F: ^{1}H NMR (400 MHz, DMSO-d_6): δ 10.29 (dd, J = 9.3, 4.7 Hz, 1H), 7.91 (dd, J = 8.6, 3.1 Hz, 1H), 7.80 (ddd, J = 9.3, 8.0, 3.1 Hz, 1H), 7.67 (t, J = 5.7 Hz, 1H), 4.01 (dd, J = 8.4, 6.4 Hz, 2H), 3.09 (q, J = 6.5 Hz, 2H), 1.93 (td, J = 12.2, 2.9 Hz, 1H), 1.81 (p, J = 6.9 Hz, 2H), 1.73 (d, J = 9.8 Hz, 4H), 1.26 (q, J = 12.2 Hz, 2H), 0.97–0.87 (m, 3H), 0.80 (s, 9H); ^{19}F NMR (376 MHz, DMSO-d_6): δ −113.21 (td, J = 8.3, 4.6 Hz); HRMS (ES-API) *m/z*: calcd for $C_{23}H_{31}FN_5O_2S$ (M + H), 460.2177; found, 460.2177.

tert-Butyl (4-((3-(7-fluoro-5-oxo-1-thioxo-1,2-dihydro-[1,2,4]triazolo[4,3-a]quinazolin-4(5H)-yl)propyl)carbamoyl)cyclohexyl)carbamate (**110**). *tert*-Butyl (4-((3-(7-fluoro-5-oxo-1-thioxo-1,2-dihydro-[1,2,4]triazolo[4,3-*a*]quinazolin-4(5H)-yl)propyl)carbamoyl)cyclohexyl)carbamate, di-TFA salt, was synthesized according to General Procedure F: ^{1}H NMR (400 MHz, DMSO-d_6): δ 10.29 (dd, J = 9.3, 4.7 Hz, 1H), 7.91 (dd, J = 8.6, 3.1 Hz, 1H), 7.80 (ddd, J = 9.4, 8.0, 3.2 Hz, 1H), 7.67 (t, J = 5.7 Hz, 1H), 6.65 (d, J = 6.5 Hz, 1H), 4.06–3.98 (m, 2H), 3.43 (s, 1H), 3.11 (q, J = 6.5 Hz, 2H), 2.10 (dq, J = 12.2, 3.8 Hz, 1H), 1.82 (p, J = 7.7, 7.3 Hz, 2H), 1.77–1.68 (m, 1H), 1.64–1.53 (m, 2H), 1.47–1.37 (m, 5H), 1.36 (s, 9H); ^{19}F NMR (376 MHz, DMSO-d_6): δ −113.17 (td, J = 8.3, 4.8 Hz); HRMS (ES-API) *m/z*: calcd for $C_{24}H_{31}FN_6NaO_4S$ (M + Na), 541.2004; found, 541.2011.

4-Amino-*N*-(3-(7-fluoro-5-oxo-1-thioxo-1,2-dihydro-[1,2,4]triazolo[4,3-a]quinazolin-4(5H)-yl)propyl)cyclohexane-1-carboxamide (**111**). *tert*-Butyl (4-((3-(7-fluoro-5-oxo-1-thioxo-1,2-dihydro-[1,2,4]triazolo[4,3-*a*]quinazolin-4(5H)-yl)propyl)carbamoyl)cyclohexyl)carbamate (0.0282 g, 0.054 mmol) was dissolved in HCl in dioxane (0.136 mL, 0.544 mmol) and the solution stirred at RT for 2 h. The reaction was concentrated and purified by HPLC to give 4-amino-*N*-(3-(7-fluoro-5-oxo-1-thioxo-1,2-dihydro-[1,2,4]triazolo[4,3-*a*]quinazolin-4(5H)-yl)propyl)cyclohexane-1-carboxamide, di-TFA salt: ^{1}H NMR (400 MHz, DMSO-d_6): δ 10.31 (dd, J = 9.3, 4.7 Hz, 1H), 7.93 (dd, J = 8.5, 3.1 Hz, 1H), 7.88–7.76 (m, 2H), 7.71 (s, 3H), 4.04 (dd, J = 8.3, 6.4 Hz, 2H), 3.14 (q, J = 6.6 Hz, 2H), 2.33–2.23 (m, 0H), 1.91–1.78 (m, 5H), 1.72–1.63 (m, 6H), 1.58–1.47 (m, 1H); ^{19}F NMR (376 MHz, DMSO-d_6): δ −113.09 (td, J = 8.4, 4.8 Hz); HRMS (ES-API) *m/z*: calcd for $C_{19}H_{24}FN_6O_2S$ (M + H), 419.1660; found, 419.1642.

N-(3-(7-Fluoro-5-oxo-1-thioxo-1,2-dihydro-[1,2,4]triazolo[4,3-a]quinazolin-4(5H)-yl)propyl)piperidine-2-carboxamide (**112**). *tert*-Butyl 2-((3-(7-fluoro-5-oxo-1-thioxo-1,2-dihydro-[1,2,4]triazolo[4,3-*a*]quinazolin-4(5H)-yl)propyl)carbamoyl)piperidine-1-carboxylate was synthesized according to General Procedure F. Then, *N*-(3-(7-fluoro-5-oxo-1-thioxo-1,2-dihydro-[1,2,4]triazolo[4,3-*a*]quinazolin-4(5H)-yl)propyl)piperidine-2-carboxamide was synthesized as follows: *tert*-butyl 2-((3-(7-fluoro-5-oxo-1-thioxo-1,2-dihydro-[1,2,4]triazolo[4,3-*a*]quinazolin-4(5H)-yl)propyl)carbamoyl)piperidine-1-carboxylate (0.172 g, 0.341 mmol) was dissolved in HCl in dioxane (0.852 mL, 3.41 mmol) and the solution stirred at RT for 2 h. The reaction was concentrated and purified by HPLC (H$_2$O + 0.1% NH$_4$OH/MeCN, 10–50%, 8 min, Waters XBridge Prep C18 OBD, 5 μm, 30 × 75 mm) to give *N*-(3-(7-fluoro-5-oxo-1-thioxo-1,2-dihydro-[1,2,4]triazolo[4,3-*a*]quinazolin-4(5H)-yl)propyl)piperidine-2-carboxamide: ^{1}H NMR (400 MHz, dmso): δ 10.46 (dd, J = 9.3, 4.8 Hz, 1H), 8.28–8.22 (m, 1H), 7.87 (dd, J = 8.6, 3.2 Hz, 1H), 7.77 (td, J = 8.7, 3.1 Hz, 1H), 4.07 (t, J = 7.2 Hz, 2H), 3.49 (s, 1H), 3.22–3.06 (m, 3H), 2.79 (t, J = 11.8 Hz, 1H), 2.00–1.93 (m, 1H), 1.91–1.82 (m, 2H), 1.76–1.71 (m, 1H), 1.61 (d, J = 12.4 Hz, 1H), 1.49–1.37 (m, 4H); HRMS (ES-API) *m/z*: calcd for $C_{18}H_{22}FN_6O_2S$ (M + H), 405.1503; found, 405.1517.

N-(3-(7-Fluoro-5-oxo-1-thioxo-1,2-dihydro-[1,2,4]triazolo[4,3-a]quinazolin-4(5H)-yl)propyl)piperidine-3-carboxamide (**113**). *tert*-Butyl 2-((3-(7-fluoro-5-oxo-1-thioxo-1,2-dihydro-[1,2,4]triazolo[4,3-*a*]quinazolin-4(5H)-yl)propyl)carbamoyl)piperidine-1-carboxylate was synthesized according to General Procedure F. Then, *N*-(3-(7-fluoro-5-oxo-1-thioxo-1,2-dihydro-[1,2,4]triazolo[4,3-*a*]quinazolin-4(5H)-yl)propyl)piperidine-3-carboxamide was synthesized as follows: *tert*-butyl 3-((3-(7-fluoro-5-oxo-1-thioxo-1,2-dihydro-[1,2,4]triazolo[4,3-*a*]quinazolin-4(5H)-yl)propyl)carbamoyl)piperidine-1-carboxylate (0.172 g, 0.341 mmol) was dissolved in HCl in dioxane (0.852 mL, 3.41 mmol) and the solution stirred at RT for 2 h. The reaction was concentrated and purified by HPLC (H$_2$O + 0.1% NH$_4$OH/MeCN, 10–50%, 8 min, Waters XBridge Prep C18 OBD, 5 μm, 30 × 75 mm) to give *N*-(3-(7-fluoro-5-oxo-1-thioxo-1,2-dihydro-[1,2,4]triazolo[4,3-*a*]quinazolin-4(5H)-yl)propyl)piperidine-3-carboxamide: ^{1}H NMR (400 MHz, dmso): δ 10.43 (s, 1H), 8.14 (t, J = 5.8 Hz, 1H), 7.87 (dd, J = 8.6, 3.2 Hz, 1H), 7.82–7.73 (m, 1H), 4.05 (t, J = 7.5 Hz, 2H), 3.11 (dq, J = 19.6, 7.8, 6.2 Hz, 5H), 2.96–2.90 (m, 1H), 2.89–2.80 (m, 2H), 1.84 (p, J = 7.1 Hz, 4H), 1.74 (app s, 1H), 1.56 (t, J = 9.7 Hz, 2H); HRMS (ES-API) *m/z*: calcd for $C_{18}H_{22}FN_6O_2S$ (M + H), 405.1503; found, 405.1491.

N-(3-(7-Fluoro-5-oxo-1-thioxo-1,2-dihydro-[1,2,4]triazolo[4,3-a]quinazolin-4(5H)-yl)propyl)piperidine-4-carboxamide (**114**). *tert*-Butyl 4-((3-(7-fluoro-5-oxo-1-thioxo-1,2-dihydro-[1,2,4]triazolo[4,3-*a*]quinazolin-4(5H)-yl)propyl)carbamoyl)piperidine-1-carboxylate was synthesized according to General Procedure F. Then, *N*-(3-(7-fluoro-5-oxo-1-thioxo-1,2-dihydro-[1,2,4]triazolo[4,3-*a*]quinazolin-4(5H)-yl)propyl)piperidine-4-carboxamide was synthesized as follows: *tert*-butyl 4-((3-(7-fluoro-5-oxo-1-thioxo-1,2-dihydro-[1,2,4]triazolo[4,3-*a*]quinazolin-4(5H)-yl)propyl)carbamoyl)piperidine-1-carboxylate (0.172 g, 0.341 mmol) was dissolved in HCl in dioxane (0.852 mL, 3.41 mmol) and the solution stirred at RT for 2 h. The reaction was concentrated and purified by HPLC (H$_2$O + 0.1% NH$_4$OH/MeCN, 10–50%, 8 min, Waters XBridge Prep C18 OBD, 5 μm, 30 × 75 mm) to give *N*-(3-(7-fluoro-5-oxo-1-thioxo-1,2-dihydro-[1,2,4]triazolo[4,3-*a*]quinazolin-4(5H)-yl)propyl)piperidine-4-carboxamide: ^{1}H NMR (400 MHz, dmso): δ 10.34 (s, 1H), 7.96 (t, J = 5.5 Hz, 1H), 7.91–7.87 (m, 1H), 7.83–7.76 (m, 1H), 4.02 (t, J = 7.4 Hz, 2H), 3.12 (dd, J = 12.4, 6.1 Hz, 2H), 2.87 (t, J = 12.2 Hz, 2H), 2.41–2.32 (m, 1H), 1.81 (d, J = 12.4 Hz, 5H), 1.69 (d, J = 13.1 Hz, 2H); HRMS (ES-API) *m/z*: calcd for $C_{18}H_{22}FN_6O_2S$ (M + H), 405.1503; found, 405.1511; purity (HPLC) 93.09%.

N-(3-(7-Fluoro-5-oxo-1-thioxo-1,2-dihydro-[1,2,4]triazolo[4,3-a]quinazolin-4(5H)-yl)propyl)tetrahydro-2H-pyran-4-carboxamide (**115**). *N*-(3-(7-Fluoro-5-oxo-1-thioxo-1,2-dihydro-[1,2,4]triazolo[4,3-*a*]quinazolin-4(5H)-yl)propyl)tetrahydro-2H-pyran-4-carboxamide, TFA salt, was synthesized according to General Procedure F: HRMS (ES-API) *m/z*: calcd for $C_{18}H_{21}FN_5O_3S$ (M + H), 406.1344; found, 406.1355.

N-(3-(7-Fluoro-5-oxo-1-thioxo-1,2-dihydro-[1,2,4]triazolo[4,3-a]quinazolin-4(5H)-yl)propyl)-2-(piperidin-4-yl)acetamide (**116**). *tert*-Butyl 4-(2-((3-(7-fluoro-5-oxo-1-thioxo-1,2-dihydro-[1,2,4]triazolo-[4,3-*a*]quinazolin-4(5H)-yl)propyl)amino)-2-oxoethyl)piperidine-1-

carboxylate was synthesized according to General Procedure F. Then, *N*-(3-(7-fluoro-5-oxo-1-thioxo-1,2-dihydro-[1,2,4]triazolo[4,3-*a*]-quinazolin-4(5*H*)-yl)propyl)-2-(piperidin-4-yl)acetamide was synthesized as follows: *tert*-butyl 4-(2-((3-(7-fluoro-5-oxo-1-thioxo-1,2-dihydro-[1,2,4]triazolo[4,3-*a*]quinazolin-4(5*H*)-yl)propyl)amino)-2-oxoethyl)piperidine-1-carboxylate (0.0209 g, 0.040 mmol) was dissolved in HCl in dioxane (0.101 mL, 0.403 mmol) and the solution stirred at RT for 2 h. The reaction was concentrated and purified by HPLC to give *N*-(3-(7-fluoro-5-oxo-1-thioxo-1,2-dihydro-[1,2,4]triazolo[4,3-*a*]quinazolin-4(5*H*)-yl)propyl)-2-(piperidin-4-yl)-acetamide, TFA: ^{1}H NMR (400 MHz, DMSO-d_6): δ 10.31 (dd, J = 9.3, 4.7 Hz, 1H), 8.43 (s, 1H), 8.12 (s, 1H), 7.96−7.89 (m, 2H), 7.83 (ddd, J = 9.3, 8.0, 3.1 Hz, 1H), 4.08−4.00 (m, 2H), 3.24 (d, J = 13.1 Hz, 2H), 3.13 (q, J = 6.6 Hz, 2H), 2.86 (dd, J = 21.5, 10.8 Hz, 3H), 2.02 (d, J = 7.0 Hz, 2H), 1.97−1.89 (m, 1H), 1.84 (p, J = 7.0 Hz, 2H), 1.77 (d, J = 14.0 Hz, 2H), 1.35−1.22 (m, 2H); ^{19}F NMR (376 MHz, DMSO-d_6): δ −113.06 to −113.17 (m).

N-(3-(7-Fluoro-5-oxo-1-thioxo-1,2-dihydro-[1,2,4]triazolo[4,3-a]-quinazolin-4(5H)-yl)propyl)-2-(4-methylpiperazin-1-yl)acetamide (**117**). *N*-(3-(7-Fluoro-5-oxo-1-thioxo-1,2-dihydro-[1,2,4]triazolo[4,3-*a*]quinazolin-4(5*H*)-yl)propyl)-2-(4-methylpiperazin-1-yl)acetamide, di-TFA salt, was synthesized according to General Procedure F: ^{1}H NMR (400 MHz, DMSO-d_6): δ 10.30 (dd, J = 9.3, 4.7, 1H), 9.49 (s, 1H), 7.97 (t, J = 5.5 Hz, 1H), 7.93 (dd, J = 8.5, 3.1 Hz, 1H), 7.82 (ddd, J = 9.3, 8.0, 3.2 Hz, 1H), 4.02 (t, J = 7.2 Hz, 2H), 3.40 (d, J = 10.2 Hz, 1H), 3.21−3.11 (m, 2H), 3.08 (s, 4H), 2.99 (d, J = 13.1 Hz, 3H), 2.78 (s, 3H), 1.84 (p, J = 6.8 Hz, 2H); ^{19}F NMR (376 MHz, DMSO-d_6): δ −113.07 (td, J = 8.2, 4.6 Hz); HRMS (ES-API) m/z: calcd for $C_{19}H_{25}FN_7O_2S$ (M + H), 434.1769; found, 434.1763.

N-(3-(7-Fluoro-5-oxo-1-thioxo-1,2-dihydro-[1,2,4]triazolo[4,3-a]-quinazolin-4(5H)-yl)propyl)-2-morpholinoacetamide (**118**). *N*-(3-(7-Fluoro-5-oxo-1-thioxo-1,2-dihydro-[1,2,4]triazolo[4,3-*a*]-quinazolin-4(5*H*)-yl)propyl)-2-morpholinoacetamide, di-TFA salt, was synthesized according to General Procedure F: ^{1}H NMR (400 MHz, DMSO-d_6): δ 10.29 (dd, J = 9.3, 4.7 Hz, 1H), 10.18 (s, 1H), 8.55 (s, 1H), 7.92 (dd, J = 8.6, 3.1 Hz, 1H), 7.82 (ddd, J = 9.3, 8.0, 3.1 Hz, 1H), 4.05 (t, J = 7.1 Hz, 2H), 3.97−3.67 (m, 8H), 3.22 (q, J = 6.6 Hz, 2H), 1.89 (p, J = 7.1 Hz, 2H); ^{19}F NMR (376 MHz, DMSO-d_6): δ −113.07 (td, J = 8.3, 4.6 Hz); HRMS (ES-API) m/z: calcd for $C_{18}H_{22}FN_6O_3S$ (M + H), 421.1453; found, 421.1449.

4-((1H-Imidazole-1-yl)methyl)-N-(3-(7-fluoro-5-oxo-1-thioxo-1,2-dihydro-[1,2,4]triazolo[4,3-a]quinazolin-4(5H)-yl)propyl)-benzamide (**119**). 4-((1*H*-Imidazol-1-yl)methyl)-*N*-(3-(7-fluoro-5-oxo-1-thioxo-1,2-dihydro-[1,2,4]triazolo[4,3-*a*]quinazolin-4(5*H*)-yl)-propyl)benzamide, TFA salt, was synthesized according to General Procedure F: ^{1}H NMR (400 MHz, DMSO-d_6): δ 10.30 (dd, J = 9.3, 4.7 Hz, 1H), 9.13 (t, J = 1.5 Hz, 1H), 8.52 (t, J = 5.7 Hz, 1H), 7.91 (dd, J = 8.5, 3.1 Hz, 1H), 7.86−7.77 (m, 3H), 7.75 (t, J = 1.7 Hz, 1H), 7.64 (t, J = 1.6 Hz, 1H), 7.57−7.45 (m, 2H), 5.46 (s, 2H), 4.11 (dd, J = 8.3, 6.3 Hz, 2H), 3.37−3.33 (m, 2H), 1.99 (p, J = 7.0 Hz, 2H); ^{19}F NMR (376 MHz, DMSO-d_6): δ −113.10 (td, J = 8.3, 4.7 Hz); HRMS (ES-API) m/z: calcd for $C_{23}H_{21}FN_7O_2S$ (M + H), 478.1456; found, 478.1454.

N-(3-(7-Fluoro-5-oxo-1-thioxo-1,2-dihydro-[1,2,4]triazolo[4,3-a]-quinazolin-4(5H)-yl)propyl)-2-phenylacetamide (**120**). *N*-(3-(7-Fluoro-5-oxo-1-thioxo-1,2-dihydro-[1,2,4]triazolo[4,3-*a*]quinazolin-4(5*H*)-yl)propyl)-2-phenylacetamide was synthesized according to General Procedure F: ^{1}H NMR (400 MHz, DMSO-d_6): δ 10.31 (dd, J = 9.3, 4.7 Hz, 1H), 8.05 (t, J = 5.7 Hz, 1H), 7.92 (dd, J = 8.6, 3.1 Hz, 1H), 7.81 (ddd, J = 9.3, 8.0, 3.1 Hz, 1H), 7.33−7.15 (m, 5H), 4.04 (dd, J = 8.2, 6.4 Hz, 2H), 3.38 (s, 2H), 3.14 (q, J = 6.7 Hz, 2H), 1.86 (p, J = 7.2 Hz, 2H); ^{19}F NMR (376 MHz, DMSO-d_6): δ −113.17 (td, J = 8.3, 4.8 Hz); HRMS (ES-API) m/z: calcd for $C_{19}H_{17}FN_5O_2S$ (M + H), 398.1082; found, 398.1063.

3-(3,5-Dimethylisoxazol-4-yl)-N-(3-(7-fluoro-5-oxo-1-thioxo-1,2-dihydro-[1,2,4]triazolo[4,3-a]quinazolin-4(5H)-yl)propyl)-propenamide (**121**). 3-(3,5-Dimethylisoxazol-4-yl)-*N*-(3-(7-fluoro-5-oxo-1-thioxo-1,2-dihydro-[1,2,4]triazolo[4,3-*a*]quinazolin-4(5*H*)-yl)-propyl)propenamide, TFA salt, was synthesized according to General Procedure F: ^{1}H NMR (400 MHz, DMSO-d_6): δ 10.31 (dd, J = 9.3, 4.7 Hz, 1H), 7.92 (dd, J = 8.6, 3.0 Hz, 1H), 7.85−7.78 (m, 2H), 4.01

(t, J = 7.2 Hz, 2H), 3.32−3.23 (m, 2H), 3.10 (q, J = 6.7 Hz, 2H), 2.25 (s, 3H), 2.19 (dd, J = 7.9, 7.0 Hz, 2H), 2.13 (s, 3H), 1.81 (p, J = 7.0 Hz, 2H); ^{19}F NMR (376 MHz, DMSO-d_6): δ −113.14 (dd, J = 8.3, 5.0 Hz); HRMS (ES-API) m/z: calcd for $C_{20}H_{22}FN_6O_3S$ (M + H), 445.1453; found, 445.1475.

N-(3-(7-Fluoro-5-oxo-1-thioxo-1,2-dihydro-[1,2,4]triazolo[4,3-a]-quinazolin-4(5H)-yl)propyl)-2-(3-fluorophenyl)acetamide (**122**). *N*-(3-(7-Fluoro-5-oxo-1-thioxo-1,2-dihydro-[1,2,4]triazolo[4,3-*a*]-quinazolin-4(5*H*)-yl)propyl)-2-(3-fluorophenyl)acetamide, TFA salt, was synthesized according to General Procedure F: ^{1}H NMR (400 MHz, DMSO-d_6): δ 10.29 (dd, J = 9.3, 4.7 Hz, 1H), 8.08 (t, J = 5.6 Hz, 1H), 7.90 (dd, J = 8.6, 3.1 Hz, 1H), 7.80 (ddd, J = 9.3, 8.0, 3.1 Hz, 1H), 7.31 (td, J = 8.1, 6.5 Hz, 1H), 7.08−6.99 (m, 3H), 4.03 (t, J = 7.3 Hz, 2H), 3.40 (s, 2H), 3.13 (q, J = 6.6 Hz, 2H), 1.84 (p, J = 7.1 Hz, 2H); ^{19}F NMR (376 MHz, DMSO-d_6): δ −113.19 (q, J = 7.7, 7.1 Hz), −113.86 to −113.98 (m); HRMS (ES-API) m/z: calcd for $C_{20}H_{18}F_2N_5O_2S$ (M + H), 430.1144; found, 430.1153.

N-(3-(7-Fluoro-5-oxo-1-thioxo-1,2-dihydro-[1,2,4]triazolo[4,3-a]-quinazolin-4(5H)-yl)propyl)-2-(4-fluorophenyl)acetamide (**123**). *N*-(3-(7-Fluoro-5-oxo-1-thioxo-1,2-dihydro-[1,2,4]triazolo[4,3-*a*]-quinazolin-4(5*H*)-yl)propyl)-2-(4-fluorophenyl)acetamide, TFA salt, was synthesized according to General Procedure F: ^{1}H NMR (400 MHz, DMSO-d_6): δ 10.29 (dd, J = 9.4, 4.7 Hz, 1H), 8.05 (t, J = 5.7 Hz, 1H), 7.91 (dd, J = 8.6, 3.1 Hz, 1H), 7.80 (ddd, J = 9.3, 8.0, 3.1 Hz, 1H), 7.30−7.22 (m, 2H), 7.14−7.05 (m, 2H), 4.02 (t, J = 7.3 Hz, 2H), 3.36 (s, 2H), 3.12 (q, J = 6.6 Hz, 2H), 1.84 (p, J = 7.1 Hz, 2H); ^{19}F NMR (376 MHz, DMSO-d_6): δ −113.18 (td, J = 8.3, 4.8 Hz), −116.95 (ddd, J = 14.6, 9.1, 5.5 Hz); HRMS (ES-API) m/z: calcd for $C_{20}H_{18}F_2N_5O_2S$ (M + H), 430.1144; found, 430.1141; purity (HPLC) 93.64%.

2-(3-Chlorophenyl)-N-(3-(7-fluoro-5-oxo-1-thioxo-1,2-dihydro-[1,2,4]triazolo[4,3-a]quinazolin-4(5H)-yl)propyl)acetamide (**124**). 2-(3-Chlorophenyl)-*N*-(3-(7-fluoro-5-oxo-1-thioxo-1,2-dihydro-[1,2,4]triazolo[4,3-*a*]quinazolin-4(5*H*)-yl)propyl)acetamide, TFA salt, was synthesized according to General Procedure F: ^{1}H NMR (400 MHz, DMSO-d_6): δ 10.29 (dd, J = 9.3, 4.7 Hz, 1H), 8.09 (t, J = 5.7 Hz, 1H), 7.91 (dd, J = 8.6, 3.1 Hz, 1H), 7.80 (ddd, J = 9.3, 8.0, 3.1 Hz, 1H), 7.33−7.24 (m, 3H), 7.19 (dt, J = 7.5, 1.5 Hz, 1H), 4.03 (t, J = 7.2 Hz, 2H), 3.39 (s, 2H), 3.27 (s, 1H), 3.12 (q, J = 6.7 Hz, 2H), 1.85 (p, J = 7.2 Hz, 2H); ^{19}F NMR (376 MHz, DMSO-d_6): δ −113.19 (d, J = 10.0 Hz); HRMS (ES-API) m/z: calcd for $C_{20}H_{18}ClFN_5O_2S$ (M + H), 446.0848; found, 446.0867; purity (HPLC) 94.66%.

2-(4-Bromophenyl)-N-(3-(7-fluoro-5-oxo-1-thioxo-1,2-dihydro-[1,2,4]triazolo[4,3-a]quinazolin-4(5H)-yl)propyl)acetamide (**125**). 2-(4-Bromophenyl)-*N*-(3-(7-fluoro-5-oxo-1-thioxo-1,2-dihydro-[1,2,4]triazolo[4,3-*a*]quinazolin-4(5*H*)-yl)propyl)acetamide, TFA salt, was synthesized according to General Procedure F: ^{1}H NMR (400 MHz, DMSO-d_6): δ 10.29 (dd, J = 9.3, 4.6 Hz, 1H), 8.08 (t, J = 5.7 Hz, 1H), 7.91 (dd, J = 8.6, 3.1 Hz, 1H), 7.80 (ddd, J = 9.2, 7.9, 3.1 Hz, 1H), 7.50−7.42 (m, 2H), 7.22−7.15 (m, 2H), 4.02 (t, J = 7.3 Hz, 2H), 3.36 (s, 2H), 3.12 (q, J = 6.6 Hz, 2H), 1.84 (p, J = 7.0 Hz, 2H); ^{19}F NMR (376 MHz, DMSO-d_6): δ −113.19; purity (HPLC) 88.26%.

N-(3-(7-Fluoro-5-oxo-1-thioxo-1,2-dihydro-[1,2,4]triazolo[4,3-a]-quinazolin-4(5H)-yl)propyl)-2-(p-tolyl)acetamide (**126**). *N*-(3-(7-Fluoro-5-oxo-1-thioxo-1,2-dihydro-[1,2,4]triazolo[4,3-*a*]quinazolin-4(5*H*)-yl)propyl)-2-(*p*-tolyl)acetamide, TFA salt, was synthesized according to General Procedure F: ^{1}H NMR (400 MHz, DMSO-d_6): δ 10.29 (dd, J = 9.4, 4.6 Hz, 1H), 7.99 (t, J = 5.8 Hz, 1H), 7.91 (dd, J = 8.6, 3.1 Hz, 1H), 7.80 (ddd, J = 10.9, 8.0, 3.1 Hz, 1H), 7.09 (q, J = 8.0 Hz, 4H), 4.02 (t, J = 7.3 Hz, 2H), 3.11 (q, J = 6.6 Hz, 2H), 2.24 (s, 3H), 1.83 (p, J = 7.2 Hz, 2H); ^{19}F NMR (376 MHz, DMSO-d_6): δ −113.20; purity (HPLC) 89.66%.

N-(3-(7-Fluoro-5-oxo-1-thioxo-1,2-dihydro-[1,2,4]triazolo[4,3-a]-quinazolin-4(5H)-yl)propyl)-2-(4-hydroxyphenyl)acetamide (**127**). *N*-(3-(7-Fluoro-5-oxo-1-thioxo-1,2-dihydro-[1,2,4]triazolo[4,3-*a*]-quinazolin-4(5*H*)-yl)propyl)-2-(4-hydroxyphenyl)acetamide, TFA salt, was synthesized according to General Procedure F: ^{1}H NMR (400 MHz, DMSO-d_6): δ 10.29 (dd, J = 9.3, 4.7 Hz, 1H), 9.16 (s, 1H), 7.94−7.87 (m, 2H), 7.80 (ddd, J = 9.3, 8.0, 3.1 Hz, 1H), 7.04−

6.98 (m, 2H), 6.69−6.60 (m, 2H), 4.06−3.98 (m, 2H), 3.23 (s, 2H), 3.10 (q, J = 6.6 Hz, 2H), 1.83 (p, J = 7.2 Hz, 2H); ^{19}F NMR (376 MHz, DMSO-d_6): δ −113.19; purity (HPLC) 90.60%.

***N*-(3-(7-Fluoro-5-oxo-1-thioxo-1,2-dihydro-[1,2,4]triazolo[4,3-a]-quinazolin-4(5H)-yl)propyl)-2-(2-methoxyphenyl)acetamide (128).** *N*-(3-(7-Fluoro-5-oxo-1-thioxo-1,2-dihydro-[1,2,4]triazolo[4,3-*a*]-quinazolin-4(5*H*)-yl)propyl)-2-(2-methoxyphenyl)acetamide, TFA salt, was synthesized according to General Procedure F: ^{1}H NMR (400 MHz, DMSO-d_6): δ 10.29 (dd, J = 9.3, 4.7 Hz, 1H), 7.91 (dd, J = 8.6, 3.1 Hz, 1H), 7.80 (ddd, J = 9.2, 7.8, 3.0 Hz, 2H), 7.22−7.16 (m, 1H), 7.13 (dd, J = 7.5, 1.7 Hz, 1H), 6.92 (dd, J = 8.2, 1.1 Hz, 1H), 6.86 (td, J = 7.4, 1.1 Hz, 1H), 4.03 (t, J = 7.3 Hz, 2H), 3.74 (s, 3H), 3.34 (s, 2H), 3.13 (q, J = 6.6 Hz, 2H), 1.84 (p, J = 7.0 Hz, 2H); ^{19}F NMR (376 MHz, DMSO-d_6): δ −113.18 (td, J = 8.3, 4.7 Hz); HRMS (ES-API) m/z: calcd for $C_{21}H_{21}FN_5O_3S$ (M + H), 442.1344; found, 442.1360.

***N*-(3-(7-Fluoro-5-oxo-1-thioxo-1,2-dihydro-[1,2,4]triazolo[4,3-a]-quinazolin-4(5H)-yl)propyl)-2-(3-methoxyphenyl)acetamide (129).** *N*-(3-(7-Fluoro-5-oxo-1-thioxo-1,2-dihydro-[1,2,4]triazolo[4,3-*a*]-quinazolin-4(5*H*)-yl)propyl)-2-(3-methoxyphenyl)acetamide, TFA salt, was synthesized according to General Procedure F: ^{1}H NMR (400 MHz, DMSO-d_6): δ 10.29 (dd, J = 9.3, 4.6 Hz, 1H), 8.01 (t, J = 5.7 Hz, 1H), 7.91 (dd, J = 8.6, 3.1 Hz, 1H), 7.80 (ddd, J = 9.3, 8.0, 3.1 Hz, 1H), 7.22−7.13 (m, 1H), 6.82−6.73 (m, 3H), 4.03 (t, J = 7.2 Hz, 2H), 3.71 (s, 3H), 3.33 (s, 2H), 3.12 (q, J = 6.7 Hz, 2H), 1.84 (p, J = 7.2 Hz, 2H); ^{19}F NMR (376 MHz, DMSO-d_6): δ −113.19.

***N*-(3-(7-Fluoro-5-oxo-1-thioxo-1,2-dihydro-[1,2,4]triazolo[4,3-a]-quinazolin-4(5H)-yl)propyl)-2-(4-methoxyphenyl)acetamide (130).** *N*-(3-(7-Fluoro-5-oxo-1-thioxo-1,2-dihydro-[1,2,4]triazolo[4,3-*a*]-quinazolin-4(5*H*)-yl)propyl)-2-(4-methoxyphenyl)acetamide, TFA salt, was synthesized according to General Procedure F: ^{1}H NMR (400 MHz, DMSO-d_6): δ 10.29 (dd, J = 9.3, 4.7 Hz, 1H), 7.96 (t, J = 5.8 Hz, 1H), 7.91 (dd, J = 8.6, 3.1 Hz, 1H), 7.80 (ddd, J = 9.3, 8.0, 3.1 Hz, 1H), 7.17−7.09 (m, 2H), 6.87−6.79 (m, 2H), 4.02 (t, J = 7.3 Hz, 2H), 3.69 (s, 3H), 3.29 (s, 2H), 3.11 (q, J = 6.6 Hz, 2H), 1.83 (p, J = 7.1 Hz, 2H); ^{19}F NMR (376 MHz, DMSO-d_6): δ −113.19 (td, J = 8.2, 4.7 Hz).

***N*-(3-(7-Fluoro-5-oxo-1-thioxo-1,2-dihydro-[1,2,4]triazolo[4,3-a]-quinazolin-4(5H)-yl)propyl)-2-(2-(trifluoromethyl)phenyl)-acetamide (131).** *N*-(3-(7-Fluoro-5-oxo-1-thioxo-1,2-dihydro-[1,2,4]triazolo[4,3-*a*]quinazolin-4(5*H*)-yl)propyl)-2-(2-(trifluoromethyl)phenyl)acetamide, TFA salt, was synthesized according to General Procedure F: ^{1}H NMR (400 MHz, DMSO-d_6): δ 10.29 (dd, J = 9.3, 4.7 Hz, 1H), 8.05 (t, J = 5.7 Hz, 1H), 7.91 (dd, J = 8.6, 3.1 Hz, 1H), 7.80 (ddd, J = 9.2, 7.9, 3.1 Hz, 1H), 7.65 (d, J = 7.7 Hz, 1H), 7.60 (t, J = 7.6 Hz, 1H), 7.44 (d, J = 7.8 Hz, 2H), 4.04 (t, J = 7.3 Hz, 2H), 3.61 (s, 2H), 3.15 (q, J = 6.7 Hz, 2H), 1.85 (p, J = 7.1 Hz, 2H); ^{19}F NMR (376 MHz, DMSO-d_6): δ −58.53, −113.20 (td, J = 8.3, 4.8 Hz).

***N*-(3-(7-Fluoro-5-oxo-1-thioxo-1,2-dihydro-[1,2,4]triazolo[4,3-a]-quinazolin-4(5H)-yl)propyl)-2-(3-(trifluoromethyl)phenyl)-acetamide (132).** *N*-(3-(7-Fluoro-5-oxo-1-thioxo-1,2-dihydro-[1,2,4]triazolo[4,3-*a*]quinazolin-4(5*H*)-yl)propyl)-2-(3-(trifluoromethyl)phenyl)acetamide, TFA salt, was synthesized according to General Procedure F: ^{1}H NMR (400 MHz, DMSO-d_6): δ 10.29 (dd, J = 9.3, 4.7 Hz, 1H), 8.14 (t, J = 5.6 Hz, 1H), 7.90 (dd, J = 8.6, 3.1 Hz, 1H), 7.80 (ddd, J = 9.3, 8.0, 3.1 Hz, 1H), 7.61−7.49 (m, 4H), 4.03 (dd, J = 8.1, 6.3 Hz, 2H), 3.50 (s, 2H), 3.13 (q, J = 6.8 Hz, 2H), 1.85 (p, J = 7.1 Hz, 2H); ^{19}F NMR (376 MHz, DMSO-d_6): δ −61.01, −113.20 (td, J = 8.2, 4.7 Hz); HRMS (ES-API) m/z: calcd for $C_{21}H_{18}F_4N_5O_2S$ (M + H), 480.1112; found, 480.1126.

2-(2-Cyanophenyl)-*N*-(3-(7-fluoro-5-oxo-1-thioxo-1,2-dihydro-[1,2,4]triazolo[4,3-a]quinazolin-4(5H)-yl)propyl)acetamide (133). 2-(2-Cyanophenyl)-*N*-(3-(7-fluoro-5-oxo-1-thioxo-1,2-dihydro-[1,2,4]triazolo[4,3-*a*]quinazolin-4(5*H*)-yl)propyl)acetamide, TFA salt, was synthesized according to General Procedure F: ^{1}H NMR (400 MHz, DMSO-d_6): δ 10.29 (dd, J = 9.3, 4.7 Hz, 1H), 8.20 (t, J = 5.6 Hz, 1H), 7.91 (dd, J = 8.6, 3.1 Hz, 1H), 7.85−7.73 (m, 2H), 7.63 (td, J = 7.7, 1.4 Hz, 1H), 7.46 (d, J = 7.8 Hz, 1H), 7.42 (td, J = 7.6, 1.2 Hz, 1H), 4.05 (t, J = 7.2 Hz, 2H), 3.65 (s, 2H), 3.16 (q, J = 6.7 Hz, 2H), 1.87 (p, J = 7.2 Hz, 2H); ^{19}F NMR (376 MHz, DMSO-d_6):

δ −113.18 (td, J = 8.4, 4.8 Hz); HRMS (ES-API) m/z: calcd for $C_{21}H_{18}FN_6O_2S$ (M + H) 437.1190; found, 437.1194.

2-(4-Cyanophenyl)-*N*-(3-(7-fluoro-5-oxo-1-thioxo-1,2-dihydro-[1,2,4]triazolo[4,3-a]quinazolin-4(5H)-yl)propyl)acetamide (134). 2-(4-Cyanophenyl)-*N*-(3-(7-fluoro-5-oxo-1-thioxo-1,2-dihydro-[1,2,4]triazolo[4,3-*a*]quinazolin-4(5*H*)-yl)propyl)acetamide, TFA salt, was synthesized according to General Procedure F: ^{1}H NMR (400 MHz, DMSO-d_6): δ 10.29 (dd, J = 9.3, 4.7 Hz, 1H), 8.16 (t, J = 5.6 Hz, 1H), 7.91 (dd, J = 8.6, 3.1 Hz, 1H), 7.80 (ddd, J = 9.3, 8.0, 3.1 Hz, 1H), 7.77−7.73 (m, 2H), 7.47−7.40 (m, 2H), 4.02 (t, J = 7.3 Hz, 2H), 3.50 (s, 2H), 3.18−3.09 (m, 2H), 1.84 (p, J = 7.1 Hz, 2H); ^{19}F NMR (376 MHz, DMSO-d_6): δ −113.17.

***tert*-Butyl (4-(2-((3-(7-Fluoro-5-oxo-1-thioxo-1,2-dihydro-[1,2,4]triazolo[4,3-a]quinazolin-4(5H)-yl)propyl)amino)-2-oxoethyl)-phenyl)carbamate (135).** *tert*-Butyl (4-(2-((3-(7-fluoro-5-oxo-1-thioxo-1,2-dihydro-[1,2,4]triazolo[4,3-*a*]quinazolin-4(5*H*)-yl)-propyl)amino)-2-oxoethyl)phenyl)carbamate, TFA salt, was synthesized according to General Procedure F: ^{1}H NMR (400 MHz, DMSO-d_6): δ 10.30 (dd, J = 9.3, 4.7 Hz, 1H), 9.23 (s, 1H), 7.98 (t, J = 5.7 Hz, 1H), 7.92 (dd, J = 8.6, 3.1 Hz, 1H), 7.81 (ddd, J = 9.3, 8.0, 3.1 Hz, 1H), 7.34 (d, J = 8.5 Hz, 2H), 7.15−7.05 (m, 2H), 4.03 (dd, J = 8.1, 6.5 Hz, 2H), 3.30 (s, 2H), 3.12 (q, J = 6.7 Hz, 2H), 1.84 (p, J = 7.1 Hz, 2H), 1.46 (s, 9H); ^{19}F NMR (376 MHz, DMSO-d_6): δ −113.16 (td, J = 8.2, 4.8 Hz).

***N*-(3-(7-Fluoro-5-oxo-1-thioxo-1,2-dihydro-[1,2,4]triazolo[4,3-a]-quinazolin-4(5H)-yl)propyl)-2-(pyridine-2-yl)acetamide (136).** *N*-(3-(7-Fluoro-5-oxo-1-thioxo-1,2-dihydro-[1,2,4]triazolo[4,3-*a*]-quinazolin-4(5*H*)-yl)propyl)-2-(pyridine-2-yl)acetamide was synthesized according to General Procedure F: ^{1}H NMR (400 MHz, dmso): δ 10.29 (dd, J = 9.3, 4.7 Hz, 1H), 8.48−8.42 (m, 1H), 8.13 (t, J = 5.8 Hz, 1H), 7.91 (dd, J = 8.6, 3.2 Hz, 1H), 7.80 (td, J = 8.6, 3.2 Hz, 1H), 7.71 (td, J = 7.8, 1.8 Hz, 1H), 7.31 (d, J = 7.8 Hz, 1H), 7.22 (dd, J = 7.5, 5.0 Hz, 1H), 4.04 (t, J = 7.2 Hz, 2H), 3.57 (s, 2H), 3.14 (q, J = 6.7 Hz, 2H), 2.52 (s, 1H), 1.85 (p, J = 7.2 Hz, 2H); ^{19}F NMR (376 MHz, dmso): δ −113.14 to −113.23 (m).

***N*-(3-(7-Fluoro-5-oxo-1-thioxo-1,2-dihydro-[1,2,4]triazolo[4,3-a]-quinazolin-4(5H)-yl)propyl)-2-(pyridine-3-yl)acetamide (137).** *N*-(3-(7-Fluoro-5-oxo-1-thioxo-1,2-dihydro-[1,2,4]triazolo[4,3-*a*]-quinazolin-4(5*H*)-yl)propyl)-2-(pyridine-3-yl)acetamide was synthesized according to General Procedure F: ^{1}H NMR (400 MHz, DMSO-d_6): δ 10.29 (dd, J = 9.3, 4.7 Hz, 1H), 8.44−8.37 (m, 2H), 8.14 (t, J = 5.7 Hz, 1H), 7.90 (dd, J = 8.6, 3.1 Hz, 1H), 7.80 (ddd, J = 9.3, 8.0, 3.1 Hz, 1H), 7.64 (dt, J = 7.8, 2.0 Hz, 1H), 7.31 (dd, J = 7.8, 4.8 Hz, 1H), 4.03 (dd, J = 8.3, 6.3 Hz, 2H), 3.42 (s, 2H), 3.13 (q, J = 6.5 Hz, 2H), 1.85 (p, J = 7.1 Hz, 2H); ^{19}F NMR (376 MHz, DMSO-d_6): δ −113.20 (d, J = 9.2 Hz).

***N*-(3-(7-Fluoro-5-oxo-1-thioxo-1,2-dihydro-[1,2,4]triazolo[4,3-a]-quinazolin-4(5H)-yl)propyl)-2-(pyridine-4-yl)acetamide (138).** *N*-(3-(7-Fluoro-5-oxo-1-thioxo-1,2-dihydro-[1,2,4]triazolo[4,3-*a*]-quinazolin-4(5*H*)-yl)propyl)-2-(pyridine-4-yl)acetamide was synthesized according to General Procedure F: ^{1}H NMR (400 MHz, dmso): δ 10.29 (dd, J = 9.3, 4.7 Hz, 1H), 8.51−8.44 (m, 2H), 8.23−8.16 (m, 1H), 7.91 (dd, J = 8.6, 3.1 Hz, 1H), 7.80 (td, J = 8.6, 3.2 Hz, 1H), 7.28 (s, 2H), 4.03 (t, J = 7.3 Hz, 2H), 3.44 (d, J = 4.1 Hz, 2H), 3.14 (q, J = 6.6 Hz, 2H), 1.85 (p, J = 7.2 Hz, 2H); ^{19}F NMR (376 MHz, dmso): δ −113.17 (td, J = 8.3, 4.7 Hz).

9-Fluoro-4-propyl-1-thioxo-2,4-dihydro-[1,2,4]triazolo[4,3-a]-quinazolin-5(1H)-one (139). 8-Fluoro-3-propyl-2-thioxo-2,3-dihydroquinazolin-4(1*H*)-one, TFA salt, was synthesized according to General Procedure A. Then, 9-fluoro-4-propyl-1-thioxo-2,4-dihydro-[1,2,4]triazolo[4,3-*a*]quinazolin-5(1*H*)-one was synthesized according to General Procedure D: ^{1}H NMR (400 MHz, DMSO-d_6): δ 13.83 (s, 1H), 8.02 (dd, J = 7.9, 1.5 Hz, 1H), 7.77 (ddd, J = 11.5, 8.3, 1.5 Hz, 1H), 7.61 (td, J = 8.0, 4.1 Hz, 1H), 3.97−3.89 (m, 2H), 1.70 (sext, J = 7.5 Hz, 2H), 0.89 (t, J = 7.5 Hz, 3H); ^{19}F NMR (376 MHz, DMSO-d_6): δ −93.30 (dd, J = 11.5, 4.2 Hz).

9-Chloro-4-propyl-1-thioxo-2,4-dihydro-[1,2,4]triazolo[4,3-a]-quinazolin-5(1H)-one (140). 8-Chloro-3-propyl-2-thioxo-2,3-dihydroquinazolin-4(1*H*)-one, TFA salt, was synthesized according to General Procedure A. Then, 9-chloro-4-propyl-1-thioxo-2,4-dihydro-[1,2,4]triazolo[4,3-*a*]quinazolin-5(1*H*)-one was synthesized accord-

ing to General Procedure D: ^{1}H NMR (400 MHz, DMSO-d_6): δ 13.78 (s, 1H), 8.10 (dd, J = 7.7, 1.5 Hz, 1H), 7.91 (dd, J = 8.0, 1.5 Hz, 1H), 7.60 (t, J = 7.9 Hz, 1H), 3.94−3.86 (m, 2H), 1.70 (sext, J = 7.5 Hz, 2H), 0.89 (t, J = 7.4 Hz, 3H).

9-Methoxy-4-propyl-1-thioxo-2,4-dihydro-[1,2,4]triazolo[4,3-a]-quinazolin-5(1H)-one (141). 8-Methoxy-3-propyl-2-thioxo-2,3-di-hydroquinazolin-4(1H)-one was synthesized according to General Procedure A. Then, 9-methoxy-4-propyl-1-thioxo-2,4-dihydro-[1,2,4]triazolo[4,3-a]quinazolin-5(1H)-one was synthesized according to General Procedure D: ^{1}H NMR (400 MHz, dmso): δ 13.67 (s, 1H), 7.71 (dd, J = 7.3, 1.7 Hz, 1H), 7.62−7.50 (m, 2H), 3.95−3.87 (m, 5H), 1.68 (sext, J = 7.5 Hz, 2H), 0.87 (t, J = 7.5 Hz, 3H).

S-(5-Oxo-4-propyl-4,5-dihydro-[1,2,4]triazolo[4,3-a]quinazolin-1-yl) Ethanethioate (142). 3-Propyl-2-thioxo-2,3-dihydroquinazolin-4(1H)-one was synthesized according to General Procedure A. Then, 4-propyl-1-thioxo-2,4-dihydro-[1,2,4]triazolo[4,3-a]-quinazolin-5(1H)-one, TFA salt, was synthesized according to General Procedure D. Then, S-(5-oxo-4-propyl-4,5-dihydro-[1,2,4]triazolo-[4,3-a]quinazolin-1-yl) ethanethioate was synthesized by the following method. Triethylamine (0.054 mL, 0.384 mmol) and acetic anhydride (0.022 mL, 0.230 mmol) were added to a solution of 4-propyl-1-thioxo-2,4-dihydro-[1,2,4]triazolo[4,3-a]quinazolin-5(1H)-one (0.05 g, 0.192 mmol) in acetonitrile (0.549 mL). The reaction was stirred for 2 h and quenched with water. The crude mixture was concentrated and purified by HPLC to give S-(5-oxo-4-propyl-4,5-dihydro-[1,2,4]triazolo[4,3-a]quinazolin-1-yl) ethanethioate, TFA: ^{1}H NMR (400 MHz, DMSO-d_6): δ 10.32 (dd, J = 8.6, 1.0 Hz, 1H), 8.24 (dd, J = 7.9, 1.6 Hz, 1H), 7.90 (ddd, J = 8.8, 7.3, 1.7 Hz, 1H), 7.64 (td, J = 7.6, 1.1 Hz, 1H), 4.06−4.00 (m, 2H), 2.65 (s, 3H), 1.77 (sext, J = 7.4 Hz, 2H), 0.93 (t, J = 7.5 Hz, 3H).

1-(Methylthio)-4-propyl-[1,2,4]triazolo[4,3-a]quinazolin-5(4H)-one (143). 4-Propyl-1-thioxo-2,4-dihydro-[1,2,4]triazolo[4,3-a]-quinazolin-5(1H)-one was synthesized as described above. Then, 1-(methylthio)-4-propyl-[1,2,4]triazolo[4,3-a]quinazolin-5(4H)-one was synthesized by the following method. K$_2$CO$_3$ (0.032 g, 0.230 mmol) and MeI (0.012 mL, 0.192 mmol) were added to a solution of 4-propyl-1-thioxo-2,4-dihydro-[1,2,4]triazolo[4,3-a]-quinazolin-5(1H)-one (0.05 g, 0.192 mmol) in DMF (0.549 mL). The reaction was stirred for 2 h and quenched with methanol. The crude mixture was concentrated and purified by HPLC (conditions) to give 1-(methylthio)-4-propyl-[1,2,4]triazolo[4,3-a]quinazolin-5(4H)-one, TFA.

7-Fluoro-1-(methylthio)-4-propyl-[1,2,4]triazolo[4,3-a]-quinazolin-5(4H)-one (144). To a solution of 7-fluoro-4-propyl-1-thioxo-2,4-dihydro-[1,2,4]triazolo[4,3-a]quinazolin-5(1H)-one (0.05 g, 0.180 mmol) in DMF (0.513 mL) was added K$_2$CO$_3$ (0.030 g, 0.216 mmol) and MeI (0.011 mL, 0.180 mmol). The reaction was stirred for 2 h and quenched with methanol. The crude mixture was concentrated and purified by HPLC (conditions) to give 7-fluoro-1-(methylthio)-4-propyl-[1,2,4]triazolo[4,3-a]quinazolin-5(4H)-one, TFA.

9-Fluoro-1-(methylthio)-4-propyl-[1,2,4]triazolo[4,3-a]-quinazolin-5(4H)-one (145). K$_2$CO$_3$ (0.027 g, 0.199 mmol) and MeI (10.36 μL, 0.166 mmol) were added to a solution of 9-fluoro-4-propyl-1-thioxo-2,4-dihydro-[1,2,4]triazolo[4,3-a]quinazolin-5(1H)-one (0.0461 g, 0.166 mmol) in DMF (0.473 mL). The reaction was stirred for 3 h and quenched with methanol. The crude mixture was concentrated and purified by HPLC to give 9-fluoro-1-(methylthio)-4-propyl-[1,2,4]triazolo[4,3-a]quinazolin-5(4H)-one, TFA.

9-Chloro-1-(methylthio)-4-propyl-[1,2,4]triazolo[4,3-a]-quinazolin-5(4H)-one (146). K$_2$CO$_3$ (0.066 g, 0.480 mmol) and MeI (0.030 mL, 0.480 mmol) were added to a solution of 9-chloro-4-propyl-1-thioxo-2,4-dihydro-[1,2,4]triazolo[4,3-a]quinazolin-5(1H)-one (0.1179 g, 0.400 mmol) in DMF (2.000 mL). The reaction was stirred for 3 h and quenched with methanol. The crude mixture was concentrated and purified by ISCO (EtOAc/hexanes, 0−75%) to give 9-chloro-1-(methylthio)-4-propyl-[1,2,4]triazolo[4,3-a]quinazolin-5(4H)-one.

9-Methoxy-1-(methylthio)-4-propyl-[1,2,4]triazolo[4,3-a]-quinazolin-5(4H)-one (147). K$_2$CO$_3$ (0.059 g, 0.426 mmol) and MeI (0.027 mL, 0.426 mmol) were added to a solution of 9-methoxy-4-propyl-1-thioxo-2,4-dihydro-[1,2,4]triazolo[4,3-a]quinazolin-5(1H)-one (0.103 g, 0.355 mmol) in DMF (1.774 mL). The reaction was stirred for 3 h and quenched with methanol. The crude mixture was concentrated and purified by ISCO (EtOAc/hexanes, 0−90%) to give 9-methoxy-1-(methylthio)-4-propyl-[1,2,4]triazolo[4,3-a]quinazolin-5(4H)-one.

Biochemical Assays. *ELISA-Based PBD-Binding Inhibition Assay.* The assay was performed essentially as described previously. Briefly, a biotinylated PBIP1 p-T78 peptide (i.e., Biotin-Ahx-C-ETFDPPLHSpTAI-NH$_2$) was first diluted with 1× coating solution (SeraCare, Gaithersburg, MD) to the final concentration of 0.3 μM, and then 100 μL of the resulting solution was immobilized onto a 96-well streptavidin-coated plate (Nalgene Nunc, Rochester, NY). The wells were washed once with PBS + 0.05% Tween 20 (PBST) and incubated with 200 μL of PBS plus 1% BSA (blocking buffer) for 1 h to prevent nonspecific binding. HEK293A lysates expressing HA-EGFP-Plk1 were prepared in a TBSN [20 mM Tris−HCl (pH 8.0), 150 mM NaCl, 0.5% NP-40, 5 mM EGTA, 2 mM MgCl$_2$, 1.5 mM EDTA, and protease inhibitor cocktail (Roche)] + 20% DMSO buffer (∼20 μg total lysates in 100 μL buffer), mixed with the indicated amount of the competitors (p-T78 peptide and its derivative compounds) for 30 min, provided onto the biotinylated peptide-coated ELISA wells, and then incubated with constant rocking for 1 h at 25 °C. Following the incubation, ELISA plates were washed five times with PBST. To detect bound HA-EGFP-Plk1, the plates were probed for 2 h with 100 μL/well of anti-HA antibody at a concentration of 0.5 μg/mL in the blocking buffer and then washed five times. The plates were further probed for 1 h with 100 μL/well of HRP-conjugated secondary antibody (GE Healthcare) at a 1:1000 dilution in the blocking buffer. The plates were washed five times with PBST and incubated with 100 μL/well of 3,3′,5,5′-tetramethylbenzidine solution (Sigma-Aldrich, St. Louis, MO) as a substrate until a desired absorbance was reached. The reactions were stopped by the addition of 100 μL/well of stop solution (Cell Signaling Technology, Danvers, MA). The optical density was measured at 450 nm by using a PerkinElmer Enspire Multimode Plate reader (PerkinElmer, Inc., Boston, MA). Data obtained from more than three independent experiments were analyzed by GraphPad (San Diego, CA) Prism software version 7.

PBD FP Binding Assays for Plk1 Specificity. FP assays were carried out essentially as described previously.[26] Briefly, an appropriate 5-carboxyfluorescein-labeled PBD-binding peptide for Plk1, Plk2, or Plk3 was incubated at a final concentration of 5 nM with various concentrations of the bacterially expressed and purified PBD of Plk1, Plk2 or Plk3, respectively, in a binding buffer [10 mM Tris (pH 8.0), 1 mM EDTA, 50 mM NaCl, and 0.01% Nonidet P-40]. Samples were analyzed 30 min after mixing all components in a 384-well format using the Molecular Devices (San Jose, CA). To eliminate the possibility that the apparent anti-Plk1 PBD activity is not the result of the compounds' ability to inhibit the ligand peptide used for the Plk1 FP assay above (i.e., FITC-Ahx-DPPLHSpTAI-NH$_2$), a second Plk1 PBD-binding peptide (FITC-Ahx-GPMQSpTPLNG-NH$_2$)[25] was used to confirm the activity (Figure S3B, Supporting Information). SpectraMax Paradigm multimode microplate detection platform. All experiments were performed in triplicate for each sample. The obtained data were plotted using GraphPad Prism software version 7.

ADME Measurements. PAMPA permeability was measured using a high-throughput protocol, as previously reported.[47] Aqueous solubility was determined by a published procedure.[48] Microsomal metabolic stability assays were performed as reported previously.[46]

Cell-Based Assays. *Culture, Immunostaining, and Confocal Microscopy.* HeLa cells were cultured as recommended by the American Type Culture Collection (ATCC). Asynchronously growing cells were treated with control DMSO or the indicated concentration of **143**. To reveal chromosome morphologies, cells were treated with DAPI, fixed, and subjected to confocal microscopy.

Immunostaining was carried out using anti-Plk1 (Santa Cruz Biotechnology, Santa Cruz, CA), anti-Cep63 (MilliporeSigma), anti-CREST (Antibodies Incorp, Davis, CA), and anti-α-tubulin (Sigma)

antibodies. Confocal images were acquired using a Zeiss LSM780 equipped with a plan-apochromat 63× (N.A. 1.4) oil-immersion objective lens, 34-channel GaAsP spectral detector (Carl Zeiss Microscopy, LLC.), and 8-bit, 0.5 μm z-steps.

Image Quantification and Statistical Analysis. To quantify fluorescence signal intensities, images were acquired under the same settings and the images obtained after the maximum-intensity projection of z-stacks were analyzed using the Zeiss ZEN v2.1 software (Carl Zeiss Microscopy, LLC). All the quantifications were performed with randomly chosen fields from at least three independent experiments. All values are given as mean ± s. d. *P* values were calculated by an unpaired *t*-test from the mean data of each group in GraphPad Prism (***$P < 0.001$). The statistical details including the definitions and value of n (e.g., number of experimental replicates, cells, etc.) and standard deviations are provided in the figure legends.

Metabolism Study. *Animals.* Male C57BL/6 mice from Charles River Laboratories (Wilmington, MA) were housed in the National Cancer Institute animal facility that is a pathogen-free environment controlled for temperature, light (25 °C, 12 h light/dark cycle), and humidity (45−65%) with free access to food and water. The National Cancer Institute Animal Care and Use Committee approved all animal experiments conducted in this study.

In Vivo Mouse Pharmacokinetics Study. 6−8-week-old male C57BL/6 mice were selected for metabolite profiling. In brief, 200 μL/20 g mice of WA (20 mg/kg dissolved in 5% DMSO and 5% Tween 80-contained saline) was administered intraperitoneally to mice. Control mice were treated with saline containing 5% DMSO and 5% Tween 80 alone. Each group consisted of three mice. Blood samples were collected by retro-orbital bleeding at 4 h postdose. After centrifugation for 10 min at 14,000g, serum was obtained and prepared by mixing 20 μL serum with 180 μL 50% aqueous acetonitrile. After centrifugation at 14,000g for 20 min, a 5 μL aliquot of the supernatants was injected into a Waters UPLC-ESI-QTOFMS system (Waters Corporation, Milford, MA).

In Vitro MLM Assay. The incubation system (200 μL) contained 100 mM phosphate buffer solution (pH = 7.4), 1.0 mg·mL^{-1} MLMs, 5 mM MgCl$_2$, and 20 μM test compound. The mixture was preincubated at 37 °C for 3 min and initiated with 2 mM NADPH or 2 mM UDPGA. The reaction was stopped by an aliquot of 200 μL of ice-cold acetonitrile after 60 min. After centrifugation at 14,000g for 10 min, a 5 μL aliquot of the supernatant was injected into a UHPLC-ESIQTOFMS.

UHPLC-ESI-QTOFMS and UHPLC-ESI-TQMS Analysis. Metabolite profiling and identification were performed on an Acquity UPLC/ Synapt HDMS Q-TOF MS system (Waters Corp., Milford, MA) with an ESI source. Separation was achieved on an Acquity C18 BEH UPLC column (1.7 mm, 2.1 × 50 mm; Waters Corp.). The mobile phase consisted of water containing 0.1% formic acid (A) and acetonitrile containing 0.1% formic acid (B). The initial condition of 2% B was held for 0.5 min, with the following linear gradient employed: 20% B at 4 min, 95% B at 8 min, to 99% B at 9 min, held for 1 min for column flushing, then returning to initial conditions for 2 min for column equilibration before the next injection. The flow rate of the mobile phase was set at 0.4 mL/min. Column temperature was maintained at 40 °C throughout the run. Data were collected in positive ion mode, which was operated in full-scan mode at 50−950 m/z. Nitrogen was used as both cone gas (50 L/h) and desolvation gas (950 L/h). Source temperature and desolvation temperature were set at 150 and 400 °C, respectively. The capillary voltage and cone voltage were 3000 and 30 V, respectively. The structures of metabolites of interest were elucidated by tandem MS fragmentography with collision energies ramping from 15 to 40 eV, employing the same chromatographic conditions described above.

ASSOCIATED CONTENT

Supporting Information

The Supporting Information is available free of charge at https://pubs.acs.org/doi/10.1021/acs.jmedchem.0c01669.

Extracted ion chromatograms of selected compounds and their glucuronides in MLM incubations with UDPGA after 60 min; MS/MS spectrum of selected compounds and their glucuronides; comparative FP-based assays showing the ability of additional triazoloquinazolinone-derived compounds (**20**, **27**, **89**, and **90**) to specifically inhibit Plk1 PBD; acyl-transfer from **142**; extracted ion chromatograms of **143** and its metabolites in MLM incubations with NADPH and UDPGA after 60 min, MS/MS spectrum of **143**, its hydroxylated metabolite, and its demethylated metabolite, and proposed metabolic pathways of **143** in mice; extracted ion chromatograms of **143** and its metabolites from MS after 20 mg/kg IP injection of C57BL/6 mice analyzed 4 h post injection and extracted ion chromatograms of **145** and its metabolites from MS after 20 mg/ kg IP injection of C57BL/6 mice analyzed 4 h post injection; inactive S-alkylated compounds; multispecies microsome and cytosol stability of selected compounds; and in vitro and in vivo stability of selected prodrugs (PDF)

Molecular formula strings (CSV)

AUTHOR INFORMATION

Corresponding Authors

Kenneth A. Jacobson − *Molecular Recognition Section, Laboratory of Bioorganic Chemistry, National Institute of Diabetes and Digestive and Kidney Diseases, National Institutes of Health, Bethesda, Maryland 20892, United States;* orcid.org/0000-0001-8104-1493; Phone: 301-496-9024; Email: kennethj@niddk.nih.gov

Kyung S. Lee − *Chemistry Section, Laboratory of Metabolism, National Cancer Institute, National Institutes of Health, Bethesda, Maryland 20892, United States;* orcid.org/ 0000-0001-8326-7162; Phone: 240-760-7276; Email: kyunglee@mail.nih.gov

Authors

Celeste N. Alverez − *Chemistry Section, Laboratory of Metabolism, National Cancer Institute, National Institutes of Health, Bethesda, Maryland 20892, United States; Division of Preclinical Innovation, National Center for Advancing Translational Sciences, National Institutes of Health, Rockville, Maryland 20850, United States*

Jung-Eun Park − *Chemistry Section, Laboratory of Metabolism, National Cancer Institute, National Institutes of Health, Bethesda, Maryland 20892, United States*

Kiran S. Toti − *Molecular Recognition Section, Laboratory of Bioorganic Chemistry, National Institute of Diabetes and Digestive and Kidney Diseases, National Institutes of Health, Bethesda, Maryland 20892, United States;* orcid.org/ 0000-0002-4528-4858

Yangliu Xia − *Chemistry Section, Laboratory of Metabolism, National Cancer Institute, National Institutes of Health, Bethesda, Maryland 20892, United States*

Kristopher W. Krausz − *Chemistry Section, Laboratory of Metabolism, National Cancer Institute, National Institutes of Health, Bethesda, Maryland 20892, United States*

Ganesha Rai − *Division of Preclinical Innovation, National Center for Advancing Translational Sciences, National Institutes of Health, Rockville, Maryland 20850, United States;* orcid.org/0000-0001-9763-9641

Jeong K. Bang − *Division of Magnetic Resonance, Korea Basic Science Institute, Cheongju 28119, Republic of Korea;* orcid.org/0000-0001-5916-0912

Frank J. Gonzalez − *Chemistry Section, Laboratory of Metabolism, National Cancer Institute, National Institutes of Health, Bethesda, Maryland 20892, United States*

Complete contact information is available at:
https://pubs.acs.org/10.1021/acs.jmedchem.0c01669

Author Contributions

C.N.A. and J.-E.P. contributed equally to this work. C.N.A. and K.S.T. carried out the chemical synthesis under the supervision of K.A.J.; J.-E.P. performed ELISA, FP, and cell-based assays under the guidance of K.S.L.; Y.X. and K.W.K. executed mouse PK analyses; G.R. and J.K.B. assisted in the synthetic chemistry and provided in vitro assay reagents, respectively. C.N.A., J.-E.P., Y.X., K.S.T., F.J.G., K.A.J., and K.S.L. designed the experiments and wrote the paper.

Notes

The authors declare no competing financial interest.

■ ACKNOWLEDGMENTS

■ ABBREVIATIONS

ADME, absorption distribution metabolism excretion; ATP, adenosine triphosphate; Boc, *tert*-butyloxycarbonyl; COMU, (1-cyano-2-ethoxy-2-oxoethylidenaminooxy)dimethylamino-morpholino-carbenium hexafluorophosphate; CYP, cytochrome P450; DCM, dichloromethane; DIPEA, *N,N*-diisopropylethylamine; DMF, *N,N*-dimethylformamide; DMSO, dimethylsulfoxide; EGFR, epidermal growth factor receptor; ELISA, enzyme-linked immunosorbent assay; FDA, Food and Drug Administration; FITC, fluorescein-5-isothiocyanate; FP, fluorescence polarization assay; HBA, H-bond acceptor; HER2, human epidermal growth factor receptor 2; HPLC, high-performance liquid chromatography; HRMS, high-resolution mass spectrometry; IP, intraperitoneal; KD, kinase domain; LCMS, liquid chromatography−mass spectrometry; MLM, mouse liver microsome; MS/MS, tandem mass spectrometry; MT, microtubule; NAPDH, reduced nicotinamide adenine dinucleotide phosphate; PAMPA, parallel artificial membrane permeability assay; PBD, polo-box domain; PBIP1, centromeric protein U; PEG, polyethylene glycol; PPI, protein−protein interaction; pyr, pyridine; RLM, rat liver microsome; RT, room temperature; SAR, structure−activity relationship; TFA, trifluoroacetic acid; UDPGA, uridine 5′-diphosphoglucuronic acid; UGT, uridine diphosphate glucuronosyltransferase

■ REFERENCES

(1) Zitouni, S.; Nabais, C.; Jana, S. C.; Guerrero, A.; Bettencourt-Dias, M. Polo-like Kinases: Structural Variations Lead to Multiple Functions. *Nat. Rev. Mol. Cell Biol.* **2014**, *15*, 433−452.

(2) Lee, K. S.; Burke, T. R., Jr.; Park, J.-E.; Bang, J. K.; Lee, E. Recent Advances and New Strategies in Targeting Plk1 for Anticancer Therapy. *Trends Pharmacol. Sci.* **2015**, *36*, 858−877.

(3) Strebhardt, K. Multifaceted Polo-like Kinases: Drug Targets and Antitargets for Cancer Therapy. *Nat. Rev. Drug Discovery* **2010**, *9*, 643−660.

(4) de Cárcer, G. The Mitotic Cancer Target Polo-like Kinase 1: Oncogene or Tumor Suppressor? *Genes* **2019**, *10*, 208−221.

(5) Luo, J.; Emanuele, M. J.; Li, D.; Creighton, C. J.; Schlabach, M. R.; Westbrook, T. F.; Wong, K.-K.; Elledge, S. J. A Genome-Wide RNAi Screen Identifies Multiple Synthetic Lethal Interactions with the Ras Oncogene. *Cell* **2009**, *137*, 835−848.

(6) Sur, S.; Pagliarini, R.; Bunz, F.; Rago, C.; Diaz, L. A.; Kinzler, K. W.; Vogelstein, B.; Papadopoulos, N. A Panel of Isogenic Human Cancer Cells Suggests a Therapeutic Approach for Cancers with Inactivated p53. *Proc. Natl. Acad. Sci. U.S.A.* **2009**, *106*, 3964−3969.

(7) Park, J.-E.; Kim, T.-S.; Kim, B. Y.; Lee, K. S. Selective Blockade of Cancer Cell Proliferation and Anchorage-Independent Growth by Plk1 Activity−Dependent Suicidal Inhibition of its Polo-Box Domain. *Cell Cycle* **2015**, *14*, 3624−3634.

(8) Weinstein, I. B. Addiction to Oncogenes − The Achilles Heal of Cancer. *Science* **2002**, *297*, 63−64.

(9) McMurray, H. R.; Sampson, E. R.; Compitello, G.; Kinsey, C.; Newman, L.; Smith, B.; Chen, S.-R.; Klebanov, L.; Salzman, P.; Yakovlev, A.; Land, H. Synergistic Response to Oncogenic Mutations Defines Gene Class Critical to Cancer Phenotype. *Nature* **2008**, *453*, 1112−1116.

(10) Luo, J.; Solimini, N. L.; Elledge, S. J. Principles of Cancer Therapy: Oncogene and Non-Oncogene Addiction. *Cell* **2009**, *136*, 823−837.

(11) Elia, A. E. H.; Rellos, P.; Haire, L. F.; Chao, J. W.; Ivins, F. J.; Hoepker, K.; Mohammad, D.; Cantley, L. C.; Smerdon, S. J.; Yaffe, M. B. The Molecular Basis for Phosphodependent Substrate Targeting and Regulation of Plks by the Polo-Box Domain. *Cell* **2003**, *115*, 83−95.

(12) Lee, K. S.; Grenfell, T. Z.; Yarm, F. R.; Erikson, R. L. Mutation of the Polo-Box Disrupts Localization and Mitotic Functions of the Mammalian Polo Kinase Plk. *Proc. Natl. Acad. Sci. U.S.A.* **1998**, *95*, 9301−9306.

(13) Seong, Y.-S.; Kamijo, K.; Lee, J.-S.; Fernandez, E.; Kuriyama, R.; Miki, T.; Lee, K. S. A Spindle Checkpoint Arrest and a Cytokinesis Failure by the Dominant-Negative Polo-Box Domain of Plk1 in U-2 OS Cells. *J. Biol. Chem.* **2002**, *277*, 32282−32293.

(14) Rudolph, D.; Steegmaier, M.; Hoffmann, M.; Grauert, M.; Baum, A.; Quant, J.; Haslinger, C.; Garin-Chesa, P.; Adolf, G. R. BI 6727, a Polo-like Kinase Inhibitor with Improved Pharmacokinetic Profile and Broad Antitumor Activity. *Clin. Cancer Res.* **2009**, *15*, 3094−3102.

(15) Steegmaier, M.; Hoffmann, M.; Baum, A.; Lénárt, P.; Petronczki, M.; Krššák, M.; Gürtler, U.; Garin-Chesa, P.; Lieb, S.; Quant, J.; Grauert, M.; Adolf, G. R.; Kraut, N.; Peters, J.-M.; Rettig, W. J. BI 2536, a Potent and Selective Inhibitor of Polo-like Kinase 1, Inhibits Tumor Growth in Vivo. *Curr. Biol.* **2007**, *17*, 316−322.

(16) Russo, M. A.; Kang, K. S.; Di Cristofano, A. The PLK1 Inhibitor GSK461364A is Effective in Poorly Differentiated and Anaplastic Thyroid Carcinoma Cells, Independent of the Nature of Their Driver Mutations. *Thyroid* **2013**, *23*, 1284−1293.

(17) Beria, I.; Bossi, R. T.; Brasca, M. G.; Caruso, M.; Ceccarelli, W.; Fachin, G.; Fasolini, M.; Forte, B.; Fiorentini, F.; Pesenti, E.; Pezzetta, D.; Posteri, H.; Scolaro, A.; Depaolini, S. R.; Valsasina, B. NMS-P937, a 4,5-dihydro-1H-Pyrazolo[4,3-h]Quinazoline Derivative as Potent and Selective Polo-like Kinase 1 Inhibitor. *Bioorg. Med. Chem. Lett.* **2011**, *21*, 2969−2974.

(18) Nie, Z.; Feher, V.; Natala, S.; McBride, C.; Kiryanov, A.; Jones, B.; Lam, B.; Liu, Y.; Kaldor, S.; Stafford, J.; Hikami, K.; Uchiyama, N.; Kawamoto, T.; Hikichi, Y.; Matsumoto, S.-i.; Amano, N.; Zhang, L.; Hosfield, D.; Skene, R.; Zou, H.; Cao, X.; Ichikawa, T. Discovery of TAK-960: An Orally Available Small Molecule Inhibitor of Polo-like Kinase 1 (PLK1). *Bioorg. Med. Chem. Lett.* **2013**, *23*, 3662−3666.

(19) Karaman, M. W.; Herrgard, S.; Treiber, D. K.; Gallant, P.; Atteridge, C. E.; Campbell, B. T.; Chan, K. W.; Ciceri, P.; Davis, M. I.; Edeen, P. T.; Faraoni, R.; Floyd, M.; Hunt, J. P.; Lockhart, D. J.;

Milanov, Z. V.; Morrison, M. J.; Pallares, G.; Patel, H. K.; Pritchard, S.; Wodicka, L. M.; Zarrinkar, P. P. A Quantitative Analysis of Kinase Inhibitor Selectivity. *Nat. Biotechnol.* **2008**, *26*, 127–132.

(20) Lee, K. S.; Burke, T. R., Jr.; Park, J.-E.; Bang, J. K.; Lee, E. Recent Advances and New Strategies in Targeting Plk1 for Anticancer Therapy. *Trends Pharmacol. Sci.* **2015**, *36*, 858–877.

(21) Park, J.-E.; Hymel, D.; Burke, T. R., Jr.; Lee, K. S. Current Progress and Future Perspectives in the Development of Anti-Polo-like Kinase 1 Therapeutic Agents. *F1000Research* **2017**, *6*, 1024.

(22) Syed, N.; Smith, P.; Sullivan, A.; Spender, L. C.; Dyer, M.; Karran, L.; O'Nions, J.; Allday, M.; Hoffmann, I.; Crawford, D.; Griffin, B.; Farrell, P. J.; Crook, T. Transcriptional Silencing of Polo-like Kinase 2 (SNK/PLK2) is a Frequent Event in B-cell Malignancies. *Blood* **2006**, *107*, 250–256.

(23) Yang, Y.; Bai, J.; Shen, R.; Brown, S. A. N.; Komissarova, E.; Huang, Y.; Jiang, N.; Alberts, G. F.; Costa, M.; Lu, L.; Winkles, J. A.; Dai, W. Polo-like Kinase 3 Functions as a Tumor Suppressor and is a Negative Regulator of Hypoxia-Inducible Factor-1 Alpha Under Hypoxic Conditions. *Cancer Res.* **2008**, *68*, 4077–4085.

(24) Hanisch, A.; Wehner, A.; Nigg, E. A.; Silljé, H. H. W. Different Plk1 Functions Show Distinct Dependencies on Polo-Box Domain-Mediated Targeting. *Mol. Biol. Cell* **2006**, *17*, 448–459.

(25) Liu, F.; Park, J.-E.; Qian, W.-J.; Lim, D.; Gräber, M.; Berg, T.; Yaffe, M. B.; Lee, K. S.; Burke, T. R., Jr. Serendipitous Alkylation of a Plk1 Ligand Uncovers a New Binding Channel. *Nat. Chem. Biol.* **2011**, *7*, 595–601.

(26) Qian, W.-J.; Park, J.-E.; Lim, D.; Lai, C. C.; Kelley, J. A.; Park, S.-Y.; Lee, K. W.; Yaffe, M. B.; Lee, K. S.; Burke, T. R., Jr. Mono-anionic Phosphopeptides Produced by Unexpected Histidine Alkylation Exhibit High Plk1 Polo-Box Domain-Binding Affinities and Enhanced Antiproliferative Effects in HeLa Cells. *Biopolymers* **2014**, *102*, 444–455.

(27) Yun, S.-M.; Moulaei, T.; Lim, D.; Bang, J. K.; Park, J.-E.; Shenoy, S. R.; Liu, F.; Kang, Y. H.; Liao, C.; Soung, N.-K.; Lee, S.; Yoon, D.-Y.; Lim, Y.; Lee, D.-H.; Otaka, A.; Appella, E.; McMahon, J. B.; Nicklaus, M. C.; Burke, T. R., Jr.; Yaffe, M. B.; Wlodawer, A.; Lee, K. S. Structural and Functional Analyses of Minimal Phosphopeptides Targeting the Polo-Box Domain of Polo-Like Kinase 1. *Nat. Struct. Mol. Biol.* **2009**, *16*, 876–882.

(28) Huggins, D. J.; Hardwick, B. S.; Sharma, P.; Emery, A.; Laraia, L.; Zhang, F.; Narvaez, A. J.; Roberts-Thomson, M.; Crooks, A. T.; Boyle, R. G.; Boyce, R.; Walker, D. W.; Mateu, N.; McKenzie, G. J.; Spring, D. R.; Venkitaraman, A. R. Development of a Novel Cell-Permeable Protein-Protein Interaction Inhibitor for the Polo-box Domain of Polo-like Kinase 1. *ACS Omega* **2020**, *5*, 822–831.

(29) Sharma, P.; Mahen, R.; Rossmann, M.; Stokes, J. E.; Hardwick, B.; Huggins, D. J.; Emery, A.; Kunciw, D. L.; Hyvonen, M.; Spring, D. R.; McKenzie, G. J.; Venkitaraman, A. R. A Cryptic Hydrophobic Pocket in the Polo-Box Domain of the Polo-like Kinase PLK1 Regulates Substrate Recognition and Mitotic Chromosome Segregation. *Sci. Rep.* **2019**, *9*, 15930.

(30) Rubner, S.; Scharow, A.; Schubert, S.; Berg, T. Selective Degradation of Polo-like Kinase 1 by a Hydrophobically Tagged Inhibitor of the Polo-Box Domain. *Angew. Chem., Int. Ed.* **2018**, *57*, 17043–17047.

(31) Abdelfatah, S.; Berg, A.; Huang, Q.; Yang, L. J.; Hamdoun, S.; Klinger, A.; Greten, H. J.; Fleischer, E.; Berg, T.; Wong, V. K. W.; Efferth, T. MCC1019, a Selective Inhibitor of the Polo-Box Domain of Polo-like Kinase 1 as Novel, Potent Anticancer Candidate. *Acta Pharm. Sin. B* **2019**, *9*, 1021–1034.

(32) Reindl, W.; Yuan, J.; Krämer, A.; Strebhardt, K.; Berg, T. A Pan-Specific Inhibitor of the Polo-Box Domains of Polo-like Kinases Arrests Cancer Cells in Mitosis. *ChemBioChem* **2009**, *10*, 1145–1148.

(33) Reindl, W.; Yuan, J.; Krämer, A.; Strebhardt, K.; Berg, T. Inhibition of Polo-Like Kinase 1 by Blocking Polo-Box Domain-Dependent Protein-Protein Interactions. *Chem. Biol.* **2008**, *15*, 459–466.

(34) Watanabe, N.; Sekine, T.; Takagi, M.; Iwasaki, J.-i.; Imamoto, N.; Kawasaki, H.; Osada, H. Deficiency in Chromosome Congression by the Inhibition of Plk1 Polo Box Domain-Dependent Recognition. *J. Biol. Chem.* **2009**, *284*, 2344–2353.

(35) Normandin, K.; Lavallee, J. F.; Futter, M.; Beautrait, A.; Duchaine, J.; Guiral, S.; Marinier, A.; Archambault, V. Identification of Polo-like Kinase 1 Interaction Inhibitors Using a Novel Cell-Based Assay. *Sci. Rep.* **2016**, *6*, 37581.

(36) Scharow, A.; Knappe, D.; Reindl, W.; Hoffmann, R.; Berg, T. Development of Bifunctional Inhibitors of Polo-like Kinase 1 with Low-Nanomolar Activities Against the Polo-Box Domain. *Chem-BioChem* **2015**, *17*, 759–767.

(37) Chen, Y.; Zhang, J.; Li, D.; Jiang, J.; Wang, Y.; Si, S. Identification of a Novel Polo-like Kinase 1 Inhibitor that Specifically Blocks the Functions of Polo-Box Domain. *Oncotarget* **2017**, *8*, 1234–1246.

(38) Kim, T. G.; Lee, J. H.; Lee, M. Y.; Kim, K.-U.; Lee, J. H.; Park, C. H.; Lee, B. H.; Oh, K.-S. Development of a High-Throughput Assay for Inhibitors of the Polo-Box Domain of Polo-Like Kinase 1 Based on Time-Resolved Fluorescence Energy Transfer. *Biol. Pharm. Bull.* **2017**, *40*, 1454–1462.

(39) Chen, Y.; Li, Z.; Liu, Y.; Lin, T.; Sun, H.; Yang, D.; Jiang, C. Identification of Novel and Selective Non-Peptide Inhibitors Targeting the Polo-Box Domain of Polo-Like Kinase 1. *Bioorg. Chem.* **2018**, *81*, 278–288.

(40) Abdelfatah, S.; Berg, A.; Böckers, M.; Efferth, T. A Selective Inhibitor of the Polo-Box Domain of Polo-like Kinase 1 Identified by Virtual Screening. *J. Adv. Res.* **2019**, *16*, 145–156.

(41) Zhou, Y.; Yan, F.; Huo, X.; Niu, M.-M. Discovery of a Potent PLK1-PBD Small-Molecule Inhibitor as an Anticancer Drug Candidate Through Structure-Based Design. *Molecules* **2019**, *24*, 4351–4360.

(42) Lee, K. S.; Idle, J. R. Pinning Down the Polo-Box Domain. *Chem. Biol.* **2008**, *15*, 415–416.

(43) Archambault, V.; Normandin, K. Several Inhibitors of the Plk1 Polo-Box Domain Turn Out to Be Non-Specific Protein Alkylators. *Cell Cycle* **2017**, *16*, 1220–1224.

(44) Kang, Y. H.; Park, J.-E.; Yu, L.-R.; Soung, N.-K.; Yun, S.-M.; Bang, J. K.; Seong, Y.-S.; Yu, H.; Garfield, S.; Veenstra, T. D.; Lee, K. S. Self-regulated Plk1 Recruitment to Kinetochores by the Plk1-PBIP1 Interaction Is Critical for Proper Chromosome Segregation. *Mol. Cell* **2006**, *24*, 409–422.

(45) Carlsson, J.; Yoo, L.; Gao, Z.-G.; Irwin, J. J.; Shoichet, B. K.; Jacobson, K. A. Structure-Based Discovery of A_{2A} Adenosine Receptor Ligands. *J. Med. Chem.* **2010**, *53*, 3748–3755.

(46) Urban, D. J.; Martinez, N. J.; Davis, M. I.; Brimacombe, K. R.; Cheff, D. M.; Lee, T. D.; Henderson, M. J.; Titus, S. A.; Pragani, R.; Rohde, J. M.; Liu, L.; Fang, Y.; Karavadhi, S.; Shah, P.; Lee, O. W.; Wang, A.; McIver, A.; Zheng, H.; Wang, X.; Xu, X.; Jadhav, A.; Simeonov, A.; Shen, M.; Boxer, M. B.; Hall, M. D. Assessing Inhibitors of Mutant Isocitrate Dehydrogenase Using a Suite of Pre-Clinical Discovery Assays. *Sci. Rep.* **2017**, *7*, 12758.

(47) Sun, H.; Nguyen, K.; Kerns, E.; Yan, Z.; Yu, K. R.; Shah, P.; Jadhav, A.; Xu, X. Highly Predictive and Interpretable Models for PAMPA Permeability. *Bioorg. Med. Chem.* **2017**, *25*, 1266–1276.

(48) Sun, H.; Shah, P.; Nguyen, K.; Yu, K. R.; Kerns, E.; Kabir, M.; Wang, Y.; Xu, X. Predictive Models of Aqueous Solubility of Organic Compounds Built on a Large Dataset of High Integrity. *Bioorg. Med. Chem.* **2019**, *27*, 3110–3114.

(49) Lénárt, P.; Petronczki, M.; Steegmaier, M.; Di Fiore, B.; Lipp, J. J.; Hoffmann, M.; Rettig, W. J.; Kraut, N.; Peters, J.-M. The Small-Molecule Inhibitor BI 2536 Reveals Novel Insights Into Mitotic Roles of Polo-Like Kinase 1. *Curr. Biol.* **2007**, *17*, 304–315.

(50) Jackson, J. R.; Patrick, D. R.; Dar, M. M.; Huang, P. S. Targeted Anti-Mitotic Therapies: Can We Improve on Tubulin Agents? *Nat. Rev. Cancer* **2007**, *7*, 107–117.

(51) Münch, C.; Dragoi, D.; Frey, A.-V.; Thurig, K.; Lübbert, M.; Wäsch, R.; Bogatyreva, L.; Hauschke, D.; Lassmann, S.; Werner, M.; May, A. M. Therapeutic Polo-Like Kinase 1 Inhibition Results in Mitotic Arrest and Subsequent Cell Death of Blasts in the Bone

Marrow of AML Patients and Has Similar Effects in Non-Neoplastic Cell Lines. *Leuk. Res.* **2015**, *39*, 462−470.

(52) Döhner, H.; Lübbert, M.; Fiedler, W.; Fouillard, L.; Haaland, A.; Brandwein, J. M.; Lepretre, S.; Reman, O.; Turlure, P.; Ottmann, O. G.; Müller-Tidow, C.; Krämer, A.; Raffoux, E.; Döhner, K.; Schlenk, R. F.; Voss, F.; Taube, T.; Fritsch, H.; Maertens, J. Randomized, Phase 2 Trial of Low-Dose Cytarabine With or Without Volasertib in AML Patients Not Suitable for Induction Therapy. *Blood* **2014**, *124*, 1426−1433.

(53) Janning, M.; Fiedler, W. Volasertib for the Treatment of Acute Myeloid Leukemia: A Review of Preclinical and Clinical Development. *Future Oncol.* **2014**, *10*, 1157−1165.

(54) Awada, A.; Dumez, H.; Aftimos, P. G.; Costermans, J.; Bartholomeus, S.; Forceville, K.; Berghmans, T.; Meeus, M.-A.; Cescutti, J.; Munzert, G.; Pilz, K.; Liu, D.; Schöffski, P. Phase I Trial of Volasertib, a Polo-like Kinase Inhibitor, Plus Platinum Agents in Solid Tumors: Safety, Pharmacokinetics and Activity. *Invest. New Drugs* **2015**, *33*, 611−620.

(55) Willemze, R.; Suciu, S.; Meloni, G.; Labar, B.; Marie, J.-P.; Halkes, C. J. M.; Muus, P.; Mistrik, M.; Amadori, S.; Specchia, G.; Fabbiano, F.; Nobile, F.; Sborgia, M.; Camera, A.; Selleslag, D. L. D.; Lefrère, F.; Magro, D.; Sica, S.; Cantore, N.; Beksac, M.; Berneman, Z.; Thomas, X.; Melillo, L.; Guimaraes, J. E.; Leoni, P.; Luppi, M.; Mitra, M. E.; Mitra, D.; Bron, G.; Marijt, E. W. A.; Venditti, A.; Hagemeijer, A.; Mancini, M.; Jansen, J.; Cilloni, D.; Meert, L.; Fazi, P.; Vignetti, M.; Trisolini, S. M.; Mandelli, F.; de Witte, T.; de Witte, T. High-Dose Cytarabine in Induction Treatment Improves the Outcome of Adult Patients Younger Than Age 46 Years With Acute Myeloid Leukemia: Results of the EORTC-GIMEMA AML-12 Trial. *J. Clin. Oncol.* **2014**, *32*, 219−228.

(56) Lin, C.-C.; Su, W.-C.; Yen, C.-J.; Hsu, C.-H.; Su, W.-P.; Yeh, K.-H.; Lu, Y.-S.; Cheng, A.-L.; Huang, D. C.-L.; Fritsch, H.; Voss, F.; Taube, T.; Yang, J. C.-H. A Phase I Study of Two Dosing Schedules of Volasertib (BI 6727), an Intravenous Polo-Like Kinase Inhibitor, in Patients With Advanced Solid Malignancies. *Br. J. Cancer* **2014**, *110*, 2434−2440.

(57) Machiels, J.-P.; Peeters, M.; Herremans, C.; Surmont, V.; Specenier, P.; De Smet, M.; Pilz, K.; Strelkowa, N.; Liu, D.; Rottey, S. A Phase I Study of Volasertib Combined With Afatinib, in Advanced Solid Tumors. *Cancer Chemother. Pharmacol.* **2015**, *76*, 843−851.

(58) de Braud, F.; Cascinu, S.; Spitaleri, G.; Pilz, K.; Clementi, L.; Liu, D.; Sikken, P.; De Pas, T. A Phase I, Dose-Escalation Study of Volasertib Combined With Nintedanib in Advanced Solid Tumors. *Ann. Oncol.* **2015**, *26*, 2341−2346.

(59) Olmos, D.; Barker, D.; Sharma, R.; Brunetto, A. T.; Yap, T. A.; Taegtmeyer, A. B.; Barriuso, J.; Medani, H.; Degenhardt, Y. Y.; Allred, A. J.; Smith, D. A.; Murray, S. C.; Lampkin, T. A.; Dar, M. M.; Wilson, R.; de Bono, J. S.; Blagden, S. P. Phase I Study of GSK461364, a Specific and Competitive Polo-like Kinase 1 Inhibitor, in Patients With Advanced Solid Malignancies. *Clin. Cancer Res.* **2011**, *17*, 3420−3430.

(60) Schöffski, P.; Awada, A.; Dumez, H.; Gil, T.; Bartholomeus, S.; Wolter, P.; Taton, M.; Fritsch, H.; Glomb, P.; Munzert, G. A Phase I, Dose-Escalation Study of the Novel Polo-like Kinase Inhibitor Volasertib (BI 6727) In Patients With Advanced Solid Tumours. *Eur. J. Cancer* **2012**, *48*, 179−186.

(61) Bojadzic, D.; Buchwald, P. Toward Small-Molecule Inhibition of Protein-Protein Interactions: General Aspects and Recent Progress in Targeting Costimulatory and Coinhibitory (Immune Checkpoint) Interactions. *Curr. Top. Med. Chem.* **2018**, *18*, 674−699.

(62) Rognan, D. Rational design of protein−protein interaction inhibitors. *MedChemComm* **2015**, *6*, 51−60.

(63) Ceesay, M. M.; Couchman, L.; Smith, M.; Wade, J.; Flanagan, R. J.; Pagliuca, A. Triazole Antifungals Used for Prophylaxis and Treatment of Invasive Fungal Disease in Adult Haematology Patients: Trough Serum Concentrations in Relation to Outcome. *Med. Mycol.* **2016**, *54*, 691−698.

(64) Lass-Flörl, C. Triazole Antifungal Agents in Invasive Fungal Infections: A Comparative Review. *Drugs* **2011**, *71*, 2405−2419.

(65) Shagufta, S.; Ahmad, I. An Insight Into the Therapeutic Potential of Quinazoline Derivatives as Anticancer Agents. *MedChemComm* **2017**, *8*, 871−885.

(66) Ritschel, T.; Hermans, S. M. A.; Schreurs, M.; van den Heuvel, J. J. M. W.; Koenderink, J. B.; Greupink, R.; Russel, F. G. M. In Silico Identification and in Vitro Validation of Potential Cholestatic Compounds Through 3D Ligand-Based Pharmacophore Modeling of BSEP Inhibitors. *Chem. Res. Toxicol.* **2014**, *27*, 873−881.

(67) Zhang, H.-J.; Jin, P.; Wang, S.-B.; Li, F.-N.; Guan, L.-P.; Quan, Z.-S. Synthesis and Anticonvulsant Activity Evaluation of 4-Phenyl-[1,2,4]triazolo[4,3-a]quinazolin-5(4H)-one and Its Derivatives. *Arch. Pharm.* **2015**, *348*, 564−574.

(68) Zhang, H.-J.; Wang, S.-B.; Quan, Z.-S. Synthesis and Antidepressant Activities of 4-(substituted-phenyl)tetrazolo[1,5-a]-quinazolin-5(4H)-ones and Their Derivatives. *Mol. Divers.* **2015**, *19*, 817−828.

(69) Agarwal, S.; Nagpal, N.; Fong, Y. PAPD5 Inhibitors and Methods of Use Thereof. U.S. Patent WO 2019084271 A1, May 2, 2019.

(70) Ram, V. J.; Srimal, R. C.; Kushwaha, D. S.; Mishra, L. Chemoterapeutic Agents. XIX. Synthesis of [1,2,4]-Triazoloquinazolinones and Related Compounds as Antihypertensive Agents. *J. Prakt. Chem.* **1990**, *332*, 629−639.

(71) Ram, V. J.; Goel, A.; Verma, M.; Kaul, I. B.; Kapil, A. Latent Leishmanicidal Activity of Quinazolinones and 1,2,4-Triazoloquinazolinones. *Bioorg. Med. Chem. Lett.* **1994**, *4*, 2087−2090.

(72) Besnard, J.; Ruda, G. F.; Setola, V.; Abecassis, K.; Rodriguiz, R. M.; Huang, X.-P.; Norval, S.; Sassano, M. F.; Shin, A. I.; Webster, L. A.; Simeons, F. R. C.; Stojanovski, L.; Prat, A.; Seidah, N. G.; Constam, D. B.; Bickerton, G. R.; Read, K. D.; Wetsel, W. C.; Gilbert, I. H.; Roth, B. L.; Hopkins, A. L. Automated Design of Ligands to Polypharmacological Profiles. *Nature* **2012**, *492*, 215−220.

(73) Brassesco, M. S.; Pezuk, J. A.; Morales, A. G.; Carvalho de Oliveira, J.; Roberto, G. M.; Nicioli da Silva, G.; Francisco de Oliveira, H.; Scrideli, C. A.; Tone, L. G. In Vitro Targeting of Polo-like Kinase 1 in Bladder Carcinoma: Comparative Effects of Four Potent Inhibitors. *Canc. Biol. Ther.* **2013**, *14*, 648−657.

(74) Bogado, R. F. E.; Pezuk, J. A.; de Oliveira, H. F.; Tone, L. G.; Brassesco, M. S. 6727 and GSK461364 Suppress Growth and Radiosensitize Osteosarcoma Cells, but Show Limited Cytotoxic Effects When Combined With Conventional Treatments. *Anticancer Drugs* **2015**, *26*, 56−63.

(75) Rudolph, D.; Impagnatiello, M. A.; Blaukopf, C.; Sommer, C.; Gerlich, D. W.; Roth, M.; Tontsch-Grunt, U.; Wernitznig, A.; Savarese, F.; Hofmann, M. H.; Albrecht, C.; Geiselmann, L.; Reschke, M.; Garin-Chesa, P.; Zuber, J.; Moll, J.; Adolf, G. R.; Kraut, N. Efficacy and Mechanism of Action of Volasertib, a Potent and Selective Inhibitor of Polo-like Kinases, in Preclinical Models of Acute Myeloid Leukemia. *J. Pharmacol. Exp. Ther.* **2015**, *352*, 579−589.

(76) Gjertsen, B. T.; Schöffski, P. Discovery and Development of the Polo-like Kinase Inhibitor Volasertib in Cancer Therapy. *Leukemia* **2015**, *29*, 11−19.

(77) Erba, H. P. Finding the Optimal Combination Therapy for the Treatment of Newly Diagnosed AML in Older Patients Unfit for Intensive Therapy. *Leuk. Res.* **2015**, *39*, 183−191.